IKE Institut für Kernenergetik und Energiesysteme

Simulation of Operational and Accidental Behaviour of Modular High Temperature Reactors with Brayton Cycle Power Conversion Unit

Ayelet Walter

November 2010 IKE 6 - 204

Universität Stuttgart

IKE Institut für Kernenergetik und Energiesysteme

Simulation of Operational and Accidental Behaviour of Modular High Temperature Reactors with Brayton Cycle Power Conversion Unit

von der Fakultät Energie-, Verfahrens- und Biotechnik der Universität Stuttgart zur Erlangung der Würde eines Doktor-Ingenieurs (Dr.-Ing.) genehmigte Abhandlung

vorgelegt von

M.Sc. Ayelet Walter

geboren in Washington, D.C. (USA)

Hauptberichter:
Prof. G. Lohnert, Ph.D.

Mitberichter:
Prof. Dr.-Ing. E. Göde

Tag der Einreichung: 22.09.2008

Tag der mündlichen Prüfung: 03.03.2010

ISSN - 0173 - 6892

November 2010 IKE 6 - 204

Universität Stuttgart

Abstract

The present work analyses and investigates the behaviour of a High Temperature Reactor (HTR) with a Pebble Bed core connected to a Brayton cycle Power Conversion Unit (PCU) during operational and accident conditions.

The modelling of a complete circuit including both the PCU and the Pebble Bed Reactor has been performed with the commercial thermal-fluid analysis simulation code Flownex. Flownex has been developed for High Temperature Pebble Bed Reactor applications, and has been extensively validated against other codes.

As the reactor core model incorporated in Flownex is a simplified model based on 0D point kinetics, the extended 1D WKIND core model was implemented in the analysis calculations using a special coupling methodology. This study introduces a new sub-routine which enables the coupling of the WKIND reactor core model to the Flownex PCU model via an external interface. The interface facilitates the data exchange between the two codes, allowing for necessary manipulations and synchronisation of the coupled codes. By doing so, the 1D diffusion equation solution implemented in WKIND core model replaces the point kinetics model implemented in Flownex. This replacement allows for a detailed accurate solution even for very fast transients, through the treatment of the space-dependent heat conduction from the graphite matrix to helium.

Flownex component models have been validated against the experimental results of the 50 MW_{el} direct helium turbine facility Energieversorgung Oberhausen (EVO II). This provided the opportunity to validate Flownex calculations against experimental data derived from a large-scale helium Brayton cycle installation. Small differences observed in the results could be explained. Based upon steady state and transient analysis it is concluded that Flownex models simulate accurately the behaviour of the components integrated in the EVO II plant. Such models could be applied to analyse the transient behaviour of the total system of the reactor and the PCU.

In the present thesis, both the reactor core and the PCU have been modelled with a very high level of details. Due to the direct coupling, the reactor core and the PCU have a large and fast influence on each other. Hence, it is important to investigate the interactions between the two for the safety analysis of the compete plant.

Furthermore, a comparison between two system layouts of the PCU was investigated in this study, namely a single and a three shaft configurations. With the complete system model created it is possible to precisely simulate a great variety of operations which were demonstrated in several selected cases. These include the withdrawal of control rods, turbo-machinery trip, load following and a helium leak. Transient simulations results incorporated also both shaft configurations. The results show that the point kinetics core model is sufficiently accurate, with an exception to strong reactivity transients. In such cases, the analyses using the Flownex point kinetics model over-predicts the core thermal power. Further investigation is needed for improving the coupling methodology and the data exchange between the codes. It was proven that from the thermo-dynamical behaviour point of view, a quick response to a range of power demands, using a simple design of the control system, advocates the single shaft system configuration. However, further investigation should be done to rectify this, especially during long-term part load performance of the system.

Kurzfassung

In den letzten paar Jahren ist das Interesse an fortgeschrittenen Reaktoren gestiegen. Dieses Interesse wurde durch die Auffassung von den neuen Kernkraftreaktoren motiviert, die Sicherheit, Hochleistungen und eine konkurrenzfähige und machbare Energiequelle für die Stromherstellung sowie für Anwendungen von industriellen Heizprozessen ermöglichen. Dies führte zur Entwicklung des Programms der Generation IV Kernenergiesysteme. Ein vielversprechender und attraktiver Gesichtspunkt ist der Hochtemperaturreaktor (HTR) mit einer Brayton-Kreislauf-Leistungserzeugungseinheit (PCU). Dieses Konzept wurde im Kugelhaufenmodularreaktor-Kernkraftwerk (Pebble Bed Modular Reactor - PBMR) angewendet, das in Südafrika für Eskom entwickelt wurde.

Der Hochtemperatur-Kugelhaufen-Reaktor und seine Leistungserzeugungseinheit werden oft als zwei separate Systeme behandelt, welche typisch in ihren Abgrenzungen zusammenwirken, indem es die Randbedingungen füreinander bestimmt. Diese Bestimmung kann für die stationäre Analyse angemessen sein. Für die transienten Berechnungen jedoch ist die Analyse eines kompletten integrierten Systems notwendig, weshalb eine genaue Simulation, welche die gesamte ausgeglichene Anlage so detailliert und präzise wie möglich modelliert, notwendig ist.

Diese Doktorarbeit stellt die Transientanalysen eines mit einer Leistungserzeugungseinheit gekoppelten Hochtemperatur-Kugelhaufenreaktors vor, der dem Projekt des Südafrikanischen PBMR Kernkraftwerks ähnelt. Um die Analysen durchzuführen, wurde ein Systemcode entwickelt. Dieser Code koppelt das Reaktorkern-Modell mit einem thermohydraulischen Modell der Leistungserzeugungseinheit. Dieses Koppeln wurde entwickelt, um eine realistischere und detailliertere Simulation des Gesamtsystems für die Reaktorsicherheitsanalysen zu schaffen. Das Hauptberechnungswerkzeug, das für die Analysen des Gesamtsystems verwendet wurde, ist der handelsübliche Netzwerkanalysecode Flownex. Flownex wurde zur Anwendung für Hochtemperatur-Kugelhaufenreaktoren entwickelt und hat sich weitgehend gegenüber anderen Codes bewährt. Flownex richtet sich auf Modelle für die diversen Komponenten in der Leistungserzeugungseinheit ein und umfasst ein weniger detailliertes Modell für den Reaktorkern.

Außerdem kann sich die Leistungserzeugungseinheit eines Hochtemperatur- Kugelhaufenreaktors aus einer Vielzahl von Zusammensetzungen und Ausführungen zusammenstellen. Das thermohydraulische Verhalten dieser diversen Systeme stellt eine Schlüsselfrage für die Beschreibung des Kerns für den Abbau der Nachwärme. Deshalb wird ein effektives verlässliches Werkzeug benötigt, um das Modellieren eines Systems zu demonstrieren, das sich aus dem Kern, dem Kernbehälter und den Kernstrukturen, den Rohren und Ventilen, dem Wärmeaustauscher and den Turbomaschinen besteht. Das Neutronikmodell, das in Flownex angewandt wurde, war nicht entwickelt, um eine detaillierte Reaktorkonstruktion zu erleichtern, sondern eher um schnelle integrierte Simulationen der Reaktors und der Leistungserzeugungseinheit durchzuführen. Daher ist das Ziel dieser Doktorarbeit doppelt.

- Voll integrierte Transientkernkraftwerksanalysen mit detaillierten Codes für die Leistungserzeugungseinheit und den Reaktorkern durchzuführen. Das WKIND Reaktorkernmodell simuliert detailliert sowohl die neutronischen als auch die thermohydraulischen Aspekte des Kerns. Dafür wurde das 1D Neutronik-WKIND-Kernmodell ausgewählt, um das in Flownex eingebaute Reaktorkernmodell zu ersetzen. Das Ersetzen des Kerns wird durch das Erzeugen eines Hochleistungsinterfaces zwischen Flownex und WKIND bewirkt. Dies ermöglicht die Transientanalyse des Gesamtsystems von beiden Einwellen- und Dreiwellen-Leistungserzeugungseinheiten an einem Hochtemperaturkugelhaufenreaktor gekoppelt zu werden.

- Die individuellen Komponentmodelle von Flownex validieren, die in den Dynamikanalysen des Kugelhaufenreaktors gekoppelt sowohl mit Einwellenanlage als auch mit Dreiwellen-Leistungserzeugungseinheit-Ausführungen verwendet wurden. Um dieser Anforderung gerecht zu werden, wurden Flownex-Modelle gegenüber den experimentellen Ergebnissen der 50 MW_{el} Direktkreislauf-Heliumturbinenanlage Energieversorgung Oberhausen (EVO II) validiert.

Die Dissertationsziele wurden ausgeführt, und sie sind folgenden massen bezeichnet:

Kopplung und Reaktorkernmodelle

Das Koppeln versucht, die Wärme, die zu den charakteristischen Werten des Heliums des WKIND-Kernmodells übertragen wird, mit der Leistungserzeugungseinheit von Flownex abzustimmen. Diese charakteristischen Werte wurden jederzeit aktualisiert. Das gekoppelte Programm kombiniert das detaillierte Neutronik- und Thermohydraulikverhalten des WKIND-Kernmodells, welches ein 1D Neutronik und Thermohydraulikanteil mit der Thermohydraulik der Leistungserzeugungseinheit enthält, um detaillierte Berechnungen des transienten Verhaltens des Gesamtsystems durchzuführen. Beide Kernmodelle sind sehr nützlich, um angemessene Randbedingungen der Kerntransiente zu erhalten. Das WKIND-Kernmodell ermöglicht jedoch die Erweiterung der Analysen und die Lösung von starken Reaktivitätstransienten. Das ist der Fall bei der Entnahme von allen Kontrollstäben bei einer Geschwindigkeit von 100 cm/s. Hier berechnet WKIND die Temperaturänderungen innerhalb des Kerns richtig voraus. Aus den in diesem Fall erhaltenen Ergebnissen ist es eindeutig, dass große Unterschiede zwischen den Fähigkeiten und den Grenzen beider Kernmodelle bestehen. WKIND berücksichtigt die Stellung der Kontrollstäbe, wodurch es ein realistischeres Verhalten des Kerns bei dem heterogenen Brennstofftemperaturmodul beschreibt. Im zweiten Transient werden die Kontrollstäbe bei einer Geschwindigkeit von 1 cm/s herausgenommen. In diesem Fall haben beide Reaktorkernmodelle ein ähnliches Verhalten gezeigt und die Analysenergebnisse sind in beiden Fällen gleichartig. Durch die Transientanalysen ist es offensichtlich, dass die thermische Trägheit des Reaktors so groß ist, dass der Einfluss auf diversen Störungen auf dem dynamischen Verhalten des Kerns schwer erkennbar ist. Während eines Entlastungstransients ist die Kernausgangstemperatur fast konstant. Deshalb zeigt sich der stark negative Temperaturkoeffizient aus sicherheitsrelevantem Gesichtspunkt sowie für den Rückgang der Temperaturschwankungen während der off-design Operation als günstig. Beide Kernmodelle haben eine gute Übereinstimmung in den Transientanalysenergebnissen in Bezug auf den Einwellen- und Dreiwellen-Ausführungen des Systems gezeigt. Die Ergebnisse entsprechen auch den Sicherheitsanforderungen der Anlage, wodurch der inhärente Sicherheitsaspekt des PBMR veranschaulicht wird. Es wird empfohlen, Leistungsprofiländerungen während der Verschiebung von Kontrollstäben im Flownex-Kernmodell einzubeziehen. Zusätzlich umfasst die Kopplung eine Rohrleitungskomponente, welche den Reaktorkern einer Wärmequelle mit einem künstlichen Widerstand in Form einer Reibung gleich stellt, um den richtigen Druckrückgang im Reaktor zu modellieren. Diese Methode könnte durch das Ersetzen des Flownex-Kernmodells durch ein Rohr mit veränderlichem Ausgang verbessert werden. Dies wird sich aus einem neu errechneten Rohrausgangsfaktor ergeben, welcher das thermohydraulische Verhalten im Kern besser vorausrechnet. Außerdem wird es empfohlen, das Koppeln durch das Verwenden von 2D- und sogar 3D-Kernneutronik zu erweitern.

Code-Validierung

Die meiste Literatur für die Validierungsstudie wurde im Rahmen des Europäischen Projekts RAPHAEL gesammelt. Die Bedeutung der Validierung ist einerseits das Modellieren und die Konstruktion eines vollständigen Kraftwerks von Grund auf – unter Verwendung und Auswer-

tung der aus der Literatur gesammelten geometrischen Daten und Informationen. Dabei wurden eine breite Vielfalt von Modellierungsaufgaben gegenübergestellt, wie das Modellieren von ausstreuenden Leckflüssen, Ventilen und der thermischen Trägheit einer Kesselwand. Andererseits wurde die Gelegenheit geboten, Flownex-Berechnungen gegenüber experimentellen von einer großflächigen Helium-Brayton-Kreislauf-Anlage abgeleiteten Daten zu validieren. Die beobachteten Unterschiede in den Hauptsystemparametern wie Leistung, Temperaturen, Druck und Massenflüsse bewegen sich innerhalb von wenigen Prozentsätzen. Außerdem rechnen die Flownex-Modelle die gleichen Tendenzen wie die experimentellen Ergebnisse für die Transiente nach einer Ladung voraus, außer für die Temperaturentwicklung in einem der in der Simulation verwendeten Heliumkessel. Alle festgestellten Unterschiede konnten erklärt werden und deshalb können die Modelle als annehmbar für die Verwendung in weiteren Analysen betrachtet werden. Einige Modelle wurden vereinfacht behandelt. Es wird empfohlen, die Transientanalyse unter Verwendung der Charakteristika der Originalmaschinen oder von ähnlichen durch die Turbomaschinengeometrie geführten Plänen zu wiederholen. Die Bereitstellung von zusätzlichen Dokumenten und insbesondere Dokumentation von ergänzenden Transientfällen würde die Erweiterung der Validierungsübung ermöglichen.

Systemtransientanalysen

Das direkte Koppeln der Leistungserzeugungseinheit mit einem Hochtemperaturkugelhaufenreaktor hat eine Menge von dynamischen Aspekten. Die enge Wechselwirkung zwischen dem Reaktorkernfluss, der Turbinenleistung und dem Druckverhältnis führt zu starken Druck- und Temperaturtransienten, welche für die eher strukturellen Konstruktionsanforderungen ausschlaggebend sind. Durch das Einplanen von ähnlichen Kernrandbedingungen sowohl für die Einwellen- als auch für die Dreiwellenanordnungen, bestehen nur vernachlässigbare Unterschiede in dem Fluss der Masse durch den Kern während eines Reaktorabschaltvorgangs. Das Transientverhalten der beiden Kreisläufe unterscheidet sich jedoch wesentlich während eines Entlastungstransients. Hier wurde gezeigt, dass das Öffnen des Bypass-Ventils in einer bestimmten Sequenz ermöglicht, die Wellengeschwindigkeit in beiden Wellenausführungen erfolgreich zu begrenzen. Das Öffnen des Bypass-Ventils ermöglicht beiden Ausführungen stabile Betriebsbedingungen aufrechtzuerhalten. Dies bewirkt auch eine große Änderung des Druckverhältnisses über der Leistungsturbine und den Kompressoren in beiden Systemen, welche die Nutzwerte der Turbomaschinen stark beeinflusst. Die Hauptkomponenten in beiden Systemen werden deutlichen Druck- und Temperaturänderungen ausgesetzt. Enge Wechselwirkungen zwischen dem Kernmassenfluss, der Turbinenleistung und das Druckverhältnis des Systems führen zu diesem Ergebnis. Höhere Turbomaschinennutzwerte im Einwellensystem zeigen den Vorteil dieser Ausführung in einem Entlastungstransient. Mit einer frei laufenden Leistungsturbine wie in der Dreiwellenausführung ist die Generatorgeschwindigkeit schwerer zu kontrollieren. Hier muss die Tendenz der Leistungsturbine zu Übergeschwindigkeit durch eine komplizierte Sequenz von Kontrollaktionen verhindert werden. Zusätzlich benötigt dieses System eine Widerstandsbank mit einer Mindestdauerleistung von 10 MW_{el}, um die Übergeschwindigkeit der Leistungsturbine zu begrenzen und das Beladen der Anlage während des Ereignisses zu gewährleisten. Die durch den Ausbau des Dreiwellensystems mit einem zusätzlichen größeren Widerstand bedingte Komplexität wird höhere Kosten und Risiken mit sich bringen. Andererseits verlangt die Einwellenanlage, die leichter zu kontrollieren ist, eine sehr lange Welle und lange Rohre, was zu einem zusätzlichen Bruchrisiko beitragen kann. In dem Transient nach der Ladung ist der Heliumbestand innerhalb ca. 6 Stunden auf 40 % reduziert und kurz danach wird der Bestand auf 100% wiederhergestellt. Diese Transiente beeinträchtigt kaum die Turbomaschinenbetriebspunkte. Die Dreiwellenausführung bietet in diesem Fall eine verbesserte Betriebsstabilität, da die Kompressoren ihrer Arbeitslinie folgen, wobei sie die Flexibilität erhöhen und eine schnelle Antwort zum Ladungsanstieg anbieten. Das Einwellensystem hat eine eingebaute Begrenzung

der Kompressoren und die Turbinenwellen drehen in der Generatorgeschwindigkeit. Dies bringt dem Einwellensystem Nachteile während der Teilladungsleistung und deshalb wird empfohlen, das Verhalten der Systeme unter Verwendung von Belastungs- und Risikoanalyse zu untersuchen. Im Fall von Heliumleckage, hat sich ein schneller Druckausgleich, begleitet von einem Turbomaschinenschluss, gezeigt. In diesem Fall wird ein Abkoppeln des Generators vom Netz eingeleitet. Die errechnete Turbomaschinengeschwindigkeit wurde bis zum kompletten Stopp in beiden Einwellen- und Dreiwellenausführungen verringert.

Aufgrund von Simulationsergebnissen wird geschlossen, dass das dynamische Verhalten der Anlage über eine weite Reihe von Bedingungen und für Zeiteinheiten, die von einigen Sekunden bis zu mehreren Stunden schwanken, korrekt vorausgesagt wird. Es wurde demonstriert, dass das Kontrollsystem der Leistungserzeugungseinheit eine wichtige Rolle beim Ermitteln des kompletten Verhaltens der Anlage spielt.

Table of contents

Nomenclature

Latin Symbols

A	m^2	cross sectional area
C	-	coefficient
Cp	J/kgK	constant pressure specific heat
D	m	diameter
$Diff$	cm	neutron diffusion constant
E	kW	energy
$\dot{E}$	kW	net energy rate
e	μm	inside wall roughness
f	-	friction factor
g	m/s^2	gravitational acceleration
H	m	height
$\dot{h}$	J/kg	enthalpy
h	W/m^2K	heat transfer coefficient
I	m^2kg	moment of the shaft inertia
j	-	Colbrun factor
K	-	loss factor
k	W/mK	thermal conductivity
L	m	length
$\dot{m}$	kg/s	mass flow rate
n	-, neutrons/cm^3	constant, neutron density
P_n	kW	reactor power
p	Pa	total pressure
Q	m^3/s	volumetric flow rate
$\dot{Q}$	kW	heat transfer rate
R	J/kgK	gas constant
s	kJ/kgK	specific entropy
T	K	temperature
t	s	time
U	J/kgK	overall heat transfer coefficient
V	m^3	volume
v	m/s	velocity
W	J/kg	work
y	kg/s	mass source or sink

Greek Symbols

β	-	delayed neutron fraction
γ	-	ratio of specific heats of gas
ε	-	void fraction
η	-	efficiency
λ	1/s	decay constant
Λ	s	average neutron lifetime
ν	-	number of neutrons emitted per fission
μ	Ns/m^2	viscosity
ρ	kg/m^3	density
$\overline{\rho}$	-	reactivity
Σ_a	1/cm	macroscopic scattering absorption cross-section
ϕ	$1/cm^2s$	neutron flux density
ψ	-	pressure drop number
ω	rev/s	rotational speed

Indices

c	compressor
d	discharge
el	electrical
ex	external
f	fin side; fuel
g	generator
h	hydraulic
i	neutron group; node
j	neutron group; node
m	metal; moderator
mech	mechanical
max, min	maximal, minimal
P	primary side
shell	shell side
st	static
S	secondary side
t	turbine
th	thermal
1, 2	upstream, downstream
x	xenon

Dimensionless Numbers

Nu	Nusselt number, $Nu = \frac{hd}{k}$
Pr	Prandtl number, $\mathrm{Pr} = \frac{C_p \mu}{k}$
Re	Reynolds number, $\mathrm{Re} = \frac{\rho v D_H}{\mu}$
M	Mach number, $M = \sqrt{\frac{2}{\gamma - 1}\left[\left(1 - \frac{\Delta p}{p_1}\right)^{\frac{1-\gamma}{\gamma}} - 1\right]}$

Abbreviations

AVR	Arbeitsgemeinschaft Versuchsreaktor
API	Application Programming Interface
BWR	Boiling Water Reactor
CFD	Computational Fluid Dynamic
CMF	Corrected Mass Flow
CS	Corrected Speed
EVO	Energieversorgung Oberhausen
GBP	Bypass valve
HHT	HTR with Helium Turbine
HHV	High Temperature Reactor Test plant for HHT
HICS	Helium Inventory Control System
HP	High Pressure
HPC	High Pressure Compressor
HPT	High Pressure Turbine
HTGR	High Temperature Gas Cooled Reactor
HTR Module	Modular High Temperature Reactor
HTTR	High Temperature Japanese Test Reactor
IC	Inter-Cooler
ICS	Injection Control system
IHX	Intermediate Heat Exchanger
IPCM	Implicit Pressure Correction Method
LP	Low Pressure
LPC	Low Pressure Compressor
LPT	Low Pressure Turbine
MOC	Method of Characteristics
NDM	Non-Dimensional Mass flow
NDS	Non-Dimensional Speed
NTU	Number of Transfer Units
PBMM	Pebble Bed Micro Model
PBMR	Pebble Bed Modular Reactor of South Africa
PC	Pre-Cooler
PCU	Power Conversion Unit
PID	Proportional Integrator Differential
PR	Pressure Ratio
SAS	Small Absorber Spheres
THTR	Thorium High Temperature Reactor

1 Introduction

1.1 Introduction

Over the last few years a growing interest in advanced reactors has emerged. This interest has been motivated by the view of new nuclear power reactors that provide safety, high efficiencies, and a competitive and feasible energy source for the generation of electricity, as well as for industrial process heat applications. This resulted in the development of the Generation IV Nuclear Energy Systems Programme, in which ten countries have agreed on a framework for international cooperation and a joined research on advanced reactors. The High Temperature Gas Cooled Reactor (HTGR) is considered as one promising and attractive generation IV reactor, illustrating inherent safety performance and improved cycle efficiencies, due to high outlet coolant temperature.

Considerable attention was given to the alternative to directly connect it to a Brayton cycle gas turbine, for the economical generation of electrical power. In the prospect of emerging technologies, the high temperature modular reactor system, such as the Pebble Bed Modular Reactor (PBMR) nuclear power plant developed in South Africa for Eskom, has drawn large attention.

This work treats the nuclear power plants with the Pebble Bed High Temperature Reactor (HTR) type as a heat source and a direct Brayton cycle Power Conversion Unit (PCU), whereby helium is used as a coolant.

The prediction of the dynamic behaviour, which includes the transient course of power, pressure, temperature, mass flow and turbo-machine speed of such a plant, is of importance for several reasons. First, problems of control must be especially paid attention to as it has to be guaranteed that accidents will not lead to major failures and to the release of radioactivity. Second, the maximum pressure and temperature gradients mainly at the turbine outlet must be known for limiting the thermal stresses in the installations. Particular difficulties in the calculation of the cycle dynamics may arise in determining the dynamic behaviour of the high temperature reactor, the heat exchanging apparatuses, and the valves, as well as in coupling all transient responses when the complete circuit has to be regarded and calculated. Third, the actions of changing power output by changing the inventory of the working gas need investigation of their dynamics, in order to render possible design and optimisation of the control equipment.

Particularly for the PBMR – the boundary conditions of the plant are of importance, as the mass flow has to be taken into account and the total mass flow strongly depends on both the reactor core and the circuit helium mass flow. Furthermore, any change in helium mass flow which occurs in the cycle will generate a heat-up of the reactor core. In order to simulate the whole system, a qualified tool is needed. The code Flownex has therefore been chosen as an appropriate tool for analysing these complex simulations, which require a realistic connection of a detailed core model with the complete thermal-fluid PCU model.

With the aid of Flownex simulation tool, all points demonstrated in the primary circuit can be calculated in respect to mass flows, temperatures, turbo-machinery, generator's speed etc. Furthermore, it can be illustrated that by linking Flownex to an external code, new improved boundary values and system behaviour can be obtained for the solution of an integrated system, which consists of the core model and the PCU. Features presented by the different tools comprise of simulating the changes in the primary circuit, which occur due to load variations, accident and operational transients and disturbances. As the reactor will then be affected by the feedback from the temperature, one should be able to analyse the effects occurring in the reactor core due to reactivity effects caused by control rods movement.

Concerning the cycle configurations of the PBMR, several options exist. In this thesis, the multi shaft and the single shaft configurations have been considered for the layout of the compressors and the turbines in the PCU.

The modelling and the analysis of the plant and its vital components were obtained for both shaft configurations by using a simulation model, where the reactor core was coupled to the PCU components. This enables the design of a control system, which accounts for the loads anticipated on the components due to pressure and temperature variations in different transient scenarios.

1.2 Background on High Temperature Gas Cooled Reactors

The need to improve the efficiency and the safety features of the future power plants has led to the development of various reactor types over the years. Among the discussed concepts, the high temperature gas cooled reactor plays an important roll. Some of the most pronounced and interesting reactor systems which have embraced this concept are discussed below.

1.2.1 Reactor Systems

From the beginning, the high temperature gas cooled reactor development evolved along two main tracks, which differ in the choice how to fuel the reactor [1]. These tracks of development are the prismatic type (also known as the block type) and the pebble bed type.

In prismatic reactors, the core is composed of prismatic graphite blocks which contain the fuel compacts as shown in Fig. 1.1 [2]. It must be mentioned that the reactors developed in the United States differ from the German reactors in terms of reactor core and fuel organisation.

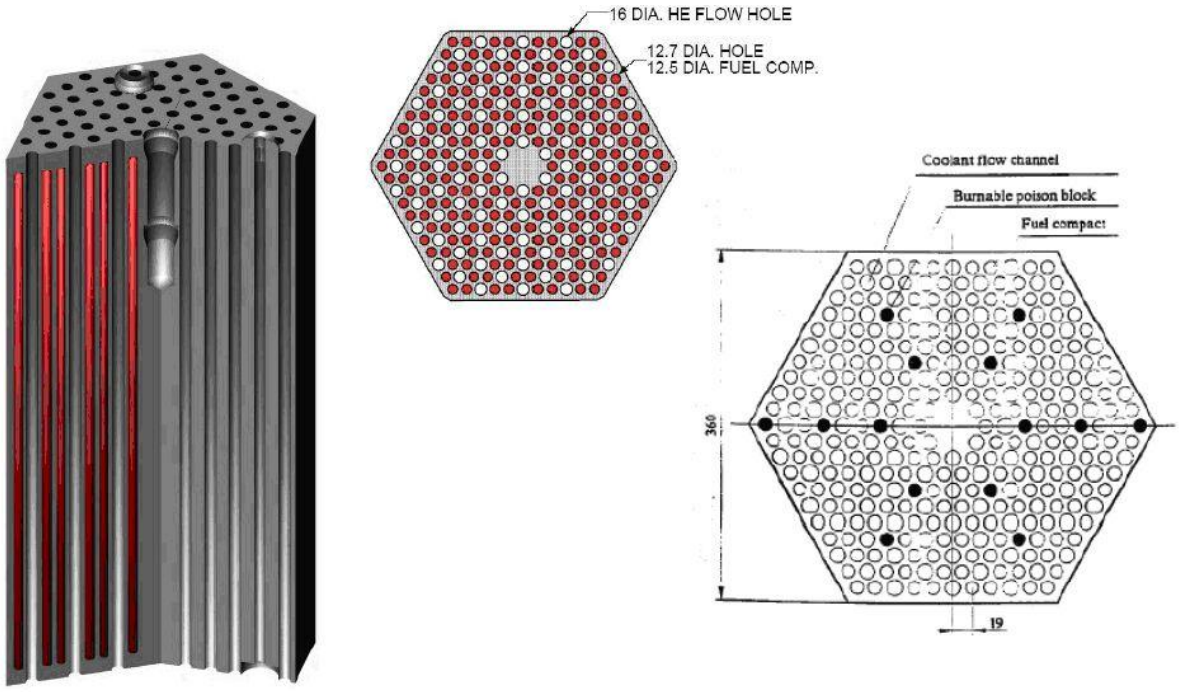

Fig. 1.1: A section through a prismatic fuel block.

The first commercial implementation was the Peach Bottom Reactor in the United State. It reached its full power in May 1967 [3], [4]. Very good operating results were achieved during the operation, before the final shutdown in 1974.

The Fort St. Vrain commercial nuclear power station with 770 MW_{th} and block fuel operated in the United States [5]. The reactor went critical for the first time in 1974 and delivered electrical power in 1976. Two years later, it reached 70% of its nominal full power [3]. Accidental water ingress in the reactor coolant system, which caused to an accelerated corrosion of the steel components led to the reactor being shut down permanently in 1989.

An important project recently initiated, which is currently under development is the Japanese High Temperature Test Reactor (HTTR). This is a block type reactor which reached its first criticality at the end of 1998, and its full power at the end of 2001. The HTTR will be used as

a test facility for fuel elements, high temperature irradiation of materials and demonstrations of industrial heat applications.

In addition, the AREVA NP has established a development project called ANTARES. The pre-conceptual design of the ANTARES HTR has been completed for a 600 MW_{th} reactor based on a block type annular core, and a coolant outlet temperature of 850°C [6]. One of the challenges set for this project has been to conduct the Very High Temperature Reactor (VHTR) for process heat for hydrogen production. This multipurpose nuclear heat source project is presently planned for operation around 2020. The attractive features of a core consisting of spherical fuel elements led to the investigation and research in the field of the pebble bed reactors by Germany, China, South Africa and Russia.

In the pebble bed core, the coated particles are embedded in spherical graphite fuel 'pebbles' with a diameter of approximately 60 mm, as shown in Fig. 1.2. A typical pebble contains some fifteen thousand coated particles. Fresh pebbles are continuously inserted into the reactor. When a pebble reaches its maximum depletion level, it is replaced with a new one. The coolant flows through the cavities between the pebbles. The 35 µm Silicon carbide layer of a coated particle acts as an extremely efficient containment. Because of its high density, this layer prevents any release of gaseous or metallic fission products outside the fuel elements up to 1600°C. The unique physics of a gas/graphite reactor in combination with the TRISO particle will therefore insure the design of an inherently safe reactor.

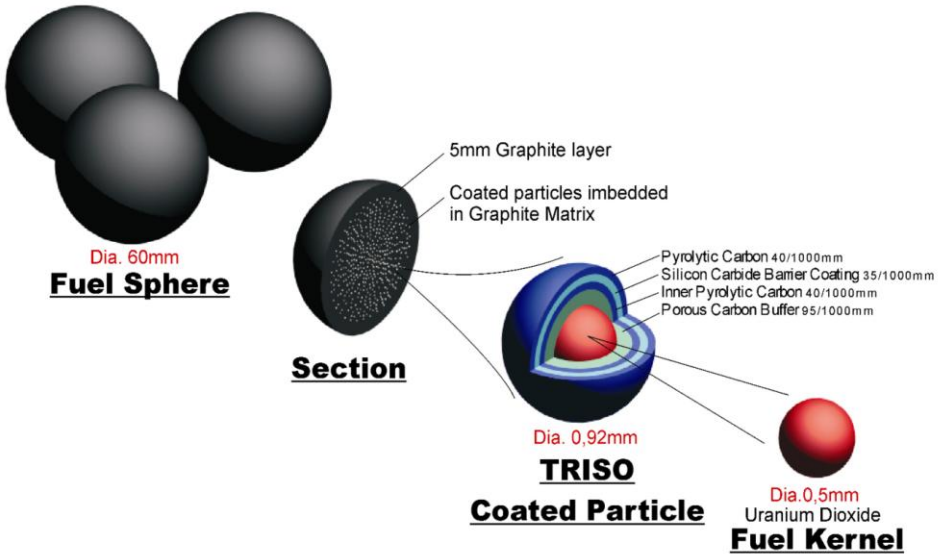

Fig. 1.2: Fuel Element Design for PBMR [7].

The attractive features of a reactor core which contains spherical fuel elements led to the investigation of the pebble bed reactors concept mainly in Europe and in the United States. The

first reactor of this kind has been developed in Germany. Among all high temperature reactors developed, the AVR has shown the longest and the most successful operation time [3]. The AVR reached criticality in August 1966 and operated until December 1988. It showed the viability of the pebble bed concept and demonstrated its reliability through physical tests, for which the plant was not initially designed. A loss of coolant flow without a scram was simulated in 1970, and a loss of coolant transient was achieved prior to the plant final shutdown [8].

Like the AVR, The THTR-300 prototype nuclear power plant in Germany was a pebble bed reactor. It included a steam cycle which generated 269 MW_{el}. This plant was shut down in 1988 after a time period of 423 days of full load operation.

1.2.2 The HTR Module

Based on the experience gained with the AVR and the THTR, the development of the HTR Module was initiated in Germany by Siemens [9]. The fuel elements were spherical, with a diameter of 6 cm as in the AVR and the THTR-300 [3].

Fig. 1.3 shows a section through the reactor and the steam generator system. Helium leaves the blower at 250°C before passing through the core, which it exits with a temperature of 750°C. The core diameter is only 3 m. Because of this limited diameter, the reactor can be shut down using the control rods, which are located in holes within the side reflector. A second design limitation is that the fuel element temperature should always be kept below this temperature. The reason is that the fission products are retained in the coated particles below 1600°C. As long as the fuel element temperature stays below 1600°C (for a limited time of 10-20 hr) [10], then all possible accidents and release of radioactive materials into the environment should be eliminated. This means that one has to layout the core and the plant around this maximum fuel element temperature of 1600°C, rather than design a core of any power and then, install auxiliary systems to cope with possible dangerous accidents. However, it is recommended to avoid even high temperatures beyond 1000°C under all operational conditions. To obtain the maximum feasible reactor power, a core height of 9.6 m was determined. The design power was thus limited to 200 MW_{th}. In the event of failure of the active cooling in the primary circuit, decay heat is removed by conduction and radiation outside the reactor pressure vessel. Due to the exploitation of inherent properties, two major dangerous situations of any nuclear reactor, i.e., the inability to remove the decay heat and the unintentional power surge due to a reactivity insertion are not existent in the HTR Module [9].

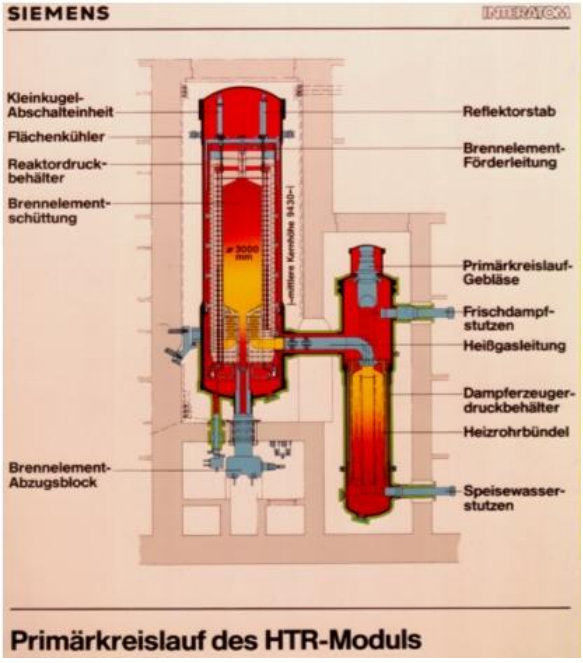

Fig. 1.3: Cross section of an HTR core unit with steam generator (SIEMENS).

The HTR Module is also suited for the generation of process heat for chemical applications. In this case, the gas exit temperature is increased to 950°C. Many years of operation of the AVR at a gas exit temperature of 950°C have shown that this is possible with the current design of the fuel elements.

1.3 Experimental Facilities

Experience gained with the design and operation of closed cycle helium turbo-machinery was obtained in Germany, South Africa, China and Japan. The Japanese project is known as the Gas Turbine High Temperature Reactor of 300 MW project.

The research and development programme in Germany was initiated in 1968 with the HHT project for electricity generation using high temperature helium cooled nuclear reactor with helium as a working fluid. The programme continued until 1982, and incorporated an international co-operation with the United States and Switzerland [11].

The programme involved two experimental facilities. The first facility known as the Energieversorgung Oberhausen (EVO II), consisted of a fossil fired heater, helium turbines and compressors and related equipment. It was constructed and operated in Oberhausen. The second facility was the High Temperature Helium Test Plant (HHV) at the research centre Jülich in Germany.

The Pebble Bed Micro Model (PBMM) in South Africa is a functional model of the PCU of the South African PBMR [12]. It was developed to gain a better understanding of the dynamic behaviour of the three shaft PBMR.

1.3.1 EVO II

The EVO II test plant was designed to provide an electrical power of 50 MW_{el} and heating for district heat of 53.5$_{th}$ MW [13]. A view of the EVO II experimental helium loop is shown in Fig. 1.4, with the two shaft design was selected for the turbo-machinery ([14], [15]).

The project was terminated due to operation difficulties which were encountered with the facility trying to fulfil the design power output. Nevertheless, a tremendous experience was gained for the helium systems and the turbo-machinery.

A detailed description of the installation, in addition to steady state and transient calculations of the complete loop, will be given in chapter 4.

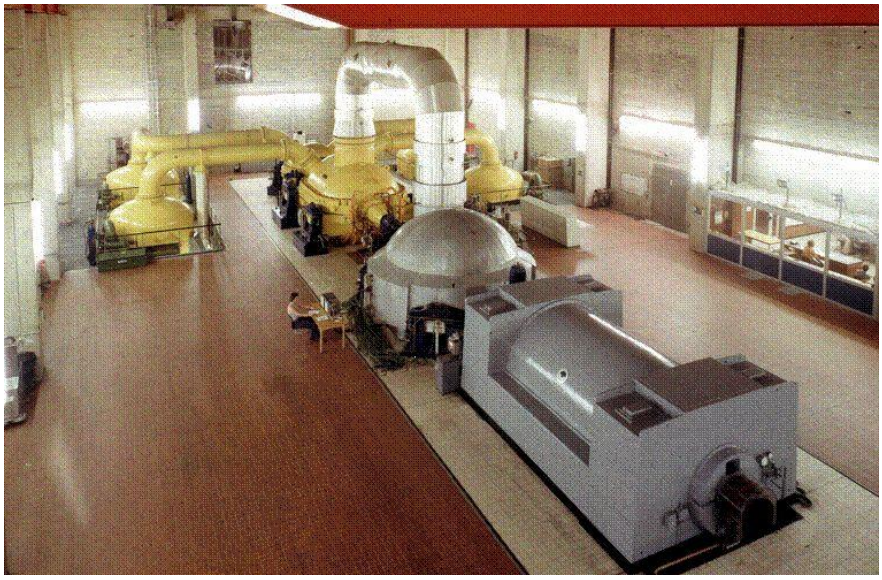

Fig. 1.4: The EVO II helium turbine.

1.3.2 The Helium Test Facility (HHV) in Jülich, Germany

The HHV test installation was built as part of the joint German-Swiss HHT project for high temperature reactor connected to a helium turbine [16]. The aim of this test installation was to develop and test large scale helium turbo-machinery and its associated components.

The HHV helium turbine is shown in Fig. 1.5.

Fig. 1.5: The HHV helium turbine, 1981.

The compressors power was 90 MW. This power was partly provided by the turbine generator with a power of about 46 MW, and the difference was supplied by a 45 MW electrical driving motor. As a result of the compressor work, helium was heated up to a temperature of 850°C, with the option to reach 1000°C for short periods. The eight stage compressor and the two stage turbine were fitted on a single shaft with a synchronous rotational speed of 3000 rpm. The maximum operating pressure was 5 Mpa, and the mass flow was approximately 200 kg/s. Hot helium could be conducted completely or partially through the test section, or bypassed back to the turbine for expansion by means of hot gas ducts with regulation valves. Helium to water cooler ensured the desired equilibrium temperature between added and removed heat. The blade feet, rotor and housing were cooled by means of a cooling or a sealing gas system. For the cooling gas system, radial-type compressors circulate the cooling helium at inlet conditions of 236°C and 4.9 MPa and outlet conditions of 5.3 MPa at 258°C. Helium mass flow of 56.8 kg/s was circulated through the compressors.

During the initial operation, oil ingress and excessive helium leakage occurred. After having overcome the initial problems, the HHV facility was successfully operated for about 1100 hours. The research and development programme which took place in this facility was successful. It demonstrated a feasible use of high temperature helium as a Brayton cycle working fluid for direct power conversion from a helium cooled nuclear reactor. In addition, the successful operation of helium turbo-machines was proven.

1.3.3 The Pebble Bed Micro Model (PBMM)

The Pebble-Bed Micro Model (PBMM) is a small-scale model, conceived to demonstrate the operability and control strategies of an early design of the South African PBMR concept [17].

The plant was designed, constructed and commissioned from January to September 2002. The experimental loop uses nitrogen instead of helium, and an electrical heater with a maximum rating of 420 kW_{th} which replaces the reactor.

Similarly to the full scale PBMR with 268 MW_{th}, the PBMM features three separate shafts for the turbine-compressor and the turbine-generator pairs. The generator is modelled by a third compressor on a separate circuit, with an additional heat exchanger which dissipates the power transferred to the fluid. Fig. 1.6 shows a schematic layout of the PBMM loop. The main components are demonstrated as following: an electrical heater, a high and a low pressure turbine (HPT and LPT respectively), a power turbine (PT), recuperator, pre-cooler, inter-cooler, high and low pressure compressors (HPC and LPC respectively), and an electric load heat exchanger.

Major operation procedures such as start-up, power variation and load rejection were demonstrated in the plant. It was furthermore shown, that the construction of the three shaft PBMR was feasible and could reach a stable and reliable operation.

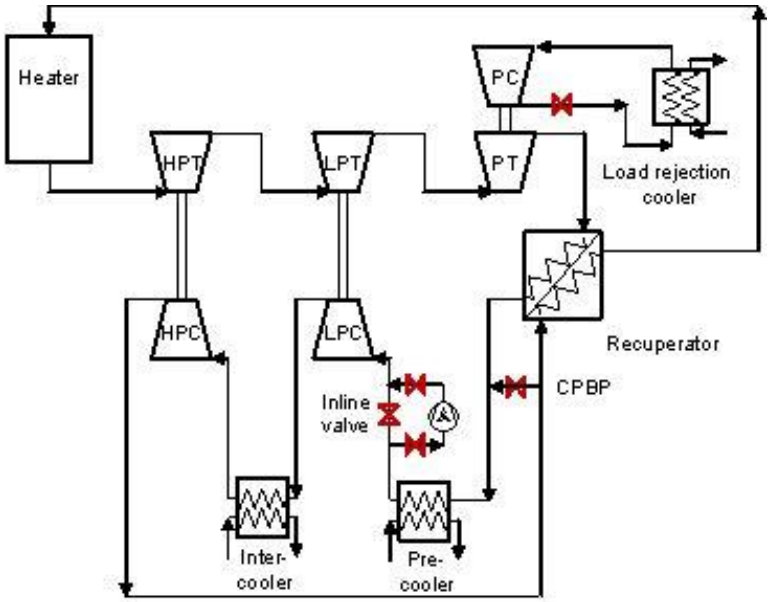

Fig. 1.6: Layout of the PBMM cycle [17].

1.4 Ongoing Experimental Research Projects

1.4.1 The HTR-10

The HTR-10 is the first important step of modular HTGR development in China. It was projected as part of the framework of China's High Technology Research and Development (R&D) Programme [5]. The objective of the HTR-10 is to verify and demonstrate the technical and the safety features of the modular HTR. The Chinese government approved the HTR-10 project in March 1992 [18].

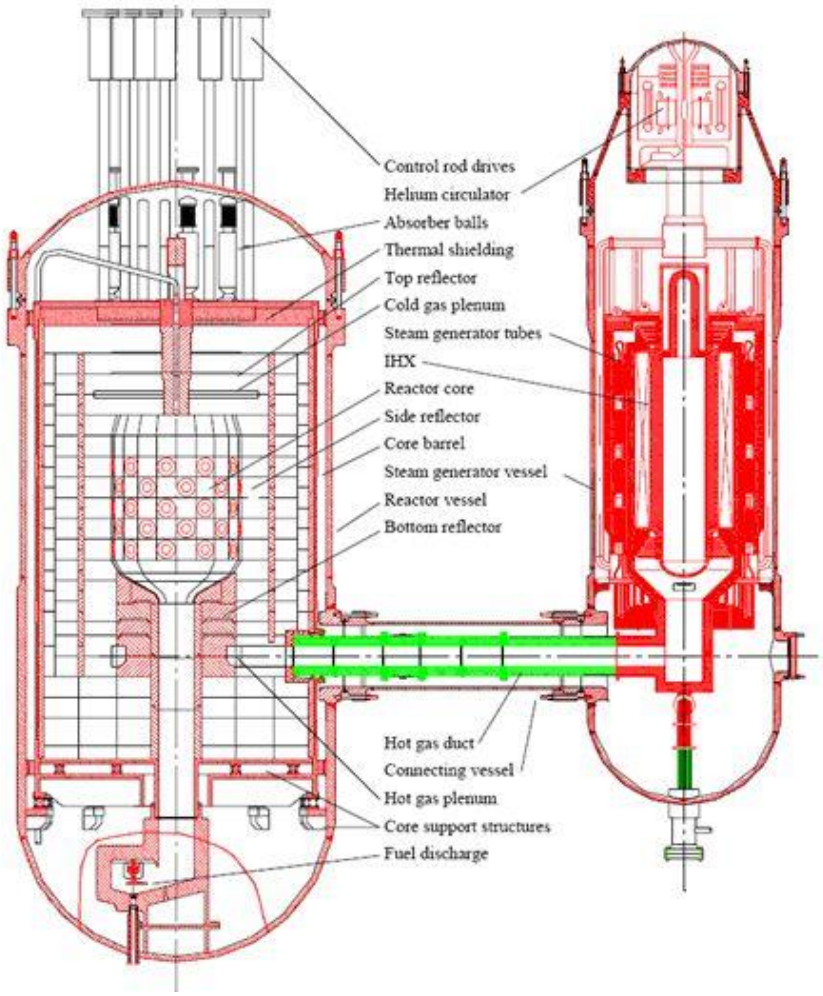

Fig. 1.7: Cross section of the HTR-10 primary circuit [20].

The design incorporates fuel pebbles with a diameter of 6 cm, as described earlier. The Pebble Bed Reactor core and the steam generator are housed in two separate steel pressure vessels. The steam generator is a once through, modular, small helical tube type. This is a unique design, in which the outer annulus contains a number of helically steam tubes generating units. Steam is generated from the high temperature helium in the primary cycle. Residual heat is

dissipated by means of passive heat transfer mechanism to the surrounding atmosphere. The project has been divided into two main phases. During the first phase a steam generator is employed, and the average core outlet temperature is limited to 700°C. At the secondary circuit, the steam generator produces steam at a temperature of 440°C and a pressure of 4.0 MPa, to provide the steam turbine-generator unit. This unit can generate electricity of about 2.6 MW_{el} at full load [19].

The research towards an inherently safe modular gas cooled reactor has shifted the interest of the HTR-10 project developers towards a combined cycle with a gas turbine-steam generator system. During the planned second phase, a 5 MW_{th} helium/nitrogen heat exchanger will be added. For research purposes this will be developed at the HTR-10 reactor, but will ultimately be included on a full-scale system, based on the modular HTR Module. Based upon investigation of both configurations, the gas turbine-steam generator combined cycle of the HTR-10 was found to be advantageous.

1.4.2 The Development of the Pebble Bed Modular Reactor

The development of improved technologies of HTGRs has led to the design of the Pebble Bed Modular Reactor (PBMR) in South Africa, as a world wide international association between the national utility Eskom, and industrial partners from the United Kingdom and the United States [21]. The PBMR aims to achieve the goals of safe, efficient and environmentally acceptable plant, with an economical generation of energy at high temperatures for electricity production and for industrial process heat applications [22].

Technological features

The fundamental concept of the reactor aims at achieving a plant which cannot cause a radiation induced hazard outside the site boundary. The peak temperature that can be reached in the reactor core is below the temperature that may cause damage to the fuel, i.e. 1600°C under the most severe conditions. Even in case of failure of the systems, which are designed to stop the nuclear reaction and remove core decay heat, the reactor is designed to stop any nuclear fission and cool down naturally. This is due to its strong negative reactivity temperature coefficient and the inherent heat removal mechanisms of conduction and convection [23]. Above all, the PBMR stands to its potential to operate as an inherently safe reactor. This concept of ‘inherently safe’ can be interpreted as the impossibility of the reactor to reach a level whereby radioactive fission products are released above predefined levels. The thermal hydraulic stabi-

lisation is achieved by having a core with a certain height-to-diameter ratio and a relatively low power density (< 4.5 MW/m^3), so that the integrated heat loss capability from the reactor exceeds the decay heat production of the core under all possible accident conditions.

The Pebble Bed reactor core is based on HTGR technology developed in Germany. This implies the use of spherical fuel elements, which have the same size and physical characteristics as the fuel, which was developed for the German HTR programme. However, instead of using the Rankine cycle power conversion followed by the HTR Module with a gas-to-steam heat exchanger; the PBMR uses a direct cycle power conversion configuration. The use of helium as a coolant, which is both chemically and radiological inert, combined with the high temperature integrity of the fuel and structural graphite, allows the use of high primary coolant temperatures of 800 to 900°C, which yield high thermal efficiencies. This enables plant efficiency of up to 42%, thus reducing the unit capital cost and the fuel cycle cost.

PBMR Design

As mentioned before, the PCU of the PBMR is based on a single loop direct Brayton thermodynamic cycle, with a helium cooled graphite moderated nuclear core assembly as a heat source ([22], [24]). The helium coolant transfers heat from the core directly to the PCU, which consists of gas turbo-machinery, a generator, gas coolers and heat exchangers. The initial design was for 268 MW_{th}, where the core geometry consisted of a dynamic central reflector column which contains dummy balls, with a diameter of 1.75 m and an effective core height of 8.5 m. This design should yield an electrical output of 110 MW_{el}. Further investigation in a later phase of the project was performed in order to test the possibilities of upgrading the power level reached with the initial design. It was found that the core thermal power could be increased to 302 MW_{th} by increasing the core height to 9.04 m. A similar study was done in order to upgrade the PCU to meet the new needs. Following this, a thorough nuclear source-term analysis confirmed that this core design would result in the release of fission products and a contamination of the system. An additional argument, which promoted the replacement of the original core design with a fixed central column, was the fact that the former ring form design would lead to strong radial outlet temperature gradients in the core. In the next stage, additional inquiry about the graphite behaviour and the core structures under irradiation was performed. It concluded in the decision to shift the core design to a core with a solid central graphite column. The new outlet diameter of the core was determined to be 3.7 m, the diameter of the fixed central reflector was 2.0 m and the core effective height was 11 m. The resulting coolant flow was 185 kg/s, and the system pressure had to be increased from

7.0 MPa to 9.0 MPa. Supplementary changes resulted at a core thermal power of 400 MW_{th}. In the same time, the design of the PCU has also been significantly changed. The three shaft baseline design has been replaced with a single shaft system, running at constant speed. In the new design, the turbine drives the Low Pressure Compressor (LPC), the High Pressure Compressor (HPC) and the generator via a speed reduction gearbox. As the Brayton cycle could now be started-up using the generator operating as its motor, the start-up blower was eliminated [24]. The early three shaft design of the PCU and the recent concept of a single shaft configuration are shown in Fig. 1.8 and in Fig. 1.9 respectively.

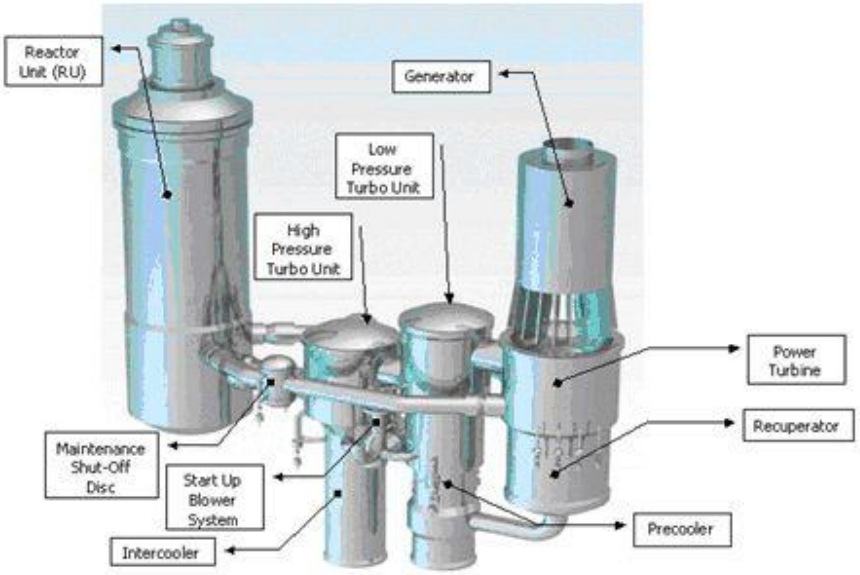

Fig. 1.8: The three shaft PBMR

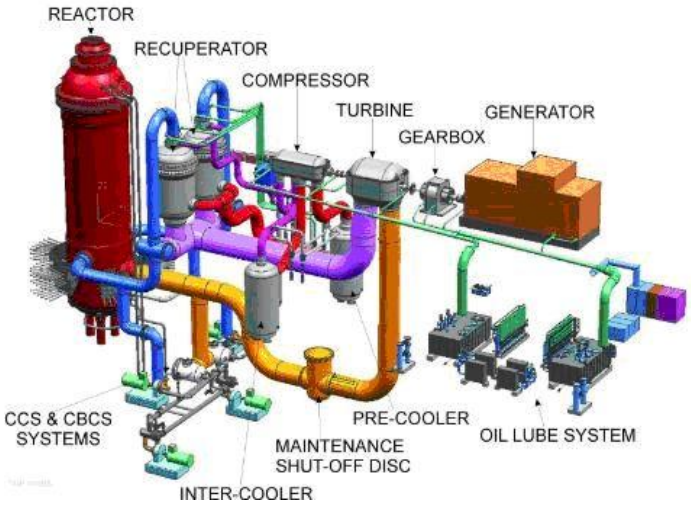

Fig. 1.9: The single shaft PBMR [7].

1.5 PBMR Thermodynamic Considerations

One of the main features of the high temperature gas cooled reactor is that it can be coupled to a variety of power conversion systems [25]. Historically, HTR plants have utilised Rankine cycle PCUs, mainly because they are technologically very similar to conventional steam plants [26]. Direct and indirect Brayton cycles, with their potential for high thermal efficiency, have been regarded for many years as attractive for HTR power conversion systems. Practically, such plants have not yet been built, mainly because the construction of a steam cycle plant involves less risk.

The choice of a thermodynamic cycle is an important step in the development of the nuclear power plant. This is due to the major influence that the cycle layout has on the cycle efficiency, the power output, the complexity of the design, the development and the construction time and the cost.

The design considerations consist of the following aspects:

- Brayton cycle versus Rankine cycle,
- Direct cycle versus indirect cycle,
- The shaft configuration,
- The choice of coolant.

These however need to be addressed based on thorough technical and economical comparisons and a simulation of all the parameters during optimisation. As the main subject of this thesis is the analysis of a system from the operating stability and the safety point view; a broad inspection, which is depicted as necessary for making a final decision, is beyond the scope of this work.

The discussion will focus on the choice of the shaft configuration and the choice of the thermodynamic cycle, which are directly related to the subject of this thesis.

1.5.1 Brayton Cycle vs. Rankine Cycle

The experience gained with helium gas turbines and with the Brayton cycle is considered very little.

An HTR with a Rankine cycle would have the advantage of using the existing HTR knowledge, and in the same time lining up with actual developments in conventional plants, whereas the Brayton cycle has only been used in experimental and tests facilities.

On the other hand, an important advantage of the Brayton cycle is that it utilises relatively compact components. Therefore, with the provision of a high core outlet temperature which is greater than 750°C, it can reach high cycle efficiencies. Moreover, it excludes the use of an additional blower to achieve forced circulation.

Furthermore, the Brayton cycle makes use of water-to-helium coolers. These could have a positive influence from an economical point of view, whereby the principal part of heat that has to be extracted by the coolers can be used in heating systems. An added advantage is that hydrogen can be exploited for additional use in the process industry.

1.5.2 Direct Cycle vs. Indirect Brayton Cycle

The direct cycle circulates working fluid exiting from the reactor core directly to the PCU and back to the core. When the turbine outlet temperature exceeds the compressor inlet temperature, the cycle efficiency can be improved by means of a recuperator type heat exchanger. The recuperator removes excess heat from the working fluid at the turbine outlet and heats up the gas before it enters the reactor [27]. In comparison with the indirect cycle, this option has the advantage of providing maximum efficiency at lower expansion ratios, thereby reducing the size of the turbo-machines. On the other hand, in the indirect cycle, the working fluid can be better exploited, especially when the reactor outlet temperature is high. In addition, the risk for water ingress in this cycle in very low.

However, in the indirect cycle, the coolant in the primary circuit circulates first through the reactor and then passes through an Intermediate Heat Exchanger (IHX) to heat the secondary cycle.

The use of an IHX is disadvantageous, as it can well limit the thermal efficiency of the indirect cycle [28], resulting in a temperature drop from the reactor outlet to the turbine inlet causing higher losses. In contrast, the coolant in the direct cycle passes directly through the power turbine, which drives the generator. The direct cycle has the advantages of higher efficiency due to higher turbine inlet temperature, and the use of fewer components as it excludes the IHX. In comparison to steam cycles, the direct gas turbine cycle with a high gas temperature of 900°C has the thermodynamic advantage of being able to make a direct use of this high upper process temperature.

1.5.3 Single Shaft vs. Multi Shaft

Two options exist for the turbo-machines configuration: a single shaft and a multi shaft configuration. The choice of the shaft configuration plays an important role together with the choice of the system layout and the turbo-machine technology.

Multi shaft

A multi shaft configuration typically consists of three shafts. This arrangement divides the compression process into two steps which are mechanically separated, allowing each section to run at a different speed.

An additional free running turbine is coupled to the generator. Having a free shaft turbine driving the generator implicates, that the speeds of both the low pressure shaft and of the high pressure shaft can be relatively high, as they are not connected to the generator and thus they are not limited by its speed. Increased cycle efficiencies can then be achieved, as the use of multiple compressors allows for higher compression ratios. Operating on a different type of work line results in a reduction in speed and pressure as the mass flow reduces. This increases the flexibility and the part load efficiency of the system, offering quick response to load increase. On the other hand, the single shaft system has only one mass flow-constraining condition imposed by a single turbine. The mass flow of the engine is then directly determined by the load shaft speed, and the compressor map consequently plays an important role in determining part load performance.

Furthermore, in a multi shaft configuration, the compressors can be driven at higher speeds than the generator. This can be done without the need for an expensive reduction gearbox, often used in the single shaft configuration. This reduces blade losses, which substantially increases the efficiencies of the turbo-machines. The three shaft design allows also for an improved maintenance of the different components because of the easier access to each. A single shaft design requires removal of the main power generator each time that maintenance is performed on any turbo-machines.

A multi shaft configuration allows for shorter shafts than in the case of a single shaft. This will further result in stiffer and tighter turbo-machine configurations, increasing the natural frequency. High natural frequency will allow for greater freedom in selecting an operating speed.

Despite of the information given here, running a three shaft configuration with a free turbine does not come without a penalty. Not having the generator connected to the shaft requires an external source to drive the compressors during start-up [27]. The lack of the breaking effect of the compressor on the generator shaft further makes the system more susceptible to over-speeding due to a sudden reduction in load. A three shaft design entails a more complex control strategy, whereby multiple bypass valves across the recuperator and the compressors must be used to compensate for loss of load operation [23].

To conclude, a multi shaft system is substantially more intricate, and this leads to additional costs and development risk.

Single shaft

The single shaft gas turbine uses a generator fitted on the same shaft together with the turbomachines for power generation. This simplifies the start-up procedure, as the generator can be used as a motor for starting. Another advantage of the single shaft configuration is its reduced risk for the shaft over-speeding in the event of loss of load, because the compressors act as a very efficient braking force for the generator shaft. As the system is less sensitive to over-speeding due to load variation, the control of the speed is easier than with a free turbine engine, as in the case of a multi shaft configuration.

A major disadvantage of single shaft systems is, however, their poor part-load efficiency and poor response to load increase. This is caused by the fact that the compressor is constrained to turn at some multiple of the generator speed (typically 3000 rpm or 50 Hz) fixed by the transmission gear ratio, whereas in the three shaft configuration only the turbine-generator shaft is running at 50 Hz. Nevertheless, the reduced efficiency can be increased by adding variable stator blades to the compressor.

On the other hand, this shaft configuration further requires longer shafts to accommodate the compressor, turbine and generator. This reduces the natural frequency of the system, thereby limiting the operating speed and reducing the cycle efficiency.

In order to improve the turbines and compressors efficiencies and to minimise their dimensions, a speed reduction gearbox is required, allowing them to run at higher rotational speeds. The gearbox and the frequency converter both lead to energy losses, which are greater during part load operation.

To conclude, the thermodynamic cycle is not affected by the choice of the shaft configuration. The design of the three shaft configuration gives shorter shafts and more degrees of freedom in the mechanical design with three shaft speeds instead of one. On the other hand, the single shaft design characterises in less stability problems and a simpler design. Therefore, the dynamics of the system are heavily affected by the choices between a single and a three shaft configuration.

Further research work is needed to find out which of the shaft options is the most promising. Hence, both shaft configurations will be investigated in this thesis based upon detailed steady state and transient analysis simulations, where they will be compared for different criteria.

1.6 Motivation of the Thesis

As the layout of the introduction showed, the PBMR and its PCU are often treated as two separate systems, which typically interact in their boundaries by providing the boundary conditions for each other. For steady state simulations this determination can be adequate. However, for transient calculations the analysis of a complete integrated system is needed. Hence, a precise simulation, which models the complete balanced plant as detailed and as accurately as possible is needed, before the final commissioning of the nuclear plant.

Furthermore, it has been pointed out that the PCU of a High Temperature Pebble Bed Reactor can consist of a variety of configurations and layouts. The thermal hydraulic behaviour of these various systems represents a key issue for decay heat removal of the core. Therefore, an effective reliable tool is needed, in order to demonstrate the modelling of a system consisting of the core, the core vessel and structures, pipes and valves, heat exchangers and turbomachines. Thus the aim of this thesis is twofold:

- To perform fully integrated plant transient analyses with detailed codes for the PCU and for the reactor core. The neutronics model as it is implemented in Flownex was not designed to facilitate detailed reactor design, but rather to do fast, integrated simulations of the reactor and the PCU. WKIND reactor core model simulates both the neutronics and thermal hydraulics aspects of the core. Therefore, the reactor core model embedded in Flownex is replaced by the 1D neutronics WKIND core model. The replacement of the core is done by creating a high-level interface between Flownex built-in component models and WKIND. This allows for the transient analy-

sis of the total system, of both three and single shaft PCUs coupled to a High Temperature Pebble Bed Reactor.

- The models obtained from the network simulation code Flownex are also compared against an experimental case. This comparison allows for further investigation of the various component models incorporated in Flowenx code, and for the validation of the models. Based on the results which include a comparison between Flownex and WKIND core models connected to the different PCU layouts, the behaviour of the complete plant can be described. It is important to note that this study also aims at creating a generic model for a single and a three shaft PCU in order to predict the boundary conditions of the reactor core model for a variety of operational and non-operational conditions. A reactor power output of 268 MW_{th} well-serves the objective of showing the dynamic behaviour of the two different cycle configurations connected to a pebble bed reactor. It is further possible to scale-up any of the systems depending on the power to be reached. This will not influence the principle thermo-dynamical behaviour of the systems investigated.

1.7 Overview of the Thesis

This thesis contains the following chapters:

Chapter 2 describes the calculation tools which were implemented to construct the layout of a single and a three shaft PCU coupled to a pebble bed reactor, as well as the EVO II system layout.

Chapter 3 describes the main component models of the PCU as they are implemented in Flownex. In addition, this chapter describes the reactor core model equations of Flownex and of WKIND. Both core models are compared in prospect of their special features accommodated from the design of the HTR applications.

Chapter 4 presents the validation and the verification of Flownex system simulation tool against the experimental data of the EVO II. Both the steady state and the dynamic calculations of the EVO II are presented. It is shown that the introduced complete system transient analysis is in good agreement with the experimental transient values of the original plant, and that very satisfying results can be obtained by choosing appropriate models and specific models performance characteristics.

Chapter 5 describes the dynamic calculations for the total plant. It is shown that a good agreement between Flwonex and WKIND core models and their respective PCUs is achieved for small reactivity changes. The design of a suitable control philosophy for the plant, especially for a load rejection, load following and a pipe leakage transient cases are presented and discussed in the context of the single and the three shaft system layouts introduced in this study. Chapter 6 presents the final conclusions of this study, as well as recommendations for the future work.

2 Main System Analysis Tools

2.1 Introduction to Computer Codes

A thermal-fluid system can consist of many interacting components, such as large scale turbines and compressors, various heat exchangers, pipes and valves, and a complex reactor core structure with helium gas which serves as energy transporting medium and as a coolant. The first of two major design challenges is to predict the performance of all components, and the second challenge is to predict the performance of the complete integrated plant, consisting of all its components and sub-systems. The solution to both is an integrated system approach, which deals with various levels of complexity and connections between the individual models. As the previous section shows, the Main Power System of the High Temperature Pebble Bed Reactor includes a number of important components. These raise the need for the selection of tools for the analysis of these complex systems.

This chapter presents the computer codes, which have been implied in order to model the various components integrated in the system. Three interconnected computer codes were used in order to fully shape a complete system model. An additional code was used for preparing the nuclear data base for the extended reactor core model. These codes are listed below:

- Flownex: steady state and dynamic calculations of the PCU and the reactor core neutronics and thermal hydraulics.
- WKIND: calculation of the core neutronics for an extended reactor core model.
- ZIRKUS: a modular programme system used for the preparation of data set for transient analyses calculations of the reactor.
- An independent software component: control of data transfer between WKIND and Flownex.

2.2 System Analysis Simulation Tools

2.2.1 Flownex

Flownex is a network simulation code, which has been developed in order to perform detailed analysis and design of complex thermal-fluid systems such as nuclear power plants. Flownex network simulation software was developed at the Engineering Faculty of Potchefstroom

University in South Africa. The idea behind Flownex was to develop a simulation programme, which would be especially useful for component design and integration, as well as for the study of the PCU of various nuclear reactor plants during operational modes and accident conditions, and the design of PID controllers and control systems. The simulation ensures complete conservation of mass, momentum and energy while accounting for non-ideal gas behaviour and compressibility effects such as choked flow through orifices. Flownex solver is based on the Implicit Pressure Correction Method (IPCM) [29]. The solver can deal with both fast and slow transients. Fast simulations on standard desktop computers allow for real time simulations. Flownex can be applied for both single and two-phase flow as well as with mixtures of fluids, for both compressible and incompressible flow. In order to insure the accuracy of the simulations run with Flownex, a wide Verification and Validation (V&V) procedure has been established. The code has been validated against other codes, as well as against experimental data [30]. The V&V of the individual components, as well as of integrated systems of components for both steady state and dynamic analyses were performed [31]. The PBMM is one of the most important experiments made to serve this purpose. The objectives fulfilled by this experimental model were demonstrating the major operational and control strategies of the PBMR, as well as demonstrating the accuracy of the computer code Flownex [12]. The validation procedure was done via comparing the results of the implemented theoretical models used in Flownex with the benchmark data obtained from various sources such as analytical data, experimental data, plant data and plant data obtained from other codes such as Spectra [32], Xnet and Star CD [33].

Flownex results were also compared with the measured results from the SANA test facility, as well as with the results of simulations calculated with the THERMIX/DIREKT code, and good comparison was obtained [34].

With the network approach, a complex thermal-fluid system is represented in form of a network of one-dimensional elements connected at common nodes [35]. Elements represent components such as pipes, compressors, turbines, heat exchangers, control valves and a pebble bed reactor core. The code can also deal with conductive heat transfer through solid structures. Flownex is able to model conduction, convection and radiation heat transfer to and from solid structures. Furthermore, solid structures can have both thermal resistance and thermal inertia, and allow also for radiation and convection heat transfer from the surface to the environment.

Compressors and turbines are modelled as grouped systems. Their performance data are obtained from interpolation of non-dimensional performance maps of pressure ratio and efficiency. The code features the ability to simultaneously solve multiple gas and liquid networks that are connected through heat exchangers. It also enables the user to construct re-usable models of complex components or sub-systems such as gas cooled nuclear reactors and heat exchangers.

The reactor and the heat exchangers are not treated as lumped systems but as distributed systems. This is done by dividing them into a number of smaller elements. The neutronics calculation in the reactor core is done using the point kinetics model. The software can also be directly linked with other external computational codes.

A detailed description of Flownex solver and its main equations, as well as a further in-depth description of the various components, will be given in chapter 3.

2.2.2 WKIND

WKIND is a 1D neutronics thermal hydraulics code, which solves the one group neutron diffusion equation in axial direction, based on a set of pre-calculated cross sections. These are weighted cross sections which depend on the material composition and on the temperature. This means, that they take into account spectrum effects from fuel, moderator, reflector, control rods, small absorber spheres (SAS) and xenon [21], [36]. The thermal hydraulics part takes into account the average axial fuel, moderator and gas temperature distribution in the core, as well as the reflector temperature distribution. An important feature is a detailed model which describes the heat transport from the fuel in the coated particle to the moderator. This plays a big role for fast transients, as the relaxation time for heat transport from the fuel is dominant for the fuel temperature and is therefore responsible for a fast negative feedback via the Doppler Effect. The cross section sets used in WKIND are calculated by the stationary HTR neutronics and thermal hydraulics system ZIRKUS [38], which was developed by SIEMENS/INTERATOM**.**

The 2D (*r*, *z*) version of WKIND is called RZKIND. The latter differs by its solver for the neutronics and the thermal hydraulics equations. The thermal hydraulics equations in the original version of RZKIND can be solved alternatively by the 2D THERMIX/KONVEK code. At the time of this study, the detailed fuel temperature model of WKIND has not yet been implemented into RZKIND. However, RZKIND can be connected to Flownex using the

same interface, as the parameters exchanged are identical in both 1D and 2D cases. By using the core models available, several transients can be treated with high accuracy by the 1D-method WKIND. Both WKIND and RZKIND were validated against theoretical calculations and experimental results, especially of the German AVR Reactor. The codes were evaluated and approved by the German licensing authorities for the HTR Module concept.

The codes WKIND and RZKIND allow for calculation of the following quasi stationary and transient simulations:

- Transients due to load changes, start-up and shut down,
- Analysis of xenon transients after load changes,
- Transients after restarting from a hot stand-by,
- Transients due to re-criticality after core heat-up accidents,
- Transients due to changes of control rod position, SAS position or loss of absorbing substances,
- Transients due to changes of coolant mass flow,
- Transients due to changes of coolant inlet temperature,
- Transients due to ingress of moderating substances such as water,
- Transients due to reactivity increase due to compression of the pebble bed.

Once these codes have been coupled with Flownex network model, the coolant inlet temperature and its mass flow rate through the core are no longer specified in the codes input. Instead, they are given by Flownex. The time dependent control rod or SAS absorber position, as well as any other external reactivity event, are specified in the core model input description. The core outlet temperature and power will be transmitted to Flownex network model. Any kind of action initiated by the reactor protection system can be formulated by the core model input description, for example: scram caused by a very high reactor power or by exceeding the maximum outlet temperature. This is done by using an interface created between WKIND core model and Flownex, or by using the input data tables of diverse Flownex components with a predefined set of conditions for a specific transient. These features allow for modelling a realistic simulation of diverse operational and accident transients, which can be formulated and executed by the coupled Flownex-WKIND or Flownex-RZKIND model. A pre-condition for a successful coupled calculation is a consistency of the core parameters and the network parameters for the initial conditions of the transient, and a synchronous solution of both the core model and the network equations.

2.2.3 ZIRKUS

The modular system programme ZIRKUS [37] was developed by INTERATOM/SIEMENS. It was designed for the realisation of various reactor physics calculations for HTR cores with pebble fuel. The programme ZIRKUS mainly consists of function modules, a general data-base and a control module for the execution of a single or a sequence of modules. These sets of modules allow for the calculation of the multi group neutron diffusion equation up to twenty groups, for the calculation of weighted cross section data for core and reflector, for the calculation of pebbles flow through the core, the core refuelling and the fuel burn-up. These must be calculated by a detailed model, taking into account the coolant flow through the reflector and the pebble bed core. The flow data chart from ZIRKUS to WKIND is shown in Fig. 2.1. The input data needed for WKIND (and RZKIND) is the cross section dependency data file.

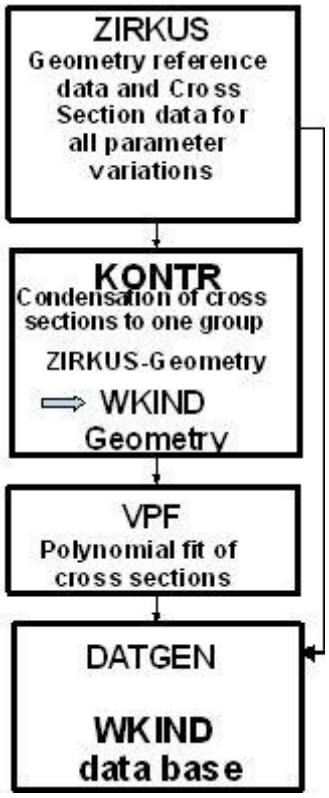

Fig. 2.1: Flow chart of the cross section set for transient calculations done by WKIND [38].

The modules contained in ZIRKUS are used for performing the following tasks [38]:

- Design of the first core, the transition core and the equilibrium core,
- Preparation of cross section data for transient calculation, with temperature dependencies from fuel, moderator, reflector, control rods movement and xenon,

- Preparation of decay heat distribution in the core for transient thermal hydraulic calculations, such as loss of coolant and loss of forced circulation accident.

For the preparation of cross sections, a variety of tasks need to be performed. The calculation of the equilibrium core is done first, followed by the calculation of the temperature change by parameters variation. For each parameter, the neutron spectrum is calculated and the diffusion equation is solved. The solution is used as the reference case for the transient calculation. Once ZIRKUS has completed the cross sections pre-calculations procedure, the cross sections are being condensed in the WKIND data file. For every axial mesh in WKIND, the temperature dependencies from fuel, moderator, control rods position and xenon, which represent the deviation from the reference case, are contained in a single parameter set. The calculation procedure is done for every time step and for each mesh.

In WKIND model, changes in the flux shape due to, for example, control rods movement, are taken into account while performing dynamic calculations. The use of appropriate reactivity coefficients in Flownex core model can correctly predict the global behaviour of the core even by using the point kinetics model. However, maintaining the same flux shape is disadvantageous for strong reactivity transients. Hence, an extended core model such as WKIND, which can treat more complex effects in the core, is needed for achieving the correct solution.

Fig. 2.2 shows the thermal flux distribution of the PBMR 268 MW_{th} with a central floating column. This is a fuel free inner column, which serves as the moderator.

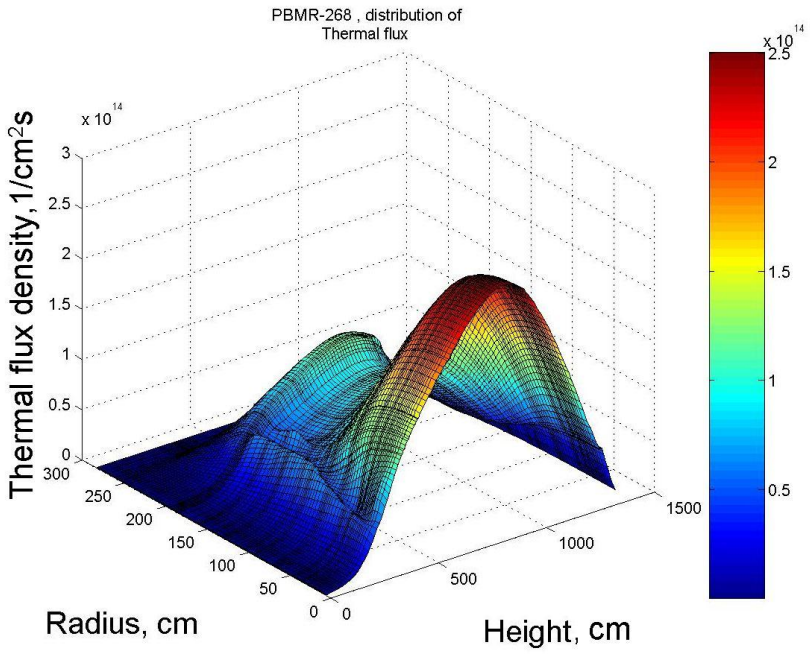

Fig. 2.2: Distribution of the thermal flux density for the PBMR 268 MW_{th}.

The reactor core presented here will be used in chapter 5 to perform the calculations, in order to compare the two different core models. The reference solution has been given in a 2D coordinate scale (*r, z* geometry). Fig. 2.2 is an example of a typical flux distribution of an equilibrium core, whereby the thermal flux has an absolute maximum in the centre of the fuel free region and a local maximum in the reflector. In the central column of the core, the fast neutrons are being thermalised. These thermal neutrons are not absorbed because of the low absorption of the graphite under high temperatures. That is the reason for the high neutron flux density seen in the centre of the core, and for a lower peak in the reflector. The reflector is also characterised by low absorption of the thermal neutrons, and by additional losses caused by streaming of the neutrons from its outer boundary.

WKIND core model uses effective cross sections for the temperature and the space dependency. An example is shown in Fig. 2.3.

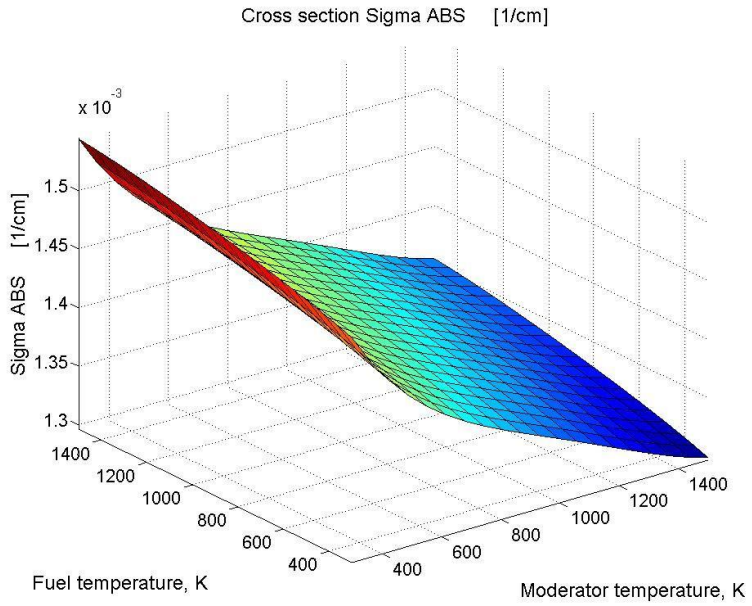

Fig. 2.3: The absorption cross section as a function of fuel and moderator temperature.

Here, the cross section as a function of moderator and of fuel temperature at a certain location is shown. The effective macroscopic cross section depends on the neutrons spectrum and on the temperature, via the Doppler Effect. The neutron spectrum depends on the graphite temperature and on the fuel burn up. High fuel temperatures together with high burn up in the fuel

zone are responsible for the resonance absorption of ^{238}U and for the hardening of the spectrum[1].

This is an example for a single parameter set in ZIRKUS. A set of cross sections should be prepared for the discretised sub-division of the core which is done in the WKIND. This implies that the solution calculated by the detailed WKIND core model will greatly differ from the solution of the point kinetics model in Flownex.

2.2.4 Coupling of Flownex PCU Model with an Alternative Core Model

A system code consisting of Flownex and of the neutron kinetic/dynamic code WKIND has been created through the use of an independent software component, a so-called connector [36], [40]. The main goal was to develop a software solution, which enables data transfer via coupling between the two applications. This is performed by implementing an external coupling method, whereby information is exchanged across the boundaries of the two coupled codes. The coupling of two codes resulted in improved boundary conditions and system behaviour via exchanging Flownex core model by the more detailed WKIND core model.

The basic coupling technique is a time step based data exchange. Data is transferred after each WKIND time step, and Flownex then adapts to it. After a steady state has been reached by both programmes, a time step is calculated by WKIND. At the end of this time step, the output data from WKIND and the current Flownex data is processed and passed as the input data for the next Flownex time step. Flownex then continues the simulation until the Flownex time is the same as WKIND time. The output data of Flownex is used to update WKIND. After each time step, both codes are interrupted, so that the data can be read from the coupling component. In order to enable the time step based data exchange, the participating codes have to provide suitable interfaces that can be used within a software component. Flownex and WKIND provide different interfaces, which are described as following:

- **Flownex:** Flownex uses a memory map file for data transfer with external programmes, and events synchronisation is provided by Windows API (Application Programming Interface). This allows for a direct interface with Flownex, without the need

[1] The absorption in thermal energies tends to remove low-energy neutrons before they come to equilibrium with the system. Since neutrons slow down into the thermal region from higher energies, the result is an increase in the average energy of the thermal neutrons. The neutrons distribution in this case is said to be absorption hardened [39].

to alter the Flownex source code. The input and output variables of the memory map file are specified in the External Controller in Flownex. The plant input variables are the parameters that will be controlled by the external controller. Conversely, the plant output variables are parameters passed to the external controller for further processing.

- **WKIND:** The interface for data exchange provided by WKIND is a file based mechanism. WKIND contains the input data file for the transient set. This file contains predefined actions such as control rod movement and scram criteria. A character at the beginning of the file indicates which of the applications, WKIND or Flownex, is active.

The data transfer for the coupling has been organised such that Flownex supplies the core inlet temperature, the helium mass flow and the time step size. These are used for generating the input for WKIND. In return, Flownex receives the value of the heat transferred to the helium, which is calculated by WKIND. In order to establish the coupling, a substitution of the Flownex core with another element was required. With the indirect coupling method [41], the reactor core incorporated in Flownex was replaced by a pipe with losses, which has about the same cross sectional flow area as the reactor simulated by Flownex. The boundary conditions for the next time step are the heat transferred to helium calculated by WKIND and the pipe pressure drop which was calculated by Flownex. This is demonstrated in Fig. 2.4.

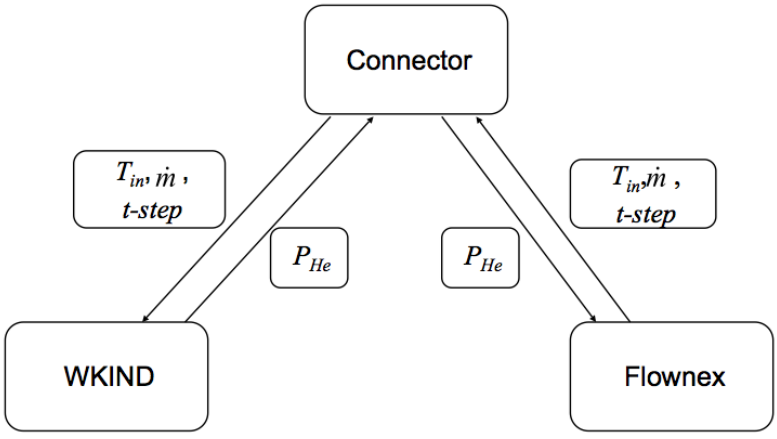

Fig. 2.4: Calculation procedure of a coupled simulation of Flownex and WKIND done via a connector. The parameter T_{in} represents the core gas inlet temperature, $\dot{m}$ is the helium mass flow rate through the core, *t-step* is the time step size and P_{He} is the thermal power transferred to the helium.

The data set for WKIND core model are contained in the programme's input file. The input file defines a linear or a quadratic polynom as a function of time. The parameters changed in

the input file during reactivity transients describe the control rods' movement. At each time step, WKIND core model calculates the heat-up of the helium coolant. The simulation of the coupled system begins with the initiation of Flownex transient simulation, which runs until the initial stationary conditions have been satisfied. In parallel, WKIND, which calculates also the stationary initial conditions, is started. Hereafter the next time step is calculated by both WKIND and Flownex alternately according to the procedure described. Updating the characteristics values of WKIND core model and of Flownex PCU after every time step eliminates the need for an iterative procedure when analysing transients.

3 Energy Conversion System Simulation Models

3.1 Flownex Network Approach

The system which has to be simulated consists of both the Pebble Bed Reactor core and the PCU, which consists of several sub-models corresponding to the various plant components. The variables which are of interest are temperatures, pressures, mass flows and rotational speeds of the shafts. Therefore, the processes which must be modelled are transformation of energy, energy storage and transport of mass, energy and momentum in all components.

Complex flows can be solved by using large-scale CFD codes. However, a CFD analysis requires complex definition of the problem, and is not well suited for a larger system where numerous variables need to be adjusted in order to reach an optimum design [42]. This, in combination with the immense computational efforts needed for modelling with a CFD code, calls for the construction of a simplified model.

The most important assumptions which Flownex is based upon, and which are used to simplify the solution of a complex thermal fluid network are discussed below.

1. **One dimensional treatment of the flow path -** Flownex employs a one-dimensional modelling methodology. Using average flow conditions across the flow area simplifies the problem to great extent. This implies that the flow velocity, the pressure and the fluid properties across the flow area are equal to the average values calculated for any cross section and vary only in the direction of the flow. A one-dimensional treatment does not capture precisely what happens inside all different components. However, as the model focuses on the interactions between various components rather than on the detailed behaviour of a component, a one-dimensional treatment of the flow is sufficient.
2. **Discretisation of the flow path -** the flow path in the components is divided into sections. These represent so called thermal nodes, which are small control volumes assumed to be perfectly mixed, and to have a constant cross sectional area. For these control volumes, the mass and the energy conservation equations are solved. The mass flow between these control volumes is determined by solving the momentum conservation equation.
3. **Point kinetics model -** the behaviour of the reactor is modelled by taking into account the relation between input conditions, control rods position and the outlet temperature. This

implies that the reactor's behaviour is regarded only in order to analyse its interaction with the PCU. This means that the reactor uses 0D point kinetics.

3.2 Flownex Flow Model and Governing Equations

The analysis of the network is based on the numerical solution of the governing equations of fluid dynamics and heat transfer. The numerical method mentioned, described elsewhere with reference to single pipe lines, is known as the Implicit Pressure Correction Method (IPCM) [29]. Following is a brief explanation of Flownex solution of the partial differential equations of mass, momentum and energy conservation solved to obtain the mass flow, pressure and temperature distributions through the complete network.

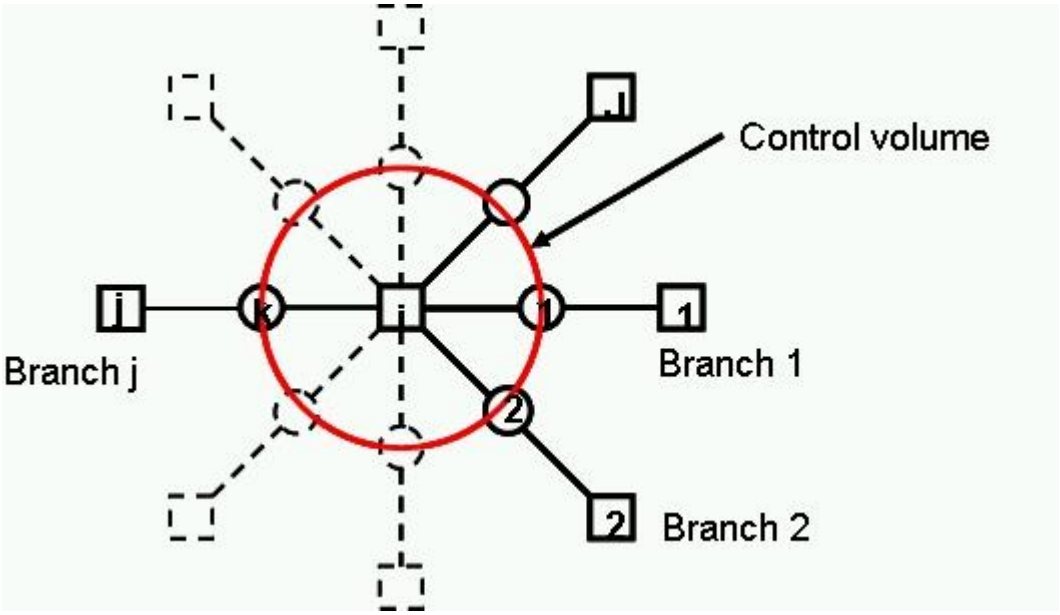

Fig. 3.1: General node with neighbouring nodes connected through branch elements [43].

In Fig. 3.1, the general flow-node i with J branches is illustrated. The figure further demonstartes, that the network is subdivided into a number of control volumes. There, the conservation of mass and energy apply.

The continuity equation for node i in Fig. 3.1 can be expressed by:

$$V_i \frac{d\rho_i}{dt} = \sum_{j=1}^{J} \rho_j Q_j s_j + y_i \tag{3.1}$$

s_j = 1 if the positive flow direction is defined as the flow from node j to node i,

s_j = -1 if the positive flow direction is defined as the flow from node i to node j,

ρ_i = average density at node i [kg/m^3],

ρ_j = average density in element j [kg/m^3],

Q_j = volumetric flow rate in element j [m^3/s],

y_i = mass source at node i [kg/s],

V_i = volume of control volume centred at node i [m^3].

The total energy balance (including internal, kinetic and potential energy) for the node i can be written as:

$$\frac{d(m_i\dot{h}_i)}{dt} - V_i\frac{dp_i}{dt} = \sum_{in,j}\left[s_j\dot{m}_j\left(\dot{h}_j + gz_j + \frac{v_j{}^2}{2}\right)\right] + \sum_{out,j}\left[s_j\dot{m}_j\left(\dot{h}_i + gz_i + \frac{v_i{}^2}{2}\right)\right] + \left(y_i{}^+ - y_i{}^-\right)\left(\dot{h}_i + gz_i + \frac{v_i{}^2}{2}\right) + \dot{E}_i \tag{3.2}$$

$y_i{}^+$ = positive (inflow) mass source at node i [kg/s],

$y_i{}^-$ = negative (outflow) mass source at node i [kg/s],

m_i = mass of fluid in control volume centred at node i [kg],

$\dot{h}_i$ = enthalpy [kJ/kg],

z = elevation [m],

g = acceleration of gravity [m/s^2],

v = velocity [m/s],

$\dot{m}$ = mass flow rate [kg/s],

$\dot{E}$ = net energy rate $\dot{Q}$ - $\dot{W}$ [kW],

$\dot{Q}$ = heat transfer rate [kW],

$\dot{W}$ = work transfer rate [kW].

where

The momentum balance for element *j* can be written in the following general form as:

$$f(\rho_j, Q_j) + \frac{\rho_j \Delta x}{A}\frac{dQ_j}{dt} + s_j(p_i - p_j) = 0 \tag{3.3}$$

where

Δx = length of element [m],

A = average cross sectional area [m^2]

p = pressure [kPa].

$f = f(\rho_j, Q_j)$ such as the Darcy Weisbach equation for a pipe element, is an element specific function, which gives the frictional pressure drop in terms of both density and volumetric flow rate. An element specific function can be given in the form of empirical models, such as a pump or a fan curve, in the form of a compressor or turbine performance characteristics, or in the form of the pressure drop through a heat exchanger etc.

The methods for solving the set of equations written above can be broadly classified as explicit, such as the Method of Characteristics (MOC) [44] and the Lax-Wendroff method [45], or as implicit. Although explicit methods are suitable for the types of flows for which they were developed, they often suffer of limitations when applied to other types of flows.

The explicit methods for the analysis of transient flows in networks focus mainly on specific types of flows, such as liquid flows, gas flows and flows in pipelines, as opposed to flows through non-pipe components, such as pumps and valves, and isothermal flows.

Explicit methods are generally simpler to programme and faster than implicit methods, and are therefore suitable for solving fast transients. However, the stability of explicit methods is governed by the relationship between time step Δt to distance Δx, which implies that Δt will be determined by the shortest time increment in the system. Therefore, such methods become very slow when solving steady state or slow transient problems, when the solution of numerous time steps is required. For example, the Method of Characteristics initially developed to analyse fast transients in liquid pipelines. Although the method has been extended to additionally deal with isothermal gas flows, the requirement for strict adherence to the time step-distance relationship becomes a serious limitation in the cases of non-isothermal gas flows, slow transients in gas pipelines and networks that comprise of different types of fluids such as heat exchanger networks. In the case of non-adiabatic gas flows, the sonic velocity is not constant, which implies that for increments with fixed length, the required time step will vary across the network. In the case of slow transients, many time steps are required, and this slows down the simulation. In the case of heat exchangers, the same length of increment must be used in the hot and the cold sides. If the sonic velocity of the two fluids differs, different time steps will be required for the hot and the cold stream, which is unacceptable.

The implicit method is particularly suited for the analysis of gas networks, where inertia forces are not as important as storage effects. Although the method is formulated in such way that the relationship between time step and length increment can be relaxed, when applied to water hammer problems it is necessary to adhere the time step-distance relationship, in order to maintain a satisfactory level of accuracy. Since the implicit method requires the simultaneous solution of all unknown variables in the system at each time step, the method can become very slow when analysing fast transients such as water hammer.

For designing plants such as the High Temperature Pebble Bed Modular Reactor, implicit methods are especially suitable for the majority of analyses required. Hence, the approach selected here is the implicit one, bearing in mind that an efficient solver for the simultaneous equations is required to avoid simplifying assumptions that will decrease accuracy. The key features of the present method are that it can deal with both pipe and non-pipe elements and it can deal with both fast and slow transients. The method uses a time step weighting factor to balance accuracy and stability.

3.3 Major PCU Components and Their Behaviour Modelled in Flownex

3.3.1 Pipes

Pipes are modelled in Flownex as distributed systems by dividing them into a number of smaller elements. Primary pressure losses are calculated with the Darcy-Weisbach equation, or with an adapted version of the equation in the case of compressible flow. Secondary losses are modelled using a loss factor.

The required input includes loss factors for flow through expansions and contractions, flow around elbows and losses at a pipe inlet and outlet. Other parameters include the length, area or outer and inner diameter, the pipe roughness and the number of parallel pipes. The roughness is used to calculate the friction losses at Reynolds numbers prevailing with time. Pipe elements can also be sub-divided into increments, depending on the degree of accuracy which is required.

Pressure drop

In the case of transient flows, the total pressure drop for incompressible flow through pipes is modelled as

$$\Delta p = \left(f \frac{L}{D} + \sum K \right) \frac{\rho v^2}{2} + \rho L \frac{dv}{dt} \tag{3.4}$$

where

f	=	Darcy friction factor [-],
L	=	pipe length [m],
D	=	pipe diameter [m],
ΣK	=	sum of loss factors of secondary loss components such as bends, valves and junctions [-],
v	=	mean velocity based on pipe diameter [m/s].

The Darcy friction factor for laminar flow (Re<2300) through a circular pipe or a conduit is

$$f = \frac{64}{\mathrm{Re}} \tag{3.5}$$

where Re is the Reynolds number based on the inside diameter of the pipe [46].

The Darcy friction factor for turbulent flow can be calculated using

$$f = \frac{0.25}{\left[\log\left\{(e/3.7D) + (5.74/\mathrm{Re}^{0.9})\right\}\right]^2} \tag{3.6}$$

where e is the mean wall roughness [μm].

The equation is valid for the ranges:

$10^{-6} \le e/D \le 10^{-2}$

$5000 \le \mathrm{Re} \le 10^8$

In the region $2300 \le \mathrm{Re} \le 5000$, a linear interpolation between equations (3.5) and (3.6) is used to calculate the friction factor [47].

Heat transfer

The laminar surface heat transfer coefficient for pipes and ducts with a circular cross section is derived from the Nusselt number Nu given by [48]:

$$Nu = \frac{hD}{k} \tag{3.7}$$

where:

h	=	heat transfer coefficient [W/m^{2}K],
D	=	diameter [m],
k	=	thermal conductivity [W/mK].

In the case of laminar flow, the Nusselt number is constant, and its value depends on the shape of the cross sectional area and on whether the heat transfer occurs at constant wall heat flux or at constant surface temperature. In the case of laminar flow through circular cross sections of pipes and ducts Nu = 4.364.

In the case of turbulent flow, Nusselt number is given by the Dittus-Boelter equation [48]:

$$Nu = 0.023 \mathrm{Re}^{0.8} \mathrm{Pr}^{n} \tag{3.8}$$

where n = 0.4 for heating, and n = 0.3 for cooling.

3.3.2 Valves and Orifices

All valves can be modelled either as a valve with its characteristics entered as data sets, or as restrictors (orifices), if the characteristics are not available. If the characteristics are known, it is possible to interpolate values from the pressure drop to flow rate curves supplied as input data.

The pressure loss relationships for valves and orifices are valid up to a Mach number of unity. Flownex can even predict the flow rates at supercritical pressure ratios when the flow is choked. This is important when simulating abnormal situations, such as a blow-down rupture in a pipe.

Orifices

Orifices are typically used to model leak flows. These flows are modelled with an RD (Restrictor with Discharge Coefficient) element. A restrictor is described by a discharge coefficient, a diameter and an equivalent number of orifices representing the number of valves. The diameter consists of the maximum outer diameter, when a minimum flow has to be maintained. When valve characteristics are available, the parameters are obtained through interpolation for a specific valve opening.

The total pressure drop for compressible flow through restrictors is given by

$$\Delta p = p_1 \left(1 - \frac{p_{st}}{p_1} \right) \tag{3.9}$$

where p_1 [Pa] is the upstream total pressure and p_{st} [Pa] is the static pressure in the throat of the restrictor.

The ratio of static pressure drop to upstream total pressure is given by

$$\frac{p_{st}}{p_1} = \left(1 + \frac{\gamma - 1}{2} M^2\right)^{\frac{-\gamma}{\gamma - 1}} \tag{3.10}$$

where

M = Mach number in the throat [-],

γ = ratio of specific heats [-].

Substitution of Eq. (3.9) into Eq. (3.10) using gas dynamics relationships for an ideal gas, leads to the following equation for the Mach number in the throat, which can be expressed in terms of $\Delta p / p_1$:

$$M = \sqrt{\frac{2}{\gamma - 1}\left[\left(1 - \frac{\Delta p}{p_1}\right)^{\frac{1-\gamma}{\gamma}} - 1\right]} \tag{3.11}$$

where γ is the ratio of specific heats.

The mass flow rate through restrictors is given by

$$\dot{m} = C_D \rho v A \tag{3.12}$$

where A [m^2] is the area of the throat and C_D is the discharge coefficient.

At very low ratios of the upstream total pressure and the pressure in the orifice throat ($\Delta p / p_1$), compressible fluids behave similarly to incompressible fluids. Under such conditions, the sizing equations for compressible flow can be taken as the standard hydrodynamic equations for Newtonian incompressible fluids. However, an increase in the values of ($\Delta p / p_1$) results in compressibility effects, which require a modification of the basic equations using correction factors. The equations for compressible fluids are for use with gas or vapour flows, and are not intended for use with multiphase streams such as gas-liquid, vapour liquid or gas-solid mixtures. The mass flow through a control valve is given by the ISA standard-75.01 1985 (Flow Equations for sizing Control Valves).

3.3.3 Heat Exchangers

Pressure drop

The primary pressure losses through heat exchangers flow passages are calculated with the Darcy-Weisbach equation (see section pipes).

Heat transfer

Heat transfer in the heat exchangers is calculated using the three-point temperature model in the cross flow direction. The three points are the average hot stream temperature, the average temperature of the metal separating the hot and the cold streams and the average cold stream temperature as shown in Fig. 3.2.

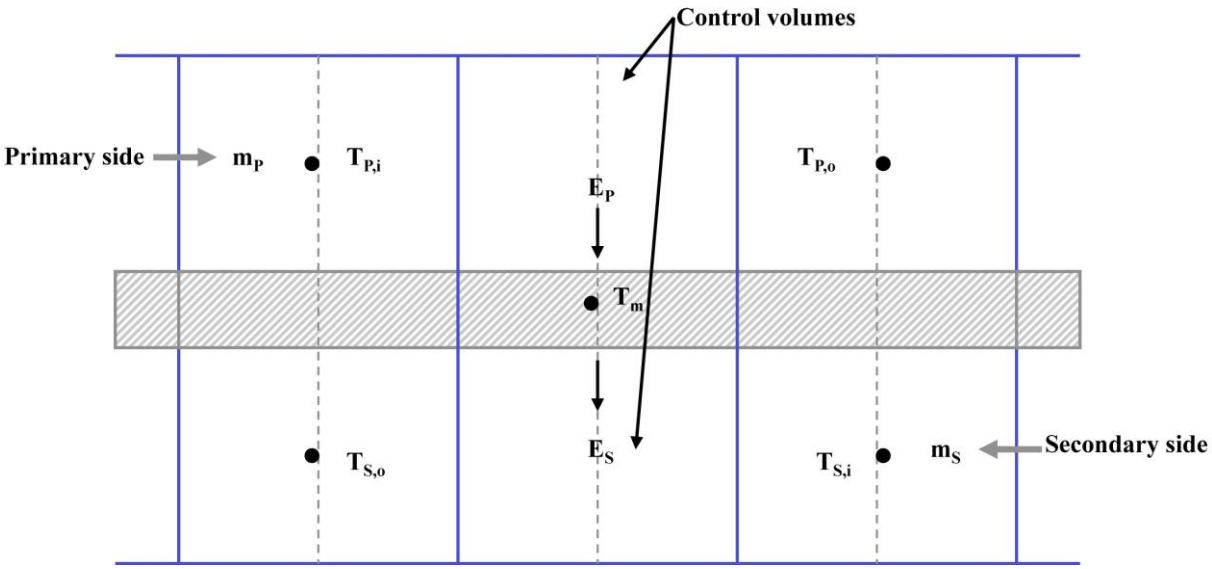

Fig. 3.2: Discretisation of a counter flow heat exchanger.

The subscripts in Fig. 3.2 denote the following:

P	=	primary side,
S	=	secondary side,
m	=	metal,
P,i	=	primary side control volume inlet,
P,o	=	primary side control volume outlet,
S,i	=	secondary side control volume inlet,
S,o	=	secondary side control volume outlet.

Consider the control volumes shown in Fig. 3.2. The governing equation for heat transfer in a heat exchanger is given by

$$\frac{d(\dot{m}C_P T_m)}{dt} = E_P - E_S \tag{3.13}$$

where

$$E_P = A_P U_P \left(0.5(T_{P,i} + T_{P,o}) - T_m\right) \tag{3.14}$$

and

$$E_S = A_P U_S \left(T_m - 0.5(T_{S,i} - T_{S,o})\right) \tag{3.15}$$

The overall heat transfer coefficients are given by

$$U_P = \frac{1}{\frac{1}{\eta_{f,P} h_P} + \frac{A_P}{A_m}} \tag{3.16}$$

and

$$U_S = \frac{1}{\frac{1}{\eta_{f,S} h_S}\frac{A_P}{A_S} + \frac{A_P}{A_m}} \tag{3.17}$$

where:

A_P = heat transfer area of the primary side [m^2],

A_S = heat transfer area of the secondary side [m^2],

A_m = heat transfer area of the wall separating the primary and the secondary side [m^2].

The surface heat transfer coefficients λ_P and λ_S, can be calculated by either using the Nusselt number calculated by the Dittus-Boelter correlation, or by the Colburn *j* factor.

The Colburn factor *j* depends on the specific heat exchanger geometry and is found in the literature [49] for different geometries, for a range of Reynolds numbers.

Pre-Cooler and Inter-Cooler

Pressure drop

Friction factors for calculating the pressure losses through the shell side of a pre-cooler and an inter-cooler are obtained from data published in the literature [49].

The pressure drop on the tube side is given by

$$\Delta p = \left(f \frac{L}{D} + \sum K \right) \frac{\rho v^2}{2} + \rho L \frac{dv}{dt} \tag{3.18}$$

whereas the pressure drop on the shell side is given by

$$\Delta p = \frac{4 f L}{D_h} \tfrac{1}{2} \rho v^2 + \rho L \frac{dv}{dt} \tag{3.19}$$

where

f = friction factor given as a function of Reynolds number [-],

v = mean velocity based on pipe diameter [m/s].

The hydraulic diameter is calculated as

$$D_h = \frac{4LA_{\min}}{A_{shell}} \tag{3.20}$$

where

A_{min} = minimum through flow area on the shell side [m^2],

A_{shell} = shell side heat transfer area [m^2].

Heat transfer

The shell side surface heat transfer coefficient is determined from a user specified curve, which provides the $StPr^{2/3}$as a function of the Reynolds number, where St is the Stanton number and Pr is the Prandtl number [50].

3.3.4 Compressors and Turbines

Compressors

Compressors performance is usually expressed in terms of pressure ratio (PR) and efficiency as functions of non-dimensional mass flow and non-dimensional speed. The reason to it is that at high Reynolds numbers, the pressure becomes insensitive to the Reynolds number.

The pressure ratio of a compressor is defined as the ratio of the total pressure at the compressor outlet (P_2) divided by the total pressure at the inlet (P_1). Hence

$$PR = \frac{P_2}{P_1} \tag{3.21}$$

The isentropic efficiency of a compressor is defined as

$$\eta = \frac{C_p T_1 (PR^{(\gamma-1)/\gamma} - 1)}{W} \tag{3.22}$$

Where W is the work done on the fluid, γ is the ratio of specific heats and T_1 is the inlet temperature [K].

The non-dimensional mass flow (NDM) and speed (NDS) are defined as

$$NDM = \frac{\dot{m}\sqrt{RT_1}}{p_1 D^2} \tag{3.23}$$

$$NDS = \frac{\omega}{\sqrt{RT_1}} \tag{3.24}$$

where and the pressure is defined at units of bar and

D = diameter [m],

R = gas constant [kJ/kgK],

ω = rotational speed [rev/s].

In order to avoid the need for specific geometry values of a turbo-machine, or by assuming that both R and D will be constant for a given machine operating with only one type of gas, the non-dimensional parameters are redefined in dimensional form. Thus, the following expressions for the corrected mass flow and for the corrected speed can be written as

$$CMF = \frac{\dot{m}\sqrt{T_1}}{P_1} \tag{3.25}$$

and

$$CS = \frac{N}{\sqrt{T_1}} \tag{3.26}$$

Turbines

Turbines' performance is also expressed in terms of pressure ratio (PR) and efficiency given as a function of corrected mass flow and corrected speed.

The pressure ratio of a turbine is defined as the ratio of the total pressure at the inlet (P_1) to the outlet pressure (P_2). Hence

$$PR = \frac{P_1}{P_2} \tag{3.27}$$

The isentropic efficiency of a turbine is defined as

$$\eta = \frac{W}{C_p T_1 (1 - PR^{(1-\gamma)/\gamma})} \tag{3.28}$$

Where W is the work done by the fluid and γ is the ratio of specific heats.

The corrected mass flow (CMF) and the corrected speed (CS) can be defined in a similar way for compressors.

Using these relationships, Flownex encompasses a model which relates the off-design behaviour to the design values, so that the optimal operating conditions can be calculated. For both compressors and turbines, this is done using performance maps which are given by two sets of maps, namely:

1. Pressure ratio versus non-dimensional mass flow rate for different values of non-dimensional rotational speed.

2. Isentropic efficiency versus non-dimensional mass flow rate for different values of non-dimensional rotational speed.

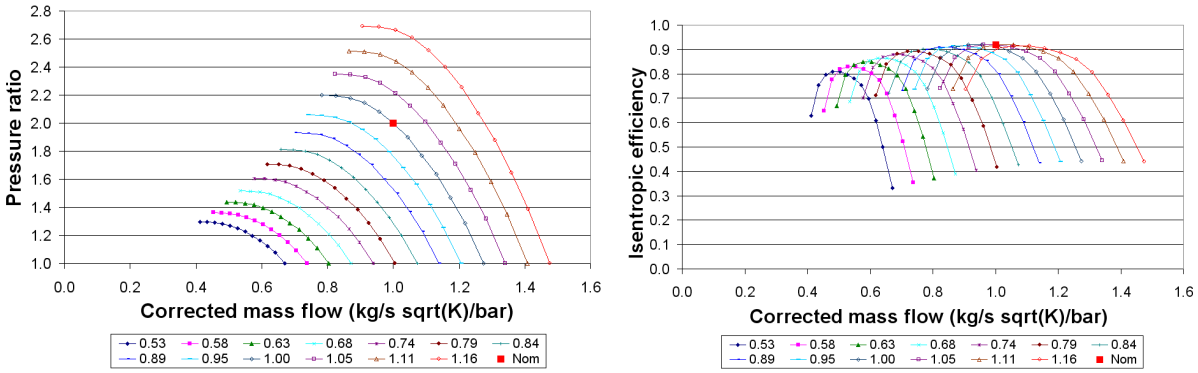

Fig. 3.3: Typical performance maps of an axial compressor (pressure ratio and efficiency vs. corrected mass flow).

Fig. 3.3 shows an example of typical maps used for an axial compressor. It can be seen that it is possible to obtain a specified pressure ratio at a specified non-dimensional speed for any mass flow and temperature resulting from the simulation. In a similar manner, the efficiency values can also be scaled so that for a given non-dimensional mass flow calculated from the simulated mass flow rate and temperatures, the specified efficiency is obtained. This can be done by scaling the non-dimensional mass-flow values in advance.

During the design and development phase of engineering systems, the performance of the compressor and turbine changes constantly, as they are being developed in parallel with other components in the system. When simulating any system for the first time, after design changes have been made to the layout or to the components, the resultant operating point will not necessarily satisfy all the boundary values. This is true with an exception concerning the maximum pressure and temperature, which are specified as boundary values in the simulation. The reactor power output will be determined by the resultant circuit mass flow rate and inlet and outlet temperatures. The mass flow rate, as well as the compressor pressure ratios, will be determined by the turbo-machine performance characteristics together with the pressure losses throughout the circuit. The resultant rotational speeds of the turbo-machines will be at a state where a power matching is obtained between the compressor and the turbine.

The closed loop configuration implies that a change at any component will influence the conditions of all other components. As the performance characteristics of the turbo-machines need to be adjusted simultaneously, a need exists for a methodology for balancing the turbo-machines, to ensure that all the specified boundary conditions are satisfied for any cycle configuration.

Scaling individual performance variables of the performance characteristics implies that modifications must be made in the design of the turbo-machine and these would result in the required in characteristics. A change in the design can lead to changing the annulus through – flow area, the blade angels, the number of stages etc. Therefore, one must be careful while scaling the individual variables so that the modifications do not result in unrealistic mechanical or aero-dynamical design criteria.

3.3.5 Calculation of turbo-machines shaft speed

Turbines and compressors can be connected with a shaft model, in which the mechanical inertia is used to predict the shaft speed from the rotational energy balance.

In steady state, the shaft with a number of turbo-machines connected to it can be power balanced. This is done by adjusting the shaft speed until the energy balance is satisfied. Taking into considerations the power losses caused by mechanical and generator related events, the power delivered to the shaft is calculated as

$$P_{shaft} = \sum_{t=1}^{n} P_t - \frac{1}{\eta_{mech}} \left(\sum_{c=1}^{n} P_c + \frac{P_g}{\eta_g} \right) \tag{3.29}$$

where $\sum P_t$ is the total power supplied by all turbines connected to the shaft, $\sum P_c$ is the total power required by all compressors connected to the shaft, P_g is the power required by the generator attached to the shaft and η_g is the generator's efficiency.

η_{mech} = shaft mechanical efficiency [-],
η_g = generator efficiency [-],
P_t = turbine fluidic power [kW],
P_c = compressor fluidic power [kW],
P_g = electrical generator power delivered to grid [kW].

During a transient simulation the rotor dynamics is governed by

$$\frac{d\omega}{dt} = \frac{P}{I\omega} \tag{3.30}$$

where

ω	=	rotational speed [rev/s]
I	=	total moment of inertia of the shaft with all rotating components attached to [kgm^2],
P	=	net shaft power [kW],
t	=	time [s].

The fact that the shaft speed in the model can be controlled allows the developer to specify a certain speed and observe the resulting turbo-machine performance.

3.4 Reactor Core Models

3.4.1 The Core Modelled by Flownex

Two core models exist in Flownex. The first is the "Generation II" core model. This model does not incorporate a fixed central column. This model is based upon a simplified two-dimensional axi-symmetrical approach, which is consistent with the overall approach followed in Flownex. The second core model is the "Generation III" advanced core model. The phenomena that can be modelled in the advanced core model include also the presence of a central column. This implies that the core itself does not extend outward from the centre, but has an inner and outer diameter. Despite the increased complexity of "Generation III" core model, it retains the simplicity of the network approach, as "Generation II" core model. Flownex reactor model integrated in the simulations is "Generation II" model. Hence, it was assumed that this core model would yield accurate results for the performance of the various simulations introduced here.

Geometry of the pebble bed reactor core

A schematic 2D representation of the geometry of the reactor core is shown in Fig. 3.4. The inner core region contains passive graphite spheres while the outer active core region is filled with fuel spheres. Helium gas enters the top of the reactor core at 500°C. The gas is heated through the active core region where heat is generated inside the fuel spheres. Upon leaving the core at the bottom, the hot gas is mixed with gas from the passive region to obtain a fully mixed exit temperature of 900°C. The core model described in Fig. 3.4 addresses the PBMR 268 MW_{th} core model design, with the core which contains dummy balls.

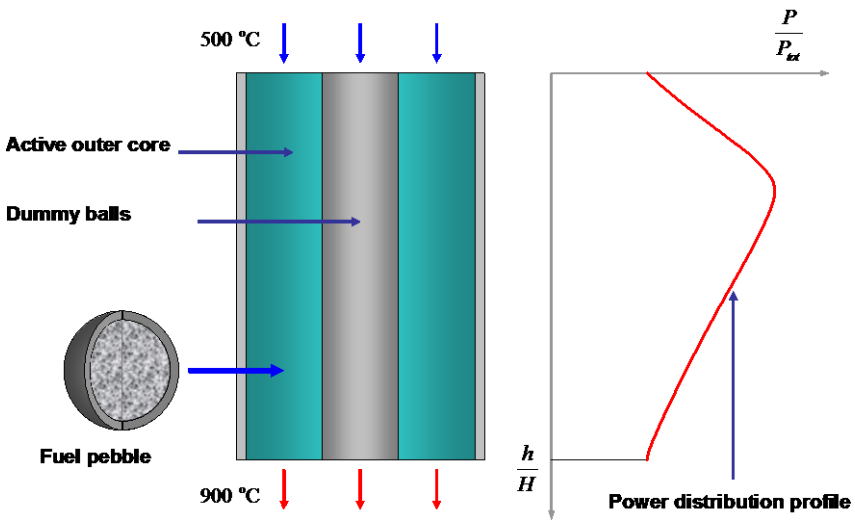

Fig. 3.4: Schematic two-dimensional representation of the core of the PBMR [52].

Integrated simulation of the reactor

The reactor model available in Flownex consists of three main parts [53]. These are schematically described in Fig. 3.5.

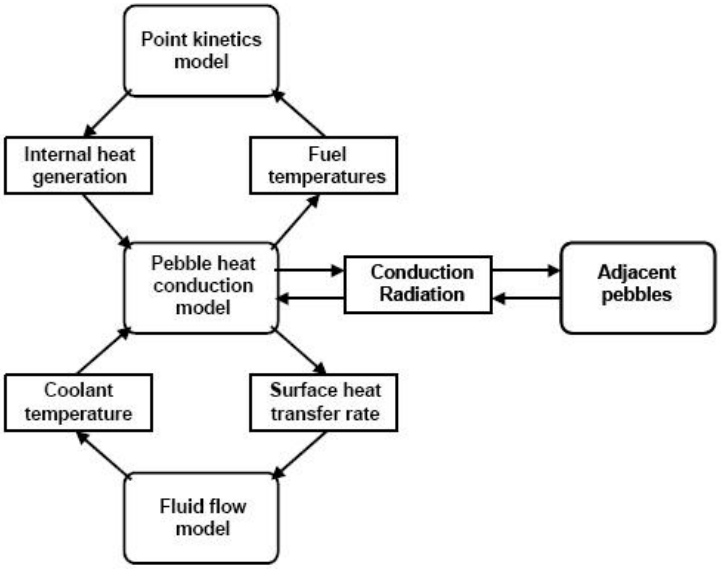

Fig. 3.5: Interaction between the point kinetics model, the heat conduction model and the fluid flow model in Flownex [54].

- *Heat transfer and fluid flow of the gas within the core*. The model is based on a discretised two dimensional axial-symmetric network, which consists of control volumes in the axial and in the radial directions. The model requires as an input the connective heat transfer rate and provides as an output the coolant temperature and pressure variations in the gas contained in each core section.
- *Heat conduction within each representative pebble in each core section*. Each pebble consists of an outer graphite layer and an inner fuel matrix region, both of which can

be discretised into any number of spherical “onion ring shaped” control volumes. This allows for the calculation of the temperature distribution within the pebbles in any region of the core. This model requires as an input the heat generation density within the fuel and the temperature of the gas surrounding the pebbles. It provides as an output the temperature distribution within the pebbles, as well as the convective heat transfer between the surfaces of the pebbles and the surrounding coolant.

- *Point kinetic neutronics and decay heat generation*. The calculation of the heat generated within the fuel is based on a point kinetics model. The point kinetics reactor model calculates the total reactor power, which has no spatial distribution, but is the integral reactor power. The power is distributed along the axial direction, but any radial power distribution profile is not taken into account. Thus, the global reactor behaviour is simulated dynamically as a single point having a certain weighted average properties assumed to be constant over time. This simplification is valid when the reactor is sufficiently small, so that it is well-coupled, and the space and time variables are essentially separable. Therefore the spatial neutron flux shape changes negligibly during a transient event, although the amplitude is strongly time dependent.

The initial purpose of Flownex core model was not to create a detailed reactor design, but rather to allow for the integrated simulation of the reactor together with the PCU within acceptable computer simulation times. Hence, the requirement for this existing model was to provide quick results of the main flow and heat transfer phenomena in the core only, in order to obtain boundary values for the simulation of the rest of the PCU [53].

The phenomena that cannot be simulated in the model described include the following:

- The presence of a central reflector column that implies that the core itself has an annular, rather than a cylindrical shape.
- The addition and extraction of gas via dedicated channels and leak paths along the inner and the outer perimeters of the core.
- The simulation of heat transfer and fluid flow through porous and solid core structures surrounding the core.
- The simulation of fluid flow and heat transfer, including radiation and natural convection, in purpose provided cavities between core structures, with a 2D rather than 1D nature.

- The ability to specify normalised radial power distribution profiles within the different axial layers in the core.
- The ability to account for heat generation occurring in any of the core structures.

This emphasises that a need exists for the development of a more comprehensive pebble bed reactor model that can still provide with integrated plant simulations, but includes the phenomena listed above. Such a reactor core model has been chosen as the WKIND core model, which will be discussed sub-chapter 3.5.2.

Thermo-mechanical analysis of the core

1. Pressure loss through the core

The pressure drop through the reactor core is calculated with the Ergun equation, which applies to the flow through a packed bed. The reactor is internally divided into two flow paths: the first represents the flow through the outer annular fuel sphere region, and the second represents the flow through the inner cylindrical moderator region. Both flow paths are divided into a number of horizontal layers, to account for the sharp change in flow properties through the reactor.

The pressure loss through the pebble bed reactor core is given by [55]

$$\Delta p = \psi \frac{1-\varepsilon}{\varepsilon^3} \frac{H}{d} \frac{1}{2\rho} \left(\frac{\dot{m}}{A} \right)^2 \text{ [Pa]} \tag{3.31}$$

where

ε	=	pebble bed void fraction [-],
H	=	reactor height [m],
d	=	sphere outer diameter [m],
ρ	=	fluid density [kg/m^3],
$\dot{m}$	=	mass flow rate [kg/s],
A	=	reactor cross sectional area [m^2],
ψ	=	pressure drop number [-].

and

$$\psi = \frac{320}{\left(\frac{\text{Re}}{1-\varepsilon} \right)} + \frac{6}{\left(\frac{\text{Re}}{1-\varepsilon} \right)^{0.1}} \tag{3.32}$$

where the Reynolds number is defined as

$$\mathrm{Re} = \frac{\dot{m}d}{A\mu} \tag{3.33}$$

$\dot{m}$ = mass flow rate [kg/s],

d = sphere diameter [m],

A = reactor cross sectional area [m^2],

μ = viscosity [kg/m.s].

The pressure drop relations are valid for $1 \le \frac{\mathrm{Re}}{1-\varepsilon} \le 10^5$ and $0.36 \le \varepsilon \le 0.42$.

2. Heat transfer between the fuel sphere and the helium

The sphere heat conduction model is based upon a finite difference solution of the transient 1D spherical heat conduction equation. Each sphere is divided into a number of discrete onion ring shaped control volumes; each ring is represented by a single node. Half of the control volumes represent the inner and the outermost layers. Implicit integration of the governing differential equations for each node creates a set of equations, which must be solved simultaneously for each node in the representative sphere.

The node on the surface of the sphere represents the surface temperature of all the spheres in that section of the reactor, which is exposed to the coolant. From the coolant viewpoint, the spheres will have the same effect as a constant surface temperature heat exchanger with a total area, which is equal to the sum of the surface areas of all the spheres in that layer. The convection heat transfer can therefore be simulated using the effectiveness-NTU method [56].

The heat transfer coefficient between the fuel spheres and helium is derived from the Nusselt number given by [55]

$$Nu = 1.27\frac{\mathrm{Pr}^{0.33}}{\varepsilon^{1.18}}\mathrm{Re}^{0.36} + 0.33\frac{\mathrm{Pr}^{0.5}}{\varepsilon^{1.07}}\mathrm{Re}^{0.86} \tag{3.34}$$

where the Nusselt number is defined as

$$Nu = \frac{hd}{k} \tag{3.35}$$

and Prandtl number is defined as

$$\mathrm{Pr} = \frac{C_p\mu}{k} \tag{3.36}$$

where

h = surface heat transfer coefficient [W/m^2K],

d	=	sphere outer diameter [m],
k	=	thermal conductivity [W/mK],
Cp	=	specific heat capacity [J/kgK],
μ	=	viscosity [Ns/m^2].

The heat transfer correlations are valid for

$$100 \le \frac{\mathrm{Re}}{1-\varepsilon} \le 10^5, 0.36 \le \varepsilon \le 0.42, \ \frac{D}{d} \ge 20 \ \text{and} \frac{H}{d} \ge 4 .$$

3. Core neutronics

This point kinetics model uses six delayed precursor groups, and is solved in a normalised form. The rate of change of the neutron density n is given by

$$\frac{dn}{dt} = \frac{(\bar{\rho} - \beta)}{\Lambda} n + \sum_{i=1}^{6} \lambda_i c_i + Q_{ex} \tag{3.37}$$

where

n	=	neutron density [neutrons/cm^3],
$\bar{\rho}$	=	reactivity,
β	=	delayed neutron fraction,
Λ	=	average neutron generation time [s],
λ_i	=	decay constant for delayed neutron group i [1/s],
c_i	=	precursor atom density for group i [atoms/cm^3]
Q_{ex}	=	external sources [neutrons/cm^{3}s].

Assuming that the neutron spectrum does not change significantly during a transient, then the reactor power level is directly proportional to the neutron density. Therefore, the rate of change of the normalised reactor power P_n can be written as

$$\frac{dP_n}{dt} = \frac{\rho - \beta}{\Lambda} P_n + \sum_{i=1}^{6} \lambda_i c_i + Q_{ex} \tag{3.38}$$

where P_n is the reactor power [kW].

When the reactor power level is directly proportional to the neutron density, the rate of change of the density (or concentration) of the precursor atom group i is given by

$$\frac{dc_i}{dt} = \frac{\beta_i n}{\Lambda} - \lambda_i c_i \tag{3.39}$$

The reactivity in the reactor is calculated as the sum of the contributions from fuel, moderator, xenon poisoning and from external influences like control rods.

The total reactivity is obtained from

$$\bar{\rho} = \bar{\rho}_f + \bar{\rho}_m + \bar{\rho}_X + \bar{\rho}_{ex} \tag{3.40}$$

where $\bar{\rho}_f$ is the reactivity from fuel, $\bar{\rho}_m$ is the reactivity due to moderator, $\bar{\rho}_X$ is the reactivity due to xenon and $\bar{\rho}_{ex}$ is the reactivity due to the insertion depth of the control rods.

Together with all reactivity contributions, the resulting net total reactivity $\bar{\rho}$ is fed back into the point kinetics reactor model. The resulting power distribution profile can be used to calculate the fuel pebbles temperature and the outlet temperature of the gas.

3.4.2 The Core Modelled by WKIND

1. Geometrical model

The reactor is described using a cylindrical geometry, which is divided to numerous axial zones. Non-cylindrical areas are treated using volumes which are cylinder-alike. It is assumed that the core material is homogenous. The inner fuel assembly is also considered to be made of a uniform type of fuel.

2. Heat conduction within the fuel elements

The heat conduction model is used in the cases of fast transients. In general, for the treatment of the source distribution of the heat production of the coated particles, the KIND codes contain three different models for the calculation of reactivity transients. Detailed description of the models can be found in Kindt and Kohtz, [57]. The relaxation time of the equalisation of temperature disturbances between the coated particle and the surrounding graphite matrix is in the range of 10^{-2} seconds. At fast power excursions, temporary storage effects of the heat in the coated particles influence the feedback provided by the Doppler Effect. In order to describe these effects, the spatial and the time dependent heat conduction equation in the sphere has been separated into two parts. The first part describes the time and the space dependency of the temperature, which is taken as an average over the coated particle and a part of the adjacent graphite matrix. The second part describes the deviation of the temperature from this average value, which occurs within the microstructure of a representative pebble.

3. Core neutronics

As oppose to the simple treatment using the point kinetics model, where reactivity transients are only treated using global coefficients, WKIND core model treats the problem in a complex manner. The numerical method solved by the code is a finite differential method. The treatment of the time and space dependent neutron diffusion equation is the following

$$\frac{1}{v}\frac{d\phi}{dt} = (1-\beta)\nu\Sigma_f\phi + \sum_{i=1}^{6}\lambda_j c_j - \Sigma_a\phi + \nabla(Diff\nabla\phi) \qquad (3.41)$$

where

v	=	velocity [cm/s],
ϕ	=	neutron flux density [1/cm^{2}s],
ν	=	number of neutrons per fission [-],
λ_j	=	decay constant of delayed neutron group *j* [1/s],
c_j	=	precursor atom density of group *j* [atoms/cm^3],
$Diff$	=	diffusion constant [cm],
Σ_f	=	macroscopic fission cross section [1/cm],
Σ_a	=	macroscopic absorption cross section [1/cm].

Equation 3.41 is solved for 1D geometry in the axial direction of the core.

The macroscopic absorption cross section is a function of several parameters and it is actualised after each time step by the temperature calculation solved by the thermal hydraulics part. In addition, WKIND calculates explicitly the temperature in the fuel particle.

Since the delayed neutron production is dependent on the precursor atom concentrations, the time dependent precursor balance must also be considered.

The balance for the precursors can be written as:

$$\frac{dc_j}{dt} = \beta_j\nu\Sigma_f\phi - \lambda_j c_j \qquad (3.42)$$

where β_j is the delayed neutron fraction for group *j*.

4 Code Validation

4.1 Oberhausen II (EVO II)

In the current chapter, Flownex will be used to verify and to validate the PCU part of the dynamic model against the existing experimental data. For this purpose, the German power plant Oberhausen II (EVO II) was chosen.

EVO II facility is a direct cycle Helium turbine plant. It was operated for more than 25000 hours by the utility EVO (Energieversorgung Oberhausen AG) between the years 1974 and 1988 ([58], [59]). The facility was part of a research and development project, which the Federal Government of Western Germany initiated in 1968. The research performed aimed at the development of helium turbo-machinery that could operate with high temperature in a Brayton cycle [11]. The facility incorporated a gas-fired helium heater, while all its other components were of the same design as the components of a power plant utilising a nuclear heat source [60].

The design and construction of a closed cycle turbine operated with air were at that time well-known. However, the change to helium, and the need to meet the development goals of using high helium temperatures and pressures to the greatest extent possible, have caused difficulties in the operation of EVO II. The helium turbine, which was designed to produce 50 MW_{el}, managed to produce only 30 MW_{el}. The efficiency of the plant reached only 23%, instead of the calculated 34.5% [61]. Because of the deficits, no successful reconditioning was possible without redesigning and constructing a new turbo-machine.

Numerous design specifications, drawings and experimental data have been obtained in the frame of the European HTR-E project, offering a unique opportunity to validate system codes on a large scale helium Brayton cycle [62].

Available measurements of temperatures, pressures and mass flows throughout the circuit have been used as basis for the simulation of the four steady state cases. These cases are the following: the design plant with 50 MW_{el}, the operating plant with 30 MW_{el} and two partial loads with 20 MW_{el} and 13 MW_{el}. An additional case is a load following transient. The scenario of a load following regards a change in the electrical power from 10.6 MW_{el} to 7.6 MW_{el} due to a change in the helium inventory in the system.

4.1.1 General Plan Description of the EVO II

Fig. 4.1 depicts the direct helium Brayton cycle EVO II plant [11]. The inlet temperature of the high pressure turbine was limited to 750°C. A two shaft design was selected for the turbo-machinery. The high pressure turbine was designed to drive both compressors on a common shaft running at a speed of 5500 rpm. The low pressure turbine was connected to the generator on a separate shaft running at 3000 rpm. The shafts are interconnected via a gearbox. The recuperator was designed as a high-efficiency baffled shell-and-tube heat exchanger. With a surface which consisted of 17500 tubes, it was designed to deliver 130 MW_{th}. The pre-cooler was a gas-to-water heat exchanger, subdivided into a heating and a cooling section. The inter-cooler was designed in a similar way, containing only a cooling section.

In the real installation, a leak flow path starting at the high pressure compressor was directed to cool the flow entering the high pressure turbine. Another leak path was the re-injection of helium from the labyrinth seal of the low pressure turbine into the circuit.

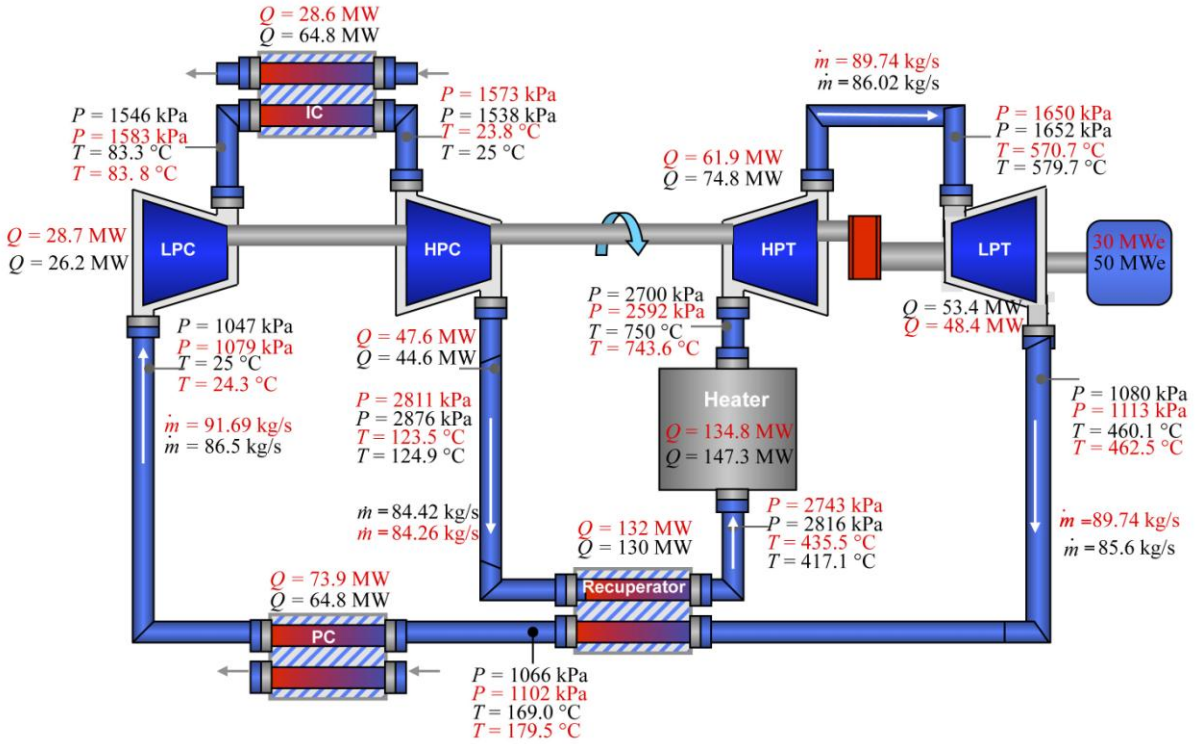

Fig.4.1: EVO II flow diagram (design parameters are marked in black, operating conditions are marked in red).

Fig. 4.1 further shows the circuit with the corresponding design values, as well as the nominal measured values, which were observed during the plant operation. Compared with the design heater thermal power, in the operating facility a thermal output of only 134.8 MW_{th} was achieved. It can be seen, that the variations in mass flow rates in the operating facility are

greater than indicated by the design parameters. This is due to leak and bypass flows, which were greater than expected. This large deficit was caused by many factors. The turbo-set had a lower output than the designed one. The nominal running speed of 5500 rpm, which is adequate for air but is considered low for helium turbo-machines, resulted in unfavourable hub to tip ratios for the compressors and the turbines. The low ratios led to poor isentropic efficiencies in the turbo-machines. In addition, the cycle pressure losses were excessive. The cooling streams and the flow through sealings were greater than predicted in a factor of four.

The following Table 4.1 indicates the different factors which had the greatest influence on the reduced performance of the plan, as they were given by Bammert [63].

Table 4.1: Major factors which contributed to decreased power output at EVO II.

Parameter	**Design Value**	**Measured Value**	**Estimated Decline in Generator Power (MW)**
Efficiency HPT (%)	88.3	82.3	-3.9
Efficiency LPT (%)	90.0	85.6	-2.4
Efficiency HPC (%)	85.5	77.9	-4.0
Efficiency LPC (%)	87.0	82.6	-1.3
Pressure losses (%)	10.25	12.79	-2.6
Cooling & leakage flow rates (kg/s)	1.78	7.53	-5.3
T inlet HPC/LPC/HPC (°C)	750.0/25.0/25.0	743.6/24.3/23.8	-0.4
ΔT across recuperator (°C)	3.0	8.7	-0.3
Sum			-20.2

Despite of the deficiency in the performance of the plant, EVO decided to accept the helium turbine from the manufacturer. This decision was made because helium-specific-experiences could nevertheless be gained with the actual plant conditions, and because the plant could be operated as a co-generation plant satisfying the required district heat demand [11].

4.2 Modelling of the EVO II System with Flownex

The validation of the EVO II design consisted of two steps:

1. Modelling and testing of separate components.
2. Modelling and testing of the integrated system.

In the first step, the separate components and their global behaviour, based upon geometrical and thermal hydraulic characteristics were modelled and tested. In the second step, the components stand-alone models were integrated into a complete system model.

The modelling of the components was based on design drawings and specifications which were provided by CEA (Commissariat à l'Energie Atomique) within the frame work of the European RAPHAEL project [64].

The diameters of pipes connecting the major components were available from plans. The diameters of the pipes connecting the heater and the high pressure turbine, as well as the pipes connecting the high pressure turbine and the low pressure turbine were calculated to obtain a velocity equivalent to the calculated fluid velocity in all other pipes. The connections between piping and exchangers' inlet and outlet volumes are represented in the simulation by specifying them on the corresponding components inlet and outlet nodes. The volumes simulate the thermal inertia associated with the heat exchangers, and are important for transient simulations.

All heat exchangers, including the recuperator, which is a gas-to-gas heat exchanger, are of shell-and-tube counter-flow design. The coolers are finned. In the case of the pre-cooler and the inter-cooler, the helium gas flows through the shell side and water flow in the tube side. In the recuperator, the low pressure hot gas coming from the low pressure turbine flows through the shell side, whereas the high pressure gas from the high pressure compressor flows through the tubes side. The modelling of the pre-cooler, which has two distinct sections, was done by simulating two finned-tube heat exchangers in series. Main design parameters of the heat exchangers are given in table 4.2.

Table 4.2: Design parameters of the heat exchangers at EVO II.

Heat exchanger	**Tube inside diameter (mm)**	**Number of**		**Heat transfer area (m^2)**	**Power (MW)**
		tubes	**baffles**		
PC hot side	10	608	-	6000	64.8
PC cold side	10	612	-	5000	
IC	10	2430	-	3900	26.6
Recuperator	10	17430	30	9530	129.5

The heat transfer correlations used are provided by Flownex and were determined adequately good for the validation. In these correlations, the Fanning friction factor and the Stanton Prandtl relationship ($StPr^{2/3}$) of the heat exchangers are given as a function of Reynolds number. The Stanton Prandtl relationship, also knows as the Colbrun correlation, depends on the fins configuration and on the spacing between tubes, and is given for various geometries. The Stanton Prandtl relationship is used to calculate the local Nusselt number for a fully developed turbulent flow.

As explained in chapter 3, the operating points of the turbo-machines are determined by the cycle operating point and are expressed in terms of pressures and corrected mass flows. Table 4.3 shows the pressure ratio, the corrected mass flow and the resulting power of the turbo-machine for a nominal mass flow rate of 84.42 kg/s and a low pressure compressor inlet pressure of 1047 kPa.

Table 4.3: pressure ratio, corrected mass flow and power for the design case with a mass flow of 84.42 kg/s and a low pressure compressor inlet pressure of 1047 kPa.

Turbo unit	**Pressure ratio**	**Corrected mass flow ($\frac{kg/s\sqrt{K}}{bar}$)**	**Power (MW)**
LPC	1.50	141.35	26.8
HPC	1.88	92.25	44.5
HPT	1.63	100.52	71.54
LPT	1.51	151.81	52.3

In order to perform the steady state calculation of the EVO II, several boundary conditions need to be specified to satisfy the solution using Flownex simulation. These are the pressure at the low pressure compressor inlet and the cooling flow rates through both the inter-cooler and the pre-cooler. The cooling water temperature known from the literature was set as 20°C. The upstream node of the low pressure compressor was set at 1047 kPa. The heater outlet temperature was kept constant at 750°C, as given by the literature. The heater was modelled in a simplified manner, using a pipe with a fixed heat transfer with an adjusted pipe pressure drop. Fig. 4.2 shows the physical layout of the EVO II circuit with a pipe as a heat source, high pressure turbo-unit, low pressure compressor, low pressure turbine, generator, heat exchngers and recuperator which are placed within one pressure boundary. The gas inside the

pressure boundary was modelled as a reservoir with a volume of 500 m^3. The figure also indicates the helium tanks and the isolation valves used during power control of the plant.

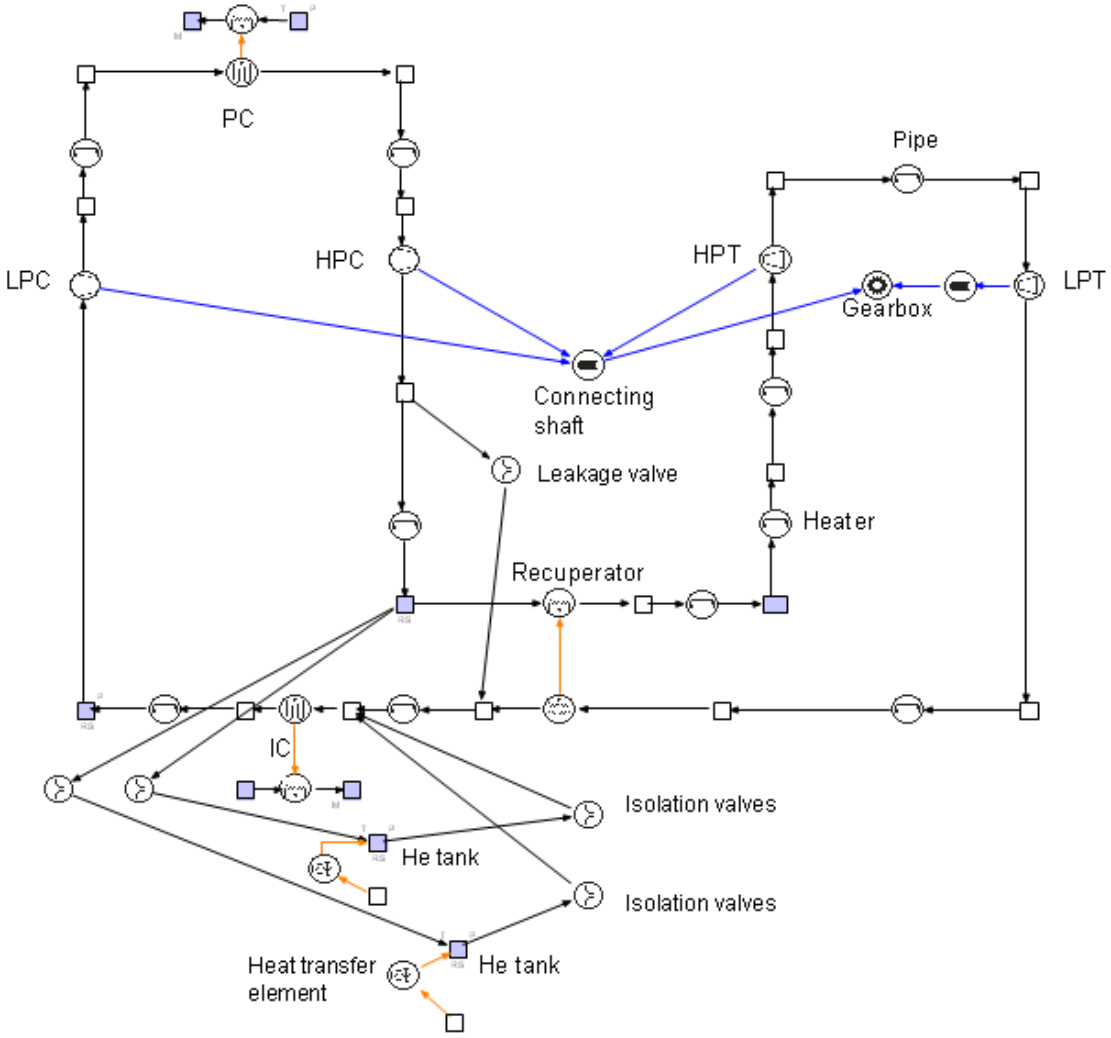

Fig. 4.2: Flownex model of the EVO II.

Flownex allows only for the addition of leak flows to the front of the turbo-machines and not to a certain stage in-between the inlet and the outlet of a turbo-machine. Therefore, it was necessary to treat the leakages in the circuit in a simplified way.

The EVO II helium turbine plant was equipped with two reservoirs, which allowed for a long-term storage of helium for periods of part-load operation. For quick power variation and for speed control, a bypass control system was designed. By opening a second bypass, the plant could be shut-down immediately. The bypass valve which connects the high pressure compressor outlet with the low pressure turbine outlet has been taken into account in the modelling. The valve is kept closed in nominal state. The valves which connect the two tanks to the

primary loop and were implemented in the simulation are kept closed in nominal state. In order to add inertia to the load following simulation, two heat-transfer elements are modelled. These elements represent the solid metal of the tanks' wall.

4.3 Steady State Calculations

The performance data of the design reference case have been viewed in numerous publications ([58], [65]). The calculation of the nominal state is based upon the information which was first established in 1972. Calculations of the partial load of the plant are based on the description of the plant during its operation time [59]. Table 4.4 shows a comparison between the cycle main thermal hydraulic parameters of the reference design case with reference to Bammert [63] and the corresponding results of Flownex.

Table 4.4: Comparison of the thermal hydraulic parameters of the design case with Flownex simulation results of EVO II.

Component	Parameter	EVO Design values	Flownex result
Low pressure compressor	P_{in} (kPa)	1050	1047
	T_{in} (°C)	25	25
	P_{out} (kPa)	1543	1570
	T_{out} (°C)	83.8	84.9
High pressure compressor	P_{in} (kPa)	1538	1552
	T_{in} (°C)	25	25
	P_{out} (kPa)	2876	2916
	T_{out} (°C)	125	124.23
Heater	P_{in} (kPa)	2833	2891
	T_{in} (°C)	420	415.45
	$\dot{m}$ (kg/s)	84.4	85.6
High pressure turbine	P_{in} (kPa)	2700	2728
	T_{in} (°C)	750	753
	P_{out} (kPa)	1650	1674
	T_{out} (°C)	579.7	592.7
Low pressure turbine	P_{out} (kPa)	1080	1096
	T_{out} (°C)	460	475.3
Power available on the shaft	Power (MW)	52.8	52.7

It can be observed that only small differences exist between the results predicted by EVO II design data and Flownex calculations. The outlet temperatures of both high and low pressure turbine are higher than the values indicated by the design plant. These differences can be ex-

plained by heat losses and deficiencies in the plant isolation, which were not taken into account in Flownex simulation. A value with much interest is the power available on the shaft. This power was calculated by subtracting the power dissipated by the pre-cooler, inter-cooler, ducts and pressure losses from the thermal power of the heater. It can be seen that the values calculated by Flownex are very close to the design specifications. The comparison between the nominal operating point of EVO II and Flownex is demonstrated in table 4.5. The geometrical input data for calculating the operational state of the plant at full-load are the same as those used for calculating the design case. The main differences are in the isentropic efficiencies specifications for the turbo-machines. These were modified to account for the decreased efficiencies and the excessive flow losses observed in the real installation. Furthermore, the excessive pressure drops observed throughout the circuit were considered.

Table 4.5: Comparison of the thermal hydraulic parameters of the nominal operational case with Flownex simulation results of EVO II.

Component	Parameter	EVO Nominal values	Flownex result
Low pressure compressor	P_{in} (kPa)	1079	1059
	T_{in} (°C)	24.3	24.8
	P_{out} (kPa)	1583	1550
	T_{out} (°C)	83.8	84.3
High pressure compressor	P_{in} (kPa)	1573	1530
	T_{in} (°C)	23.8	24.3
	P_{out} (kPa)	2811	2683
	T_{out} (°C)	123.5	121.9
Heater	P_{in} (kPa)	2743	2657
	T_{out} (°C)	742.5	742.5
	$\dot{m}$ (kg/s)	84.2	84.0
High pressure turbine	P_{in} (kPa)	2592	2485
	T_{in} (°C)	743.6	731.1
	P_{out} (kPa)	1650	1593
	T_{out} (°C)	570.7	599.13
Low pressure turbine	P_{out} (kPa)	1113	1109
	T_{out} (°C)	462.5	480.0
Power available on the shaft	Power (MW)	30.7	36.4

It can be seen that the differences between the calculated results and the real installation case are larger than the values predicted by the design calculations. A possible reason is that certain properties of the real installation differ from the design specifications [66]. Another reason is the simplified treatment of the mass losses in the plant, which were much greater in the actual installation than in the design case. In the actual installation, the blades of the high pressure turbine are cooled with a small slip stream of gas coming from the high pressure compressor. A circuit of oil in rotating labyrinth seals of the turbo-machines receives gas leaking from the primary circuit. Once the helium was separated from the oil, the gas is re-injected into the main circuit. This could further influence the results, depending on whether the bulk of these gas streams were introduced closer to the outlet of the high pressure turbine or to the inlet.

Except for the plant nominal state, two supplementary operational cases were calculated using Flownex. These correspond to the plant producing nominal power of 20 MW_{el} and 12.9 MW_{el}. These states are in principle similar to the nominal full load case, and they differ only in the mass flow and pressure distribution in the circuit. Flownex simulation results show good agreement with the literature for both cases. To summarise, the data which were not used to calculate the design and the nominal states of EVO II, and their anticipated influence on the results are as follows; regarding the turbo-machinery, the gearbox parameters, the shaft friction parameters and the generator friction parameters were not used. In order to determine the turbo-machines' characteristics, scaled performance maps provided by Flownex, rather than the original maps, were used. The inlet and outlet volumes of the turbo-machines were not used in the overall computation. The volumes represented by the turbo-machines and by the pipes are important in order to determine the total helium mass in the circuit (1300 kg). These volumes are important for the simulation of a load following transient, in order to determine the re-partition of helium between the high and the low pressure sides of the circuit, which influences the pressure evolution. The pressure drop and heat transfer correlations of heat exchangers provided by Flownex were used. These have a major influence on the total computation.

4.4 Transient Analysis

Load following is a principle way to control the power output of the plant. By extracting helium from the main circuit and storing it, the pressure level in the circuit varies, and the power

is affected and lessened. Two helium tanks are used in the current transient. Each tank has a volume of 120 m^3 and an initial temperature of 12.3°C. The initial pressures assigned to the tanks are 1075 kPa and 264 kPa for the first and for the second tank (tanks 1 and 2) respectively. The steady state conditions from which the transient starts are a plant mass flow rate of 51.9 kg/s, a power output of 10.6 MW_{el} and a maximum cycle pressure of 1660 kPa. In the current transient, it is justified to apply the scaled turbo-machines' characteristics, since they maintain their nominal design point. The predefined sequence of events is the following:

- At time t=231 s: beginning of the transient by opening the valves connecting the high pressure compressor outlet and tank 1.
- At time t=515 s: closing the valves connecting the high pressure compressor outlet and tank 1.
- At time t=597 s: opening the valves connecting the high pressure compressor outlet and tank 2.
- At time t=1170 s: closing the valves connecting the high pressure compressor outlet and tank 1.
- At time t=1200 s: end of the transient.

Fig. 4.3 presents the results obtained from Flownex simulations for the high pressure turbine and the low pressure compressor outlet pressure.

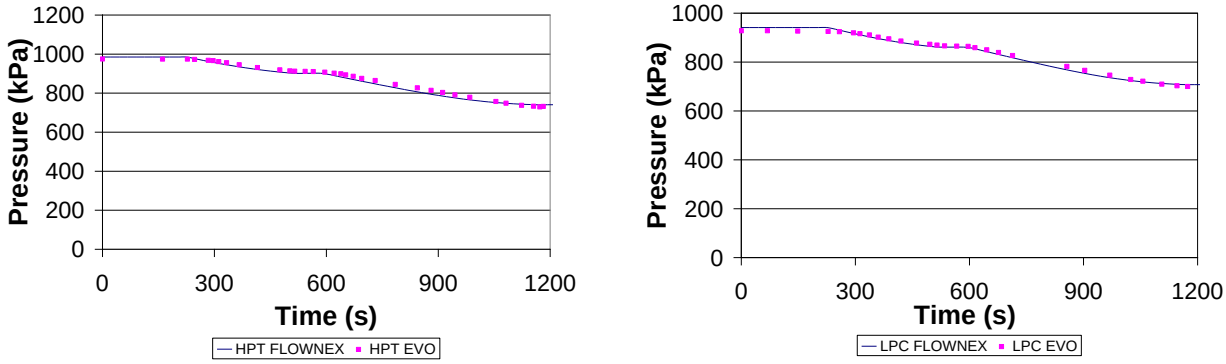

Fig. 4.3: Variations in high pressure turbine and low pressure compressor outlet pressure – comparison between EVO II measurements and Flownex simulation results during a load following transient.

The changes in pressure in the high pressure turbine outlet and in the low pressure compressor outlet follow the trend exhibited by both the mass flow in the circuit and the generator power. A similar behaviour was also demonstrated by the various components: pressure changes in the low pressure turbine inlet and outlet, the high pressure turbine inlet and the low pressure compressor inlet. Due to the extraction of helium, the pressure in the low pressure compressor outlet decreases from 700 kPa to 650 kPa at the end of the transient. The plateau in the plot represents the time between the closing of the valve connecting to tank 1 and the opening of the valve connecting to tank 2. In a similar manner, the high pressure turbine outlet pressure

decreases during the same period of time from 974 kPa to 726 kPa. It can be seen that also here good agreement is achieved. The maximal difference between the calculation and the experimental data is of about 50 kPa.

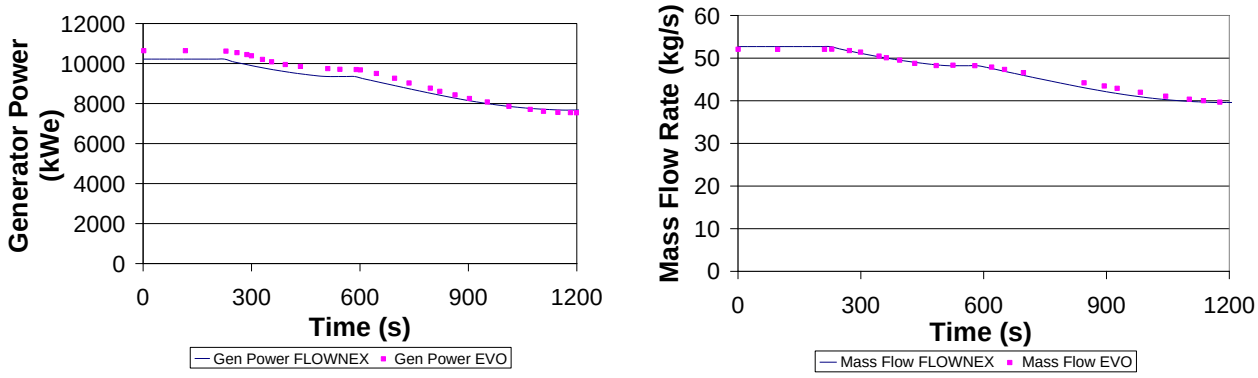

Fig. 4.4: Variations in generator power and in mass flow due to extraction of helium from the primary circuit – comparison between EVO II measurements and Flownex simulation results during a load following transient.

Fig 4.4 depicts the generator power nominal and mass flow rate during a load following transient in comparison to the published experimental results. It can be concluded that simulation's results show good agreement with those obtained at the EVO II. Fig 4.3 shows that the changes in mass flow rate in the primary circuit follow a similar pattern as the changes occurring in the generator power. The mass flow rate varies greatly during the transient, and it decreases from 51.1 kg/s at steady state to 39.8 kg/s at t=1170 s. It can be seen that the experimental results are well predicted by Flownex. The maximal difference obtained between Flownex calculation and EVO II experimental data is of about 0.8 kg/s. Fig. 4.4 further depicts the decrease in generator power due to the opening of the valves, which allows the helium to flow from the main circuit into the tanks. After opening the valve connecting to tank 1, the power decreases to about 9.7 MW_{el}. During the following 82 s, no decrease in mass flow rate is observed, and therefore the power stays constant. After opening the valve connecting to tank 2, a further decrease in power is observed. After closing this valve at t=1170 s, the power reaches its final level of about 7.6 MW_{el}. Flownex results show a satisfactory agreement with the experimental results.

The pressure and temperature evolutions in the tanks are demonstrated in the following Fig. 4.5 and Fig 4.6. It can be seen that good agreement is achieved for the pressure variations in both tanks. From Fig. 4.4 it can be seen, that after the valve connecting this tank to the main circuit opens at t=231 s, the pressure in tank 1 increases from 1075 kPa to 1538 kPa at t=5151

s. The response to the change in helium inventory causes the pressure in tank 1 to continuously decrease. At t=1200 s the pressure in the tank reaches a minimum of 1424 kPa. During the time tank 2 is coupled to the primary circuit, the pressure in it rises from 264 kPa to 1280 kPa.

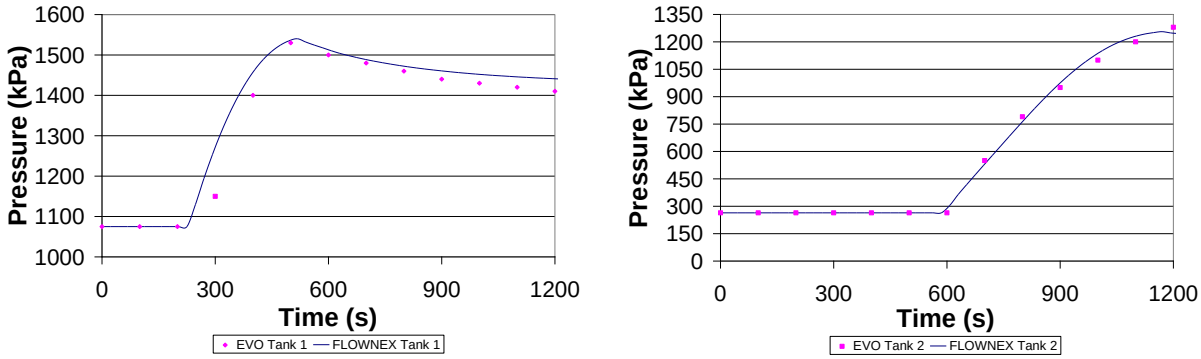

Fig. 4.5: Pressure variations in tank 1 and Tank 2 - comparison between EVO II measurements and Flownex simulation results during a load following transient.

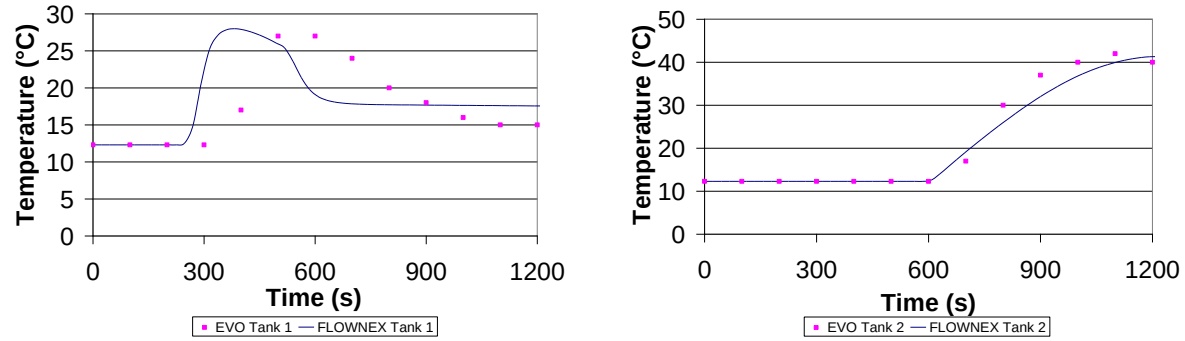

Fig. 4.6: Temperature variations in tank 1and Tank 2 - comparison between EVO measurements and Flownex simulation results during a load following transient.

As for the temperature: in the experiment, the temperature in tank 1 increases from 12.3°C to a maximal value of 27.6°C. From this maximum, 50 s after filling the tank was initiated at t=565 s, the temperature starts to sink again. At t=1200 s, the temperature in the tank is 15.7 °C, and is still higher than the initial temperature in the beginning of the transient. The temperature in tank 2 changes together with the pressure, and rises from 12.3°C to 40.9°C. The maximal temperature in this tank reaches its maximum already 60 s before closing the valve, and then it starts to sink in the same manner as the pressure, to reach a stationary state.

According to Fig. 4.6, Flownex simulation results show good agreement, except for the temperature evolution in tank 1. Several explanations are given for this disagreement. First, the information about the location of the measurement devices in the tank is not provided in the literature. Placement of the thermocouples has a very large effect on the temperature meas-

ured. Therefore, the actual temperatures measured in the experiment can differ from the representative value of the tanks temperature.

CEA has suggested that the tanks were externally cooled, and therefore heat sinks were additionally modelled. Furthermore, it has been determined that the temperature evolution highly depends on the imposed parameters for the cooling tank regulation [63]. However, the control philosophy in this case is not provided, and neither is the amount of heat removed from the tanks.

In terms of the delayed response, additional information about the types of valves used in the experiment is needed to predict better results using Flownex. Moreover, the dimensions of the tanks in the experiment are not known. In the literature, only the tanks volumes have been reported. The temperature rise observed in both tanks was extremely high without adding thermal inertia. This was performed by modelling of the tank wall with the aid of heat transfer elements added to each tank. In order to reduce the temperature variation in the gas contained in the tank, it was further needed to enlarge the capacitance of the wall, and its dimensions. The heat transfer elements were modelled so that they would have geometrical dimensions and mass in the same order of magnitude as the tanks metal.

As it has been observed, before the temperature transient in the experiment began, Flownex already simulated a cooling-off of the tank temperature due to the reduction in pressure. However, modifying the thermal inertia alone did not cause the temperature peaks of Flownex and the experiment to coincide.

5 Complete System Analyses

5.1 Introduction

During the lifetime of the nuclear plant, many transient situations can occur. These are of importance for the operational and the safety analysis of the High Temperature Pebble Bed Reactor plant. These include, for example, start-up, power transitions, shut-down and different accident scenarios. Simulations of the PCU coupled to the reactor can be used to analyse the effects that the transient response has on the various components during different operational and accident modes.

Therefore, the complete coupled Flownex-WKIND system is simulated for various transient conditions, and the results of important transient cases will be shown. For the reactor related transients, a hypothetical transient and a control rods withdrawal followed by a scram signal are analysed. Three additional transients, which were defined as system related, were calculated for both single and three shaft configurations. These transients were performed in order to demonstrate the dynamics of the PCU, and to show its interaction with the reactor core, providing realistic boundary conditions to it. These transient cases comprise a load rejection transient within less than 1 s with prevention of the turbine over-speed. The second transient is a long term load following transient. The third transient demonstrates the consequences of a helium leak due to a break in the pipe at the high pressure compressor outlet. Based on the results, it is possible to determine realistic boundary conditions for the pebble bed core, as well as operational limitations for the complete plant with respect to temperatures, pressures and mass flow rates of the different components. The basis for the dynamic calculations is a 268 MW_{th} direct cycle with a recuperator and two stages of inter-cooling, which are employed by both shaft configurations, as explained in the following subsection. The main system parameters were obtained by using the thermal-simulation code Flownex.

5.2 Main Power System Description

The Main Power System (MPS) of the High Temperature Pebble Bed Reactor, which runs on a Brayton cycle, circulates helium through the reactor core and through the different components, which constitute the PCU. The helium flow path through the system can be explained with reference to the three and to the single shaft system configurations. In order to directly compare the two systems, it is necessary to ensure that the same input parameters are set to

the same values in both system layouts. Therefore, both systems have a maximum cycle pressure of 7 MPa set as a boundary condition at the manifold. In addition, the outlet temperature of the reactor is 900°C in both systems, and the cooling water temperature is set to 33°C. The main system parameters are provided by the four figures indicated below. The three shaft PCU design which follows the early PBMR concept and its corresponding T-s diagram are demonstrated in Fig. 5.1 and Fig. 5.2 respectively, whereas the recent design of a single shaft PCU with its corresponding T-s diagram are depicted in Fig. 5.3 and Fig. 5.4. For both cycle configurations, a detailed cycle analysis was performed.

5.2.1 Main Components of a Three Shaft Recuperated and Inter-Cooled Brayton Cycle

Fig. 5.1 shows the layout of a typical three shaft reuceperative Brayton cycle similar to an earlier version of the PBMR. With reference to the figure: starting at state 1, the helium gas is initially characterised by relatively low pressure and temperature of 2.6 MPa and 33°C. Helium is compressed by a low pressure compressor to an intermediate pressure at state 2, after which it is cooled in an inter-cooler to state 3 at 33°C and 4.7 MPa. A high pressure compressor then compresses the helium to state 4 at 100°C and 7.0 MPa. Hereafter it is preheated in the recuperator from state 4 to 5 to 500°C, before entering the reactor, which heats the helium to state 6 to 900°C. After the reactor, the hot high pressure helium is expanded in a high pressure turbine to state 7 at 5.7 MPa, after which it is further expanded in a low pressure turbine to state 8 at 4.3 MPa. The high pressure turbine drives the high pressure compressor and the low pressure turbine drives the low pressure compressor. After expanding in the low pressure turbine, the heated helium is further expanded in the power turbine, which drives the generator to the pressure at state 9, which is approximately the same pressure as at the initial state. The hot helium is then cooled in the recuperator to 150°C, after which it is further cooled in the pre-cooler to the initial state. This completes the cycle. The power output of the cycle is controlled via an inventory control system through which helium can be injected or extracted from the system.

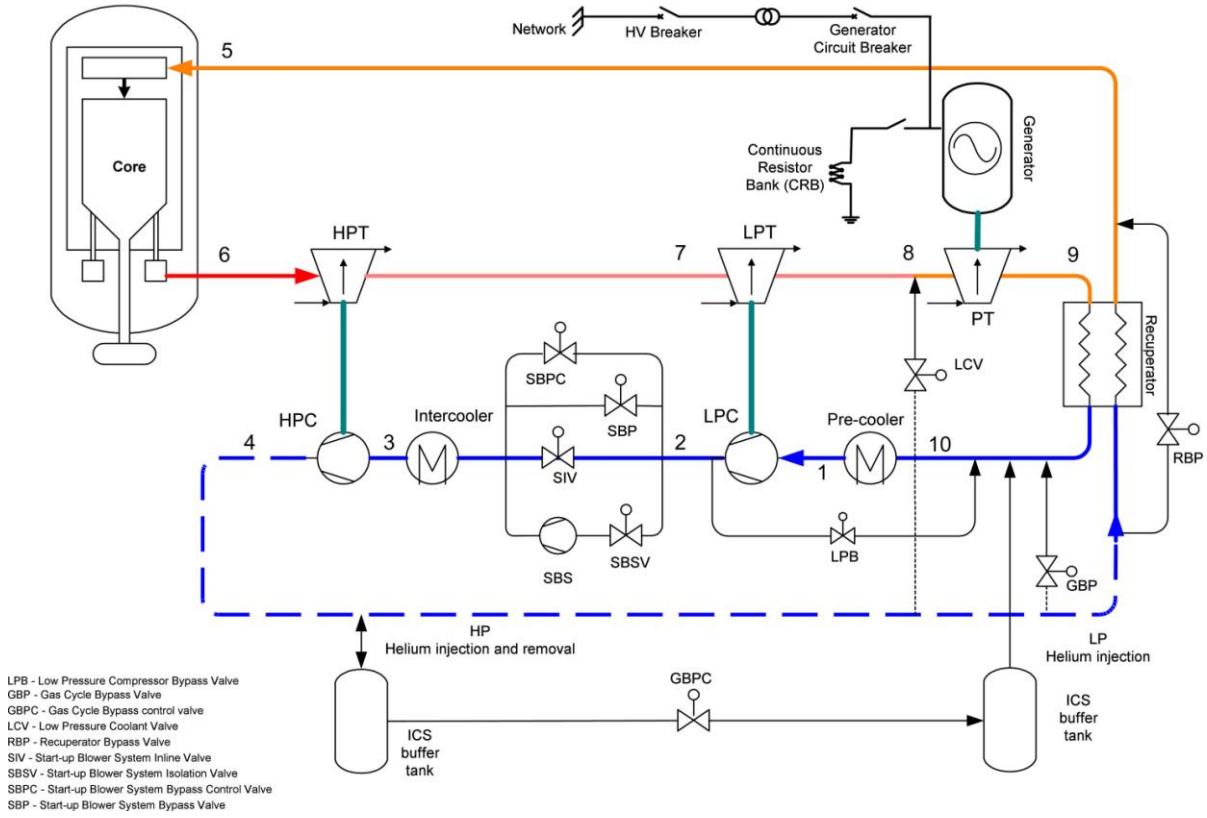

Fig. 5.1: Schematic diagram of an HTR connected to a three shaft Brayton cycle PCU [22]

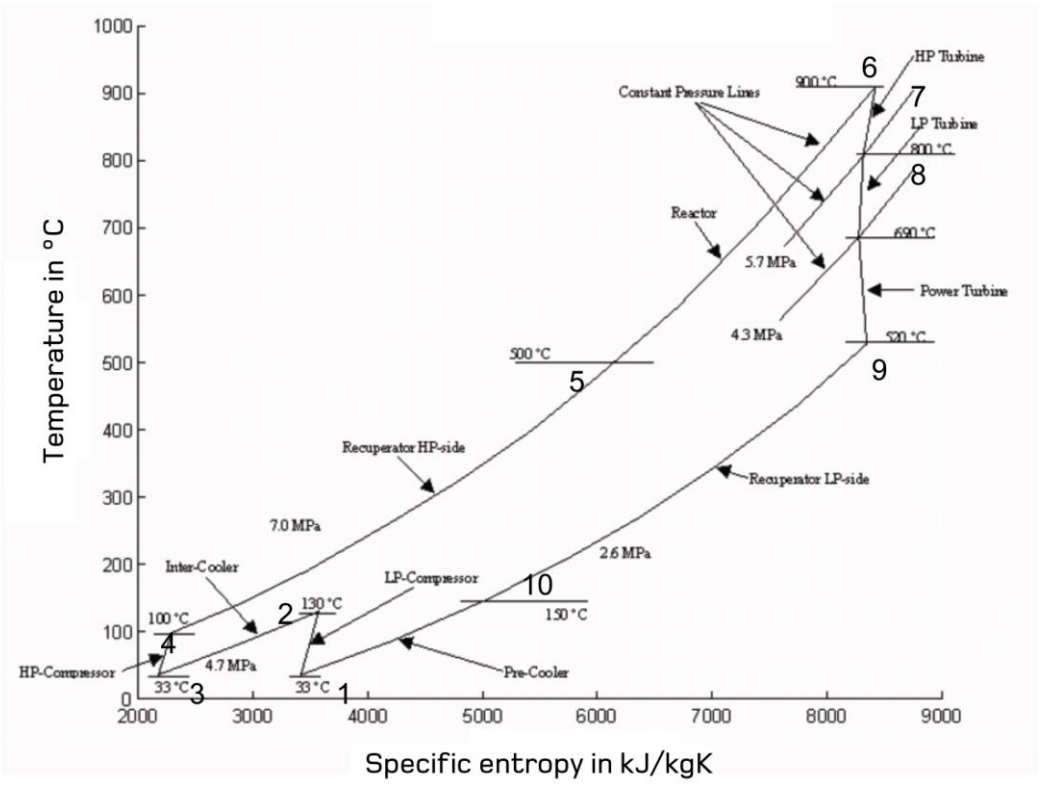

Fig. 5.2: The three shaft Brayton cycle T-s diagram.

5.2.2 Main Components of a Single Shaft Recuperated and Inter-Cooled Brayton Cycle

Fig. 5.3 demonstrates the system description and its main components as they are depicted in the single-shaft layout.

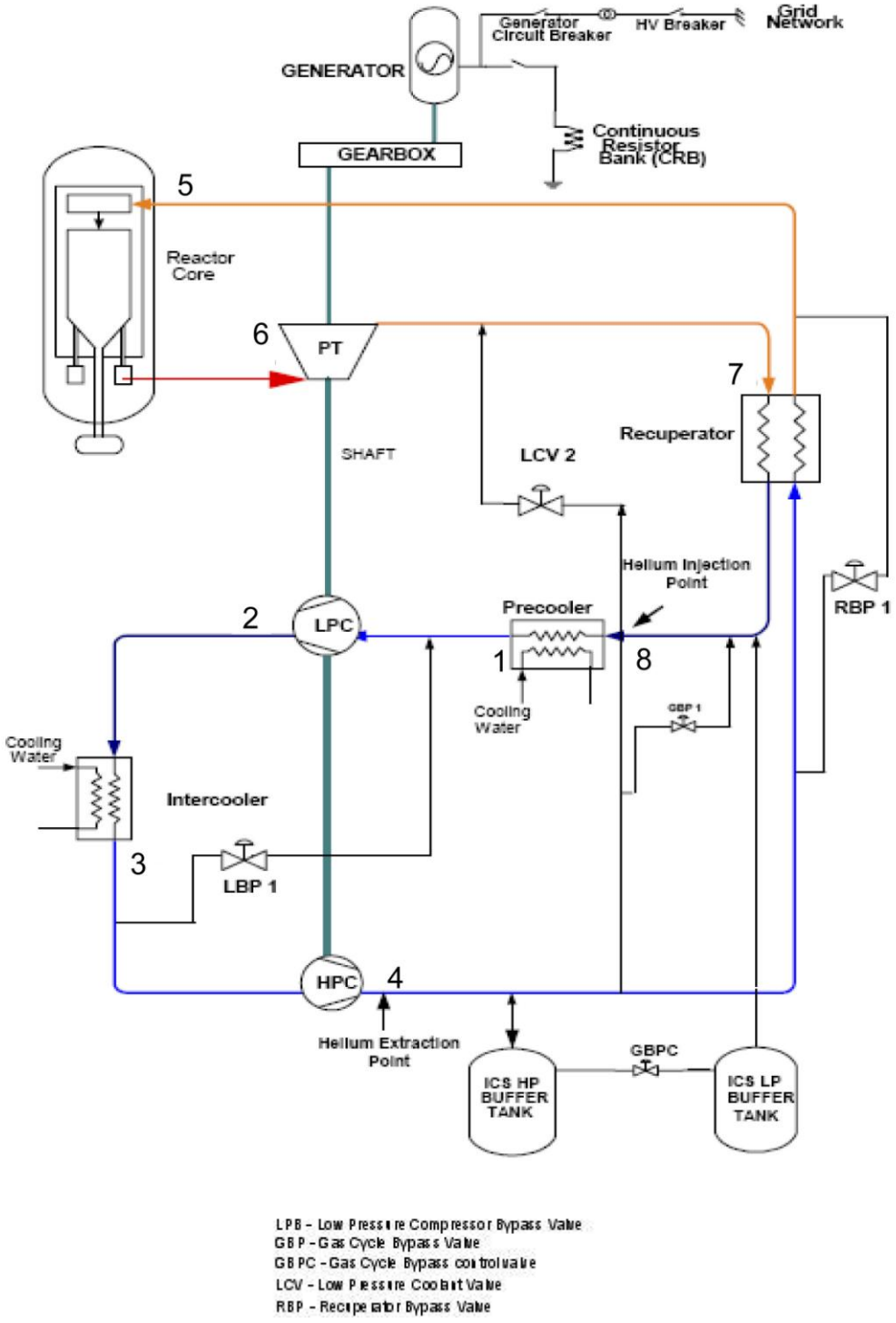

Fig. 5.3: Schematic diagram of an HTR connected to a single shaft Brayton cycle PCU [67].

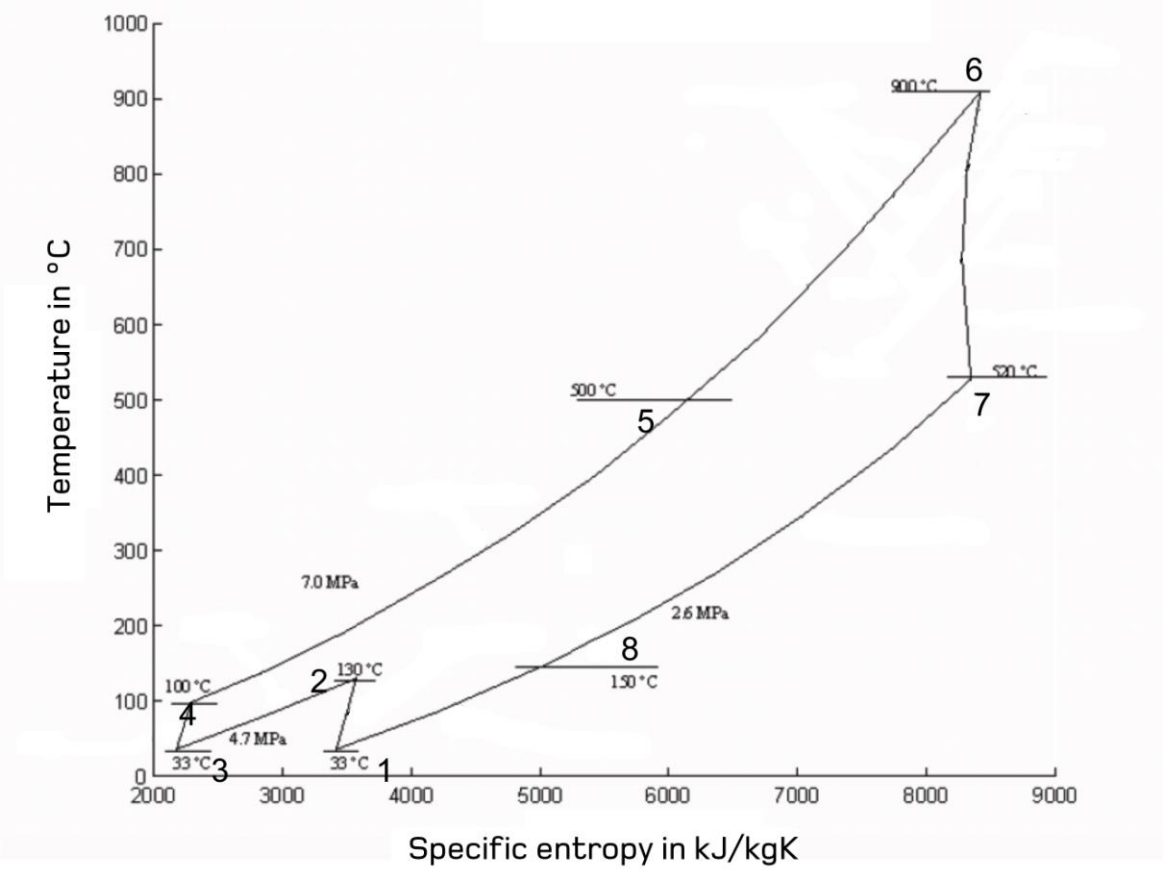

Fig. 5.4: The single shaft Brayton cycle T-s diagram.

Fig. 5.4 shows a schematic layout of the PBMR demonstrated by a high temperature gas cooled reactor connected to a single shaft recuperative inter-cooled closed Brayton cycle loop using helium as coolant. Here, the helium enters the power turbine at state 6, where the gas expansion drives the shaft, on which the power turbine is mounted. The power produced by the power turbine is then partially transmitted to the low pressure and the high pressure compressors, which are both located downstream in the flow path. The rest of the power is transmitted to the grid via a gearbox. All other states in the circuit can be described in a similar way to the gas cycle demonstrated for the three shaft system.

Also in the single shaft configuration, the helium inventory is adjusted for long-term part load operation.

5.2.3 Pebble Bed Reactor Basic Design Data

Fig. 5.5 exhibits a schematic representation of the 268 MW_{th} core, as an example for an equilibrium core used in the transient analyses. The main design parameters of the reactor core are shown in Table 5.1.

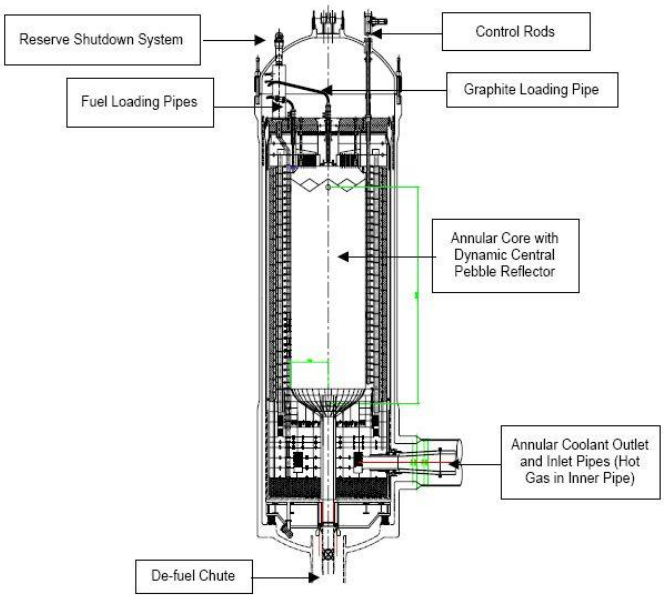

Fig. 5.5: The 268 MW_{th} PBMR reactor unit [22].

Table 5.1: Main design parameters of the 268 MW_{th} PBMR reactor unit [40].

Description	**Value**
Core outer radius (m)	1.75
Core height (m)	8.5
Radius of dynamic central column (m)	0.786
Mixing zone outer radius (m)	1.109
U-235 content for equilibrium fuel (g/fs)	0.72
Fuel kernel diameter (μm)	500
Particle material type (-)	UO_2
He inlet/outlet temperature (°C)	500/900
Total inlet mass flow rate (kg/s)	129
Inlet pressure (MPa)	7

5.3 Reactor Core related Transients

5.3.1 Fast Withdrawal of All Control Rods

In the following transient simulation it is assumed that due to an unknown malfunction of the power plant all control rods are withdrawn at a high hypothetical speed of 1 m/s. This causes an instantaneous increase in reactor power. The action of withdrawal of all control rods is initiated in both WKIND and Flownex core models. It is further assumed that both scram signals have been eliminated. In reality, these signals would be activated during such an extreme accident. The starting time for the transient event is 30 s after the beginning of the simulation, which was arbitrarily chosen. This indicates the ability of the plant to maintain stable operation. The withdrawal event is accompanied by a plant shut down. A complete plant shut down is a necessary measure in order to stop the helium mass flow circulating in the system, assuring that no further heat-up of reactor core will occur. It is assumed that despite of the elimination of all scram signals, no damage is caused to the PCU. Opening the bypass valve is used as the main measure to keep the temperatures of the plant components within the acceptable range, and to initiate a reactor shut down. Similar accident cases in the Rankine cycle can be controlled by stopping the blower, which will bring the plant to a complete shut down. However, in the case analysed here, the only way to stop the helium mass flow circulating in the plant is by opening the bypass valve. Such an accident case was investigated and reported in several publications in the past ([38], [69]).

Fig. 5.6 shows the change in WKIND reactor power and the change in control rods position initiated after a 30 s simulation run time.

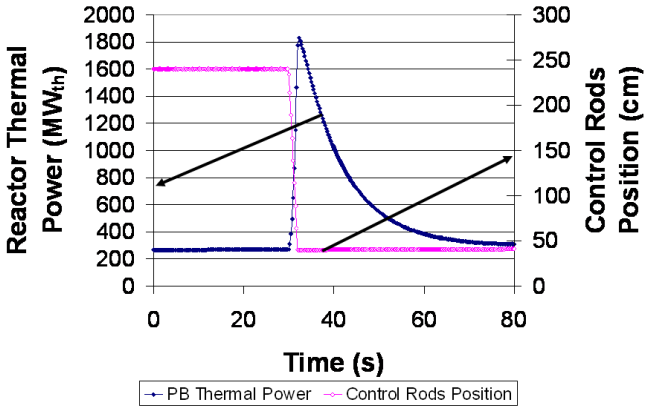

Fig. 5.6: Reactor power and control rods position (measured from top reflector) after withdrawal of all control rods in a speed of 1m/s.

It can clearly be seen, that simultaneously with the withdrawal, a very strong increase occurs in the reactor thermal power. This increase is almost seven folds greater than the reactor initial power. The sharp increase is followed by a rapid power decrease. This is due to the effect of the prompt increase in fuel temperature on the position of the control rods, which is calculated by the heterogeneous fuel temperature module in WKIND. Fig. 5.7 shows the discretisation in the core and the change in the axial temperature profile during the event.

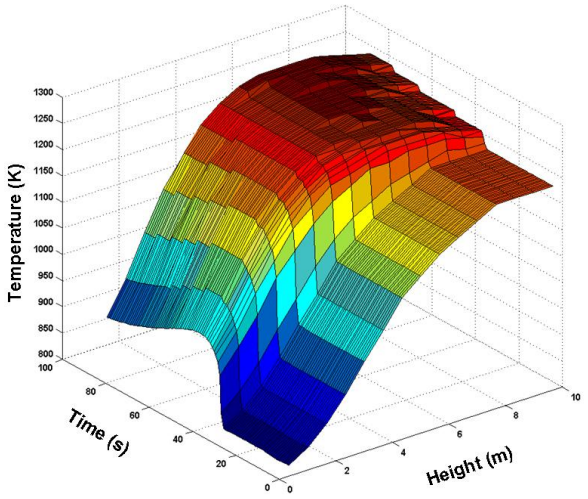

Fig. 5.7: Reactor axial fuel temperature as a function of time after withdrawal of all control rods without scram.

The immediate increase in reactor thermal power is evident. The change in the axial power distribution can be observed for each point in the matrix. The increase in power, caused by the strong insertion of reactivity into the reactor, plays a significant role for the change in the reactor fuel temperature.

For a short time, the temperature of the coated particles greatly differs from the moderator temperature (see Fig. 5.8). The reactivity equivalent of the withdrawal of all control rods from a stationary position to an end position is about 2$[2]. This reactivity is compensated by an increase of 130 K in the fuel temperature. After about 20 s also the average moderator temperature reaches a corresponding higher level, so that the isothermal temperature coefficient affects the global reactivity.

---

[2] Dollar ($) is a term used in nuclear chain reaction kinetics to define the increase in reactivity between critical and prompt critical.

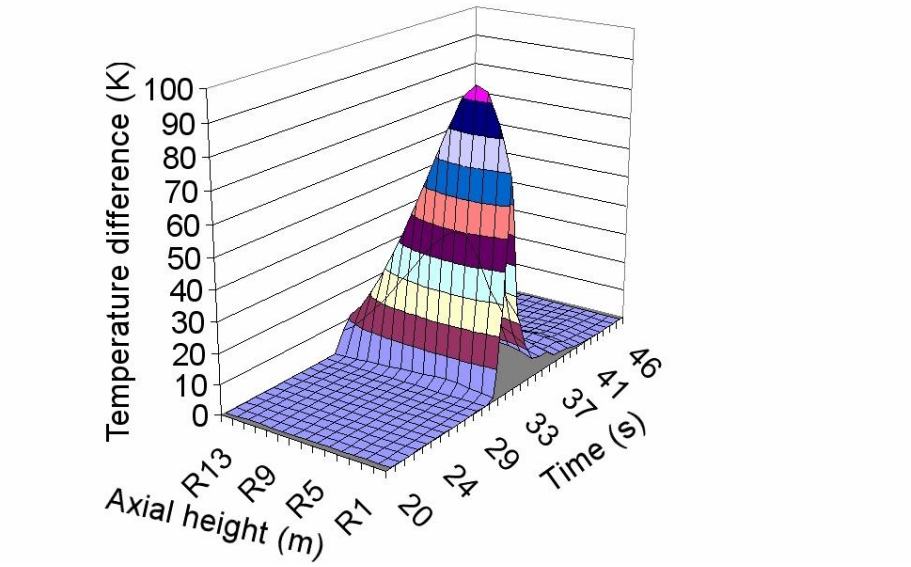

Fig. 5.8: Temperature difference between moderator and fuel temperature in the axial centre of the core after withdrawal of all control rods without scram.

This emphasises the fact that for a short relaxation time, the difference between the fuel and the moderator temperature reduces the power of the core remarkably. The heterogeneous particle model implemented in WKIND is more realistic compared with Flownex. Flownex homogeneous model predicts an unacceptable power increase by a factor of about 140, since the fuel temperature is strongly coupled to the slowly increasing moderator temperature. Fig. 5.9 shows a plot of fuel temperature, coating temperatures, average moderator temperature and surface temperature of the spheres in the axial centre of the core.

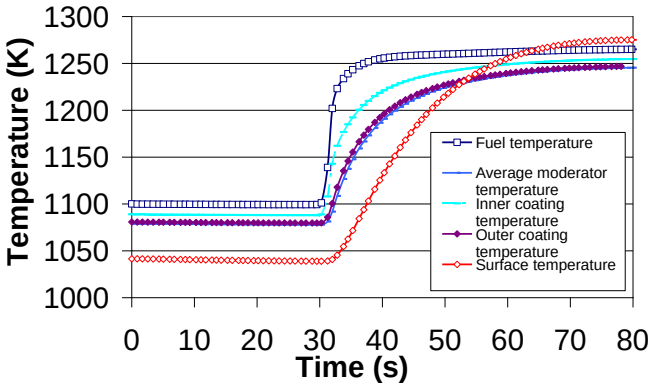

Fig. 5.9: Fuel temperature, coating temperatures, average moderator temperature and surface temperature in the axial centre of the core after withdrawal of all control rods without scram.

As the control rods are removed, the addition of external reactivity increases the fission power, which causes an increase in the fuel temperature. As for the fuel, which is represented by the UO_2 layer in the kernel; the fuel temperature increases much above the average temperature of the matrix, before the kernel reaches a homogeneous temperature. It can further be

seen, that by the time the peak has been created, the fuel temperature increases in more than 84 K, compared with the moderator temperature. This phenomenon takes place in the short time during which over power and over temperature occur in the particle. The strong reactivity feedback will then cause the total reactivity to drop to a negative value, and hence the reactor power will decrease. Due to the large heat capacity of the graphite, no large change occurs in the reactor outlet temperature and in the average fuel temperature despite of the increase in reactor power, as shown in Fig. 5.10. The following figures show the simulation results done with Flownex core model, assuming the same boundary conditions as in the case calculated with WKIND core model.

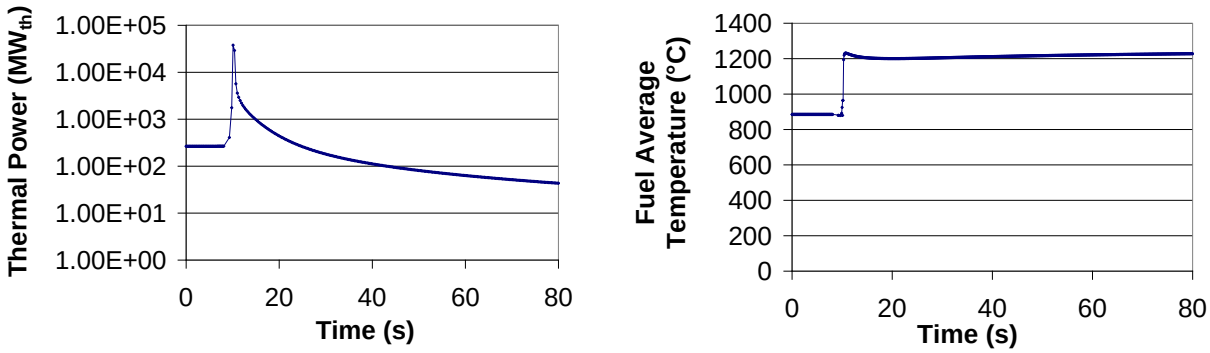

Fig. 5.10: Reactor thermal power and fuel temperature after withdrawal of all control rods without scram, three shaft configuration simulated using Flowenx core model.

As emphasised earlier, the power reaches unacceptably high levels. As a consequence, a complete plant shut down is initiated. The reactor power drops immediately, whereas the fuel temperature continues to rise. Under such conditions, the fuel particles are destroyed, and a release of fission products will occur. This example also strengthens the need for using a more detailed model than the Flownex core model, which over-predicts the reactor power level and under-predicts the average fuel temperature. In addition, it must be mentioned that a depressurisation accident is not assumed in this case. In such a severe incident the decay heat should be removed by means of natural convection. Under such extreme conditions, the system must be completely isolated from the core, and hence it is no longer of importance to treat the PCU as an integral part of the simulation. The evolution of the core temperature after a depressurisation event and the natural convection heat removal mechanism which takes place in the core could be analysed with the aid of THERMIX [70].

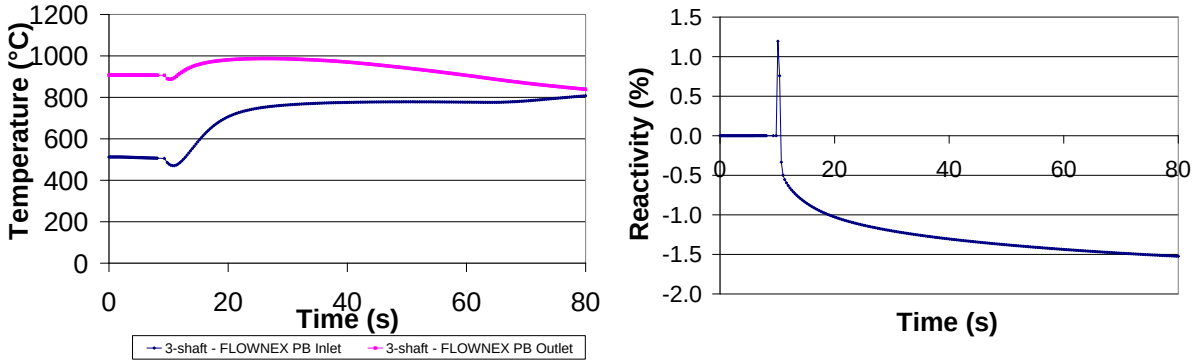

Fig. 5.11: Reactor temperatures and reactivity after withdrawal of all control rods without scram, three shaft configuration simulated using Flownex core model.

The increase in the core inlet temperature leads to a negative reactivity, and therefore the reactor power is reduced. Less heat is transferred to the helium, and this large effect causes the reactor outlet temperature to decrease, as it can be seen in Fig. 5.11. During the same period of time, the bypass valve is maintained at an opened position. Further description about the bypass valve is given in load rejection transient case. The loss of forced circulation in the circuit is stopped (Fig. 5.12). Similar effects to those discussed in a load rejection case appear here as well, but increased, since the system pressure ratio reduces to unity for pressure equalisation. The cooling of the core is done by means of radiation and convection mechanisms via the reactor cavity cooling system.

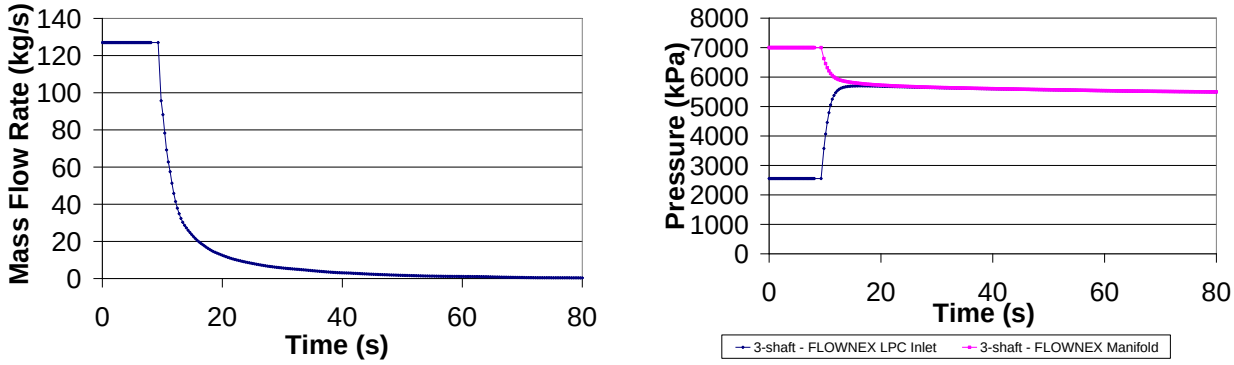

Fig. 5.12: Reactor mass flow and system pressure after opening of the bypass valve, three shaft configuration simulated using Flownex core model.

5.3.2 Withdrawal of all Control Rods with Scram and a Plant Shutdown

The withdrawal of all control rods at a speed of 1 cm/s is initiated and simulated by both Flownex and the WKIND core models at a predefined time of 8 s. It was furthermore specified that a complete shut down by control rods would be initiated as soon as a power level of

120% has been reached. The first scram signal, which is a shutdown criterion for the reactor protection system, is activated at a neutron flux which is equal or greater than 120% of the nominal value. At t=25 s, the criteria for shut down has been reached, and all control rods are inserted. This causes an immediate decrease in reactor power. Hence, the system cannot maintain a full power operation and a decoupling from the grid and a shut down of the power turbine is requested. Another option for a sub-critical reactor core in this case is maintaining a hot stand-by of the reactor, whereby a stable operation of the power turbine is maintained using the bypass valve. This is necessary in order to prevent the turbine from coasting down and to prevent further severe consequences to the components. The current simulation has been performed using both three shaft and single shaft system configurations. It is shown in Fig. 5.13 that the shut down causes the reactor power to decrease. Both core models show a good agreement qualitatively. Yet, the results achieved by the WKIND core model indicate that the core reaches a slightly higher power level than the power level reached by Flownex core model. These small differences between the models are a result of the reactivity coefficients in Flownex, which were not completely consistent with the coefficients implemented in the WKIND core model.

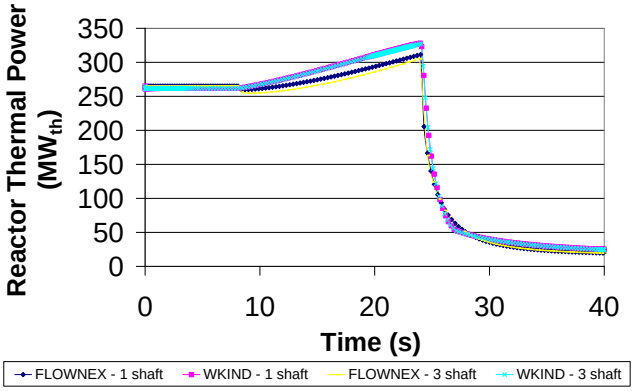

Fig. 5.13: Reactor power after a control rods withdrawal with scram and load rejection, single and three shaft configurations, WKIND and Flownex core models.

The interactions between the PCU and the pebble bed core are great, and hence, due to the opening of the bypass valve, the mass flow decreases as the compressors power decreases. Fig. 5.14 indicates that the reactor inlet temperature increases rapidly because of the opening of the bypass valve. As the power turbine which uses as the main heat sink for the reactor thermal power is bypassed, the hot helium returns via the recuperator into the system and into the inlet of the core. This result is also shown later for a load rejection case. Furthermore, the

models demonstrated the same trends in the dynamic characteristics of other system components parameters, such as the recuperator temperatures, the system pressures etc. [21].

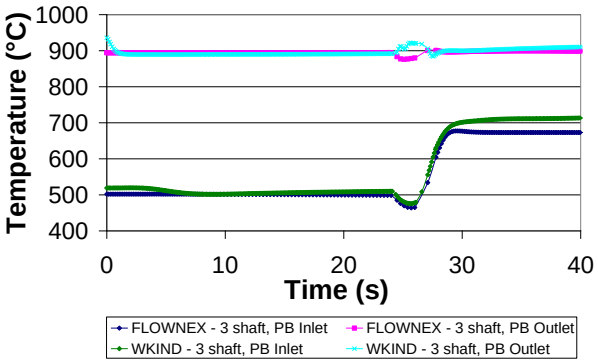

Fig. 5.14: Reactor temperatures after a control rods withdrawal with scram and load rejection, three shaft configuration, WKIND and Flownex core models.

It has been observed in both core models, that the large thermal capacity of the reactor core allows relatively fast load changes in the system, without requiring fast response from the core. Thus, the energy stored in the core can be decreased or increased, with minimal core temperature changes. It must be mentioned that similar results were achieved using the single shaft system configuration coupled to each of the core models. Furthermore, it is possible to observe that small differences exist between WKIND and Flownex core models. These can be contributed to the reactivity coefficients applied in the point kinetics model used in Flownex, which differ than those used in the space dependent model in WKIND. In addition, WKIND uses a certain dependency of the control rods position implemented in its 1D neutronics approximation, which is somewhat different than the reactivity curve used in Flownex. However, the discrepancies observed between the fuel temperature and the temperature of the surrounding matrix are not strong, due to the relative slow decrease in reactor power. The strong changes in the core inlet temperature are observed in the results calculated by both core models and they correspond to the changes in the reactor power. As the agreement between the core models is deemed acceptable, the following transient simulations will only employ the Flownex core model, and will mostly treat the differences between the single and the three shaft configurations. Furthermore, the effect that the design of the plant has on the major system components during normal and upset conditions shall be investigated.

5.4 System Related Transients

5.4.1 Load Rejection Transient

Full load rejection due to the loss of grid power is one of the most severe load control scenarios for a power plant. Despite of the steep temperature and pressure gradients which can occur during a load rejection event, the system must be designed to minimise the stresses on the components and the temperature and pressure conditions must be kept within operating limits. Once the electric load has been decreased, the large amount of excess power on the turbine-generator shaft will drive the power turbine to speed up. In both single and three shaft system configurations, a gas bypass valve control is used to maintain the power turbine shaft at the nominal operating speed. The bypass valve connects the points of the highest and lowest pressure within the system and reduces the overall system pressure ratio and also the power output [21]. Furthermore, in the three shaft system each of the compressors was also equipped with a local bypass valve, in order to insure stable operation of the compressors during and after a load rejection event. In the single shaft configuration, the bypass valve connects the high pressure compressor outlet to the inlet of the low pressure side of the recuperator, and no local compressor bypass valves were employed. In addition, in the three shaft system the grid power is stepped down from full load of 112 MW_{el} to 10 MW_{el}. This is the power level of the resistor bank, which is activated to dissipate the excess energy of the shaft and to secure that the power turbine does not over speed. However, since the fluid power cannot be dissipated instantaneously due to inertia and compressibility effects, some degree of over-speed will always occur [71].

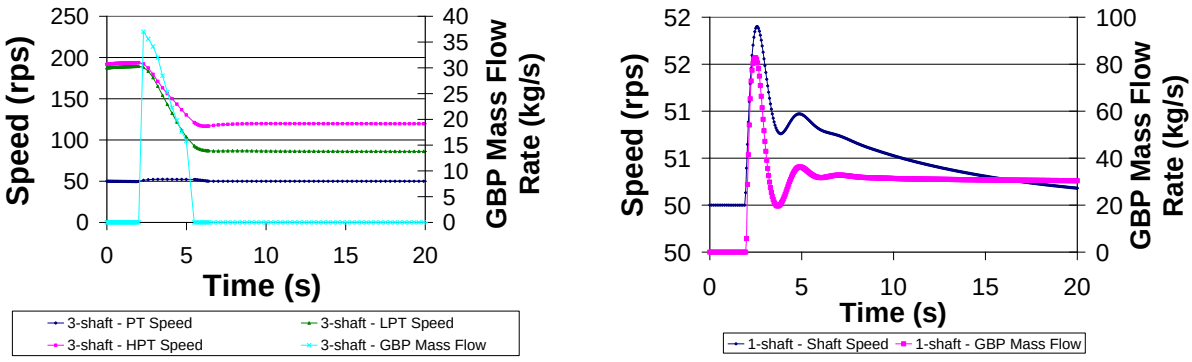

Fig. 5.15: Turbo units' rotational speed and bypass valve mass flow rate during load rejection transient, single and three shaft configurations.

Fig. 5.15 shows the variations in turbo units' speeds and the bypass flow during a loss of load transient in the single and the three shaft configurations. In the three shaft system it can be seen that the controller managed successfully to prevent the power turbine over speed and to stabilise it at the normal operation conditions at 3000 rpm (50 Hz). This is done by means of opening the bypass valve. Additionally, the speeds of both high and low pressure turbines decrease substantially due to the reduced mass flow. Both units manage to reach a new steady state, stabilising the system at the new power level. It is also possible to see that during the event, the bypass flow reaches a maximum of 37 kg/s. In order to avoid a very large flow through the valve, 8 valves are used in parallel. The total flow which is bypassed is equivalent to about 150% of the power turbine nominal flow. Fig. 5.15 further indicates that the shaft speed of the singe shaft system reaches a value of approximately 3150 rpm before decreasing again. It is furthermore shown that the controller adjusted the helium mass flow which passes through the bypass valve, via a change in the valve diameter after sensing the power turbine speed. Each of the bypass valves employed obtains a maximum flow rate of 82 kg/s. The total maximal flow rate contributed to the three valves opening in parallel is about 190% of the nominal turbine flow. In both systems, the shaft speed increases before it reaches again the nominal speed value. This can be explained by the time it takes to reach a new pressure ratio in the system and the time needed for the redistribution of the mass between the high and the low pressure zones, especially in the three shaft case. The temperature transients are a non-avoidable consequence of the pressure ratio variations over the turbo-machines.

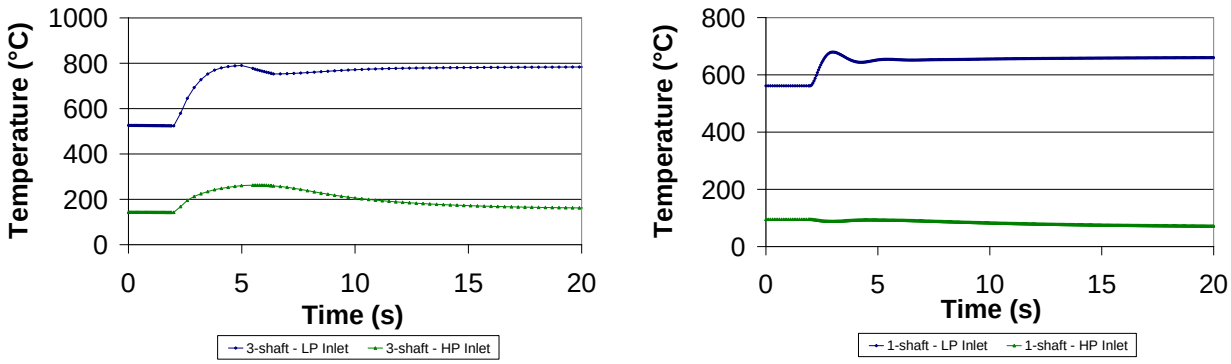

Fig. 5.16: Recuperator's inlet temperatures during load rejection transient, single and three shaft configurations.

The impact of the temperature and pressure transients could lead to high stresses on materials of the main components. Therefore they must be taken into account at the design phase of the plant. Fig. 5.16 shows the temperature evolution in the recuperator heat exchanger at the inlet of the primary and of the secondary side of both single and three shaft configurations. It can

be seen that short-circuiting the system results in hot helium entering the primary side, i.e. the low pressure side of the recuperator. The secondary side experiences only a small decrease. This is due to the large thermal mass of the recuperator, which delays a temperature increase of the high pressure gas. The recuperator low pressure inlet temperature increases in approximately 250°C to 300°C during the event in both systems. Fig. 5.17 shows the change in system pressures during the event in the two different shaft configurations.

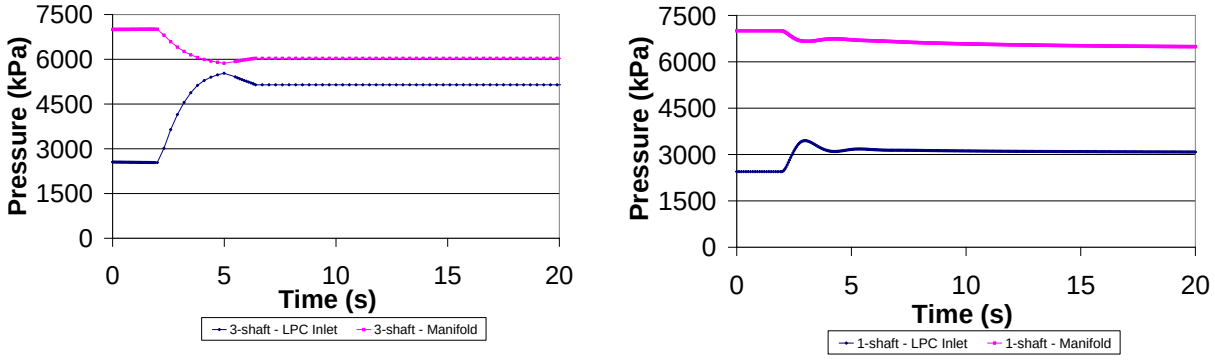

Fig. 5.17: System pressure at LP Compressor inlet and at the manifold during rejection transient, single and three shaft configurations.

It can be seen that the circuit's pressure ratio decreases after opening the bypass valve. The single shaft configuration tends towards stabilisation at a new steady state with a significantly smaller pressure difference than the difference reached in the three shaft configuration, due to the difference in the valve opening between the two systems. Fig. 5.18 shows the variation in reactor temperatures during the transient.

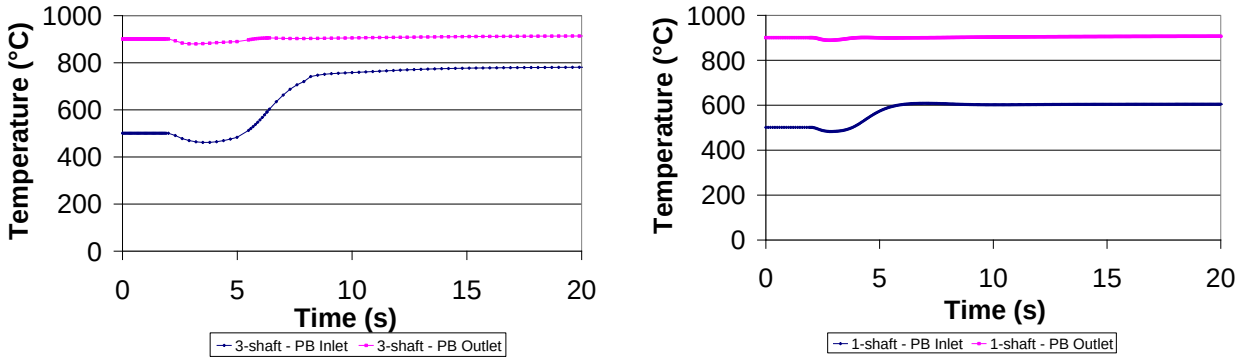

Fig. 5.18: Pebble Bed Reactor temperatures during load rejection transient, single and three shaft configuration.

While the reactor inlet temperature slightly decreases and then significantly increases, the reactor outlet temperature remains almost constant in both shaft configurations. The steep change in the inlet temperature occurs due to the high level of interdependence between the

recuperator and the reactor. The large bypass flow, in combination with a decreased pressure ratio, causes a higher turbine outlet temperature, which feeds back through the recuperator and results in a higher reactor inlet temperature. On the other hand, the nearly constant value of the reactor outlet temperature reflects the rapid feedback from the fuel temperature to reactivity, by which the power output is adjusted to match the cooling capacity of the reduced helium flow. Fig. 5.19 shows the variations in turbo-machines' efficiencies during the event in the three and in the single shaft configurations respectively. The change in the helium flow velocities reduces the machines efficiencies. It is clear that during the event, the efficiency of the three shaft power turbine drops to zero. At this stage, the turbine will not have any electrical output, and the efficiency increases again as the resistor bank has been activated. On the other hand, in the single shaft configuration, since the shaft speed and consequently all other turbo-machines speeds are controlled to operate close to their design point at 50 Hz, the variation in efficiencies is not as severe as in the three shaft configuration. The temporary reduction in the PCU efficiency must be retrieved by means of long term adjustments of storage or addition of helium in order to maintain a sufficient power level efficiency. Such changes will be discussed in the next transient analysis of load following.

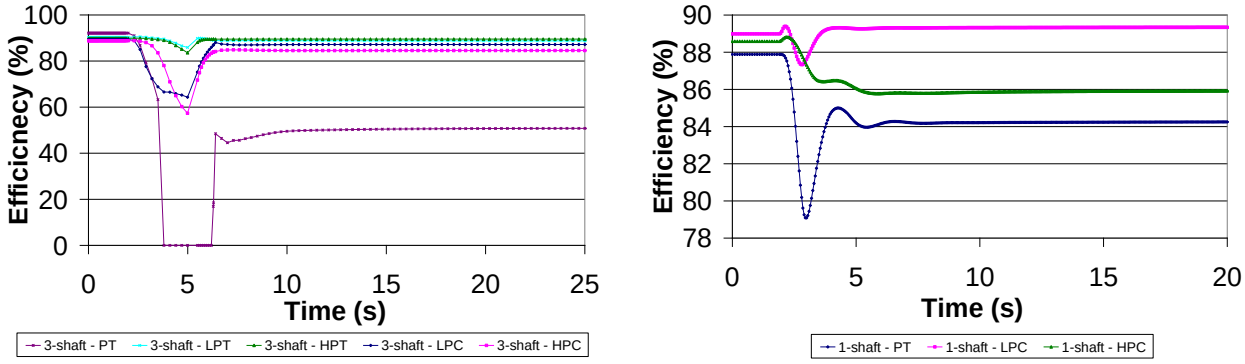

Fig. 5.19: Turbo-machines' efficiencies, single and three shaft configurations.

In order to ensure stable operating conditions of the system it is also important to prevent the compressors from entering the surge region.

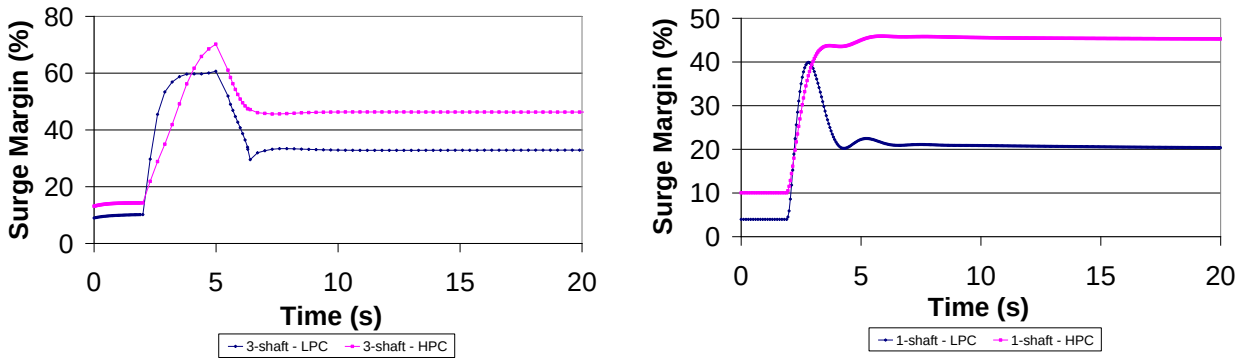

Fig. 5.20: Compressors' surge margins, single and three shaft configurations.

Fig. 5.20 shows that during the transient, the operating conditions of both high and low pressure compressors in both configurations and especially in the three shaft system change substantially. This effect is contributed to the use of bypass valves, which causes a significant change in mass flow rate through the high pressure and the low pressure turbines in the three shaft system followed by a substantial drop in their speeds. It is seen that the compressors do not go into surge. A negative surge margin in the plot indicates that the compressor has crossed the surge line. The use of local compressor bypass valves in the three shaft configuration allows the compressors to maintain stable operation. The analysis of a load rejection transient shows that both systems behave in a rather similar way. In both configurations, the operating conditions of the high pressure and the low pressure compressors significantly change during the simulation. Yet, both compressors succeed in moving away from surge. The efficiencies of the turbo-machines in both configurations have degraded substantially, especially the efficiency of the power turbine of the three shaft configuration. Moreover, the power turbine in both systems speeds up, due to the larger excess in power after the event. In both systems, the reactor outlet temperature hardly changes, yet the temperature of the recuperator low pressure side increases, and so does the core inlet temperature. A special care must be then given to avoid potential thermal stresses on material structures.

5.4.2 Load Following Transient

Under normal operating conditions, it is possible to control the electrical output of the power plant and to maintain high efficiency by changing the power output at a certain rate. Such a change can normally be followed by controlling the helium inventory level in the primary circuit. This implies that the helium coolant is either extracted from or injected into the system, resulting in changes in the system pressure. Load following in the PBMR is done using

the Helium Inventory Control System (HICS), and the helium is stored in the inventory system tanks after it is being extracted from the system [72]. The helium tank is modelled in Flownex as a reservoir at a constant pressure. In the following transient scenario, a load ramp from 100% to a partial load operation of approximately 40% and then back to 100% is simulated. The transient starts by opening the valve connecting the helium tank to the high pressure compressor outlet plenum, where the pressure in the system is maximal. This allows the helium inventory in the system to reduce to a 40% level. During this time the valve is choked, so that the mass flow through it is reduced linearly with the reduction in system pressure. After 5.6 hr, a load increase procedure is initiated in order to restore the helium inventory. This is done by opening a valve connecting the low pressure side of the system and the helium tank, which allows helium flow into the system. In both shaft configurations, helium is injected to the pre-cooler inlet, and is extracted after the manifold. Despite of the change in helium inventory in the system, the pressure ratio and the temperatures within the circuit remain nearly constant, and only the helium density and the system power are changed. In this manner, the circulating mass flow is reduced linearly with the power produced, but the gas velocities remain the same. Therefore, the turbo-machines operate at inlet conditions which are close to their design conditions, yielding a comparable high efficiency [73]. As similar simulation results were obtained in both shaft configurations, the three shaft configuration has been chosen for the demonstration. The plant behaviour during the transient is demonstrated in the following figures. Fig. 5.21 shows the effect of helium injection and thereafter extraction on the maximum and the minimum system pressures and the pressure in the helium inventory tank.

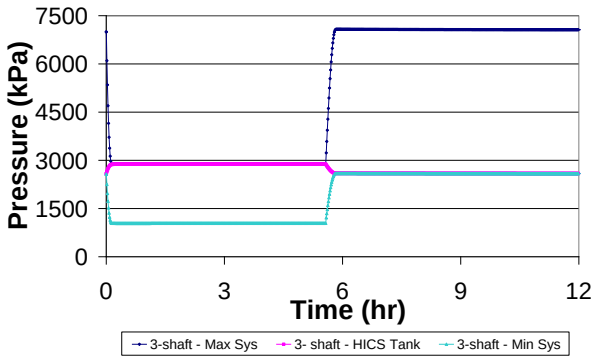

Fig. 5.21: Variation in the maximum system pressure, the minimum system pressure and the tank pressure during load following transient, three shaft configuration.

Extraction of helium from the high pressure zone of the PCU causes the pressure to drop from 7000 kPa to about 3000 kPa. In the same time, the pressure in the tank increases, as more he-

lium is stored in it. Fig. 5.22 shows that the power produced by the power turbine is reduced linearly with the reduction of helium inventory. In the same manner, injection of helium causes the power to reach its initial value, returning to nominal operating conditions.

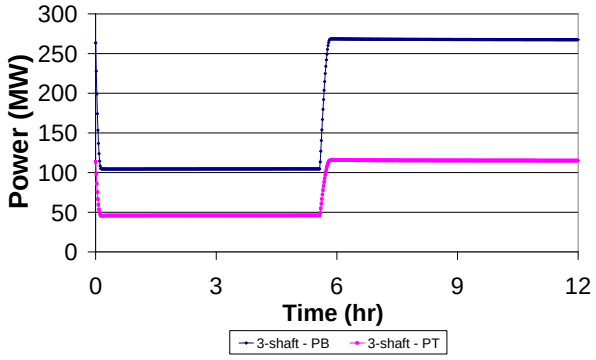

Fig. 5.22: Variation in the pebble bed reactor thermal power and in the power turbine power during load following transient, three shaft configuration.

It is shown that the power output first decreases, when mass is extracted, due to the decreasing pressure difference across the power turbine. Then power starts to increase when mass is injected into the system. Once the power demand declines, the power produced by the turbine will decrease. Due to the increase in reactor outlet temperature, the reactivity will become negative and accordingly the flux and the fission power will decrease, in order to adjust the amount of the heat produced by the reactor to the amount of heat removed by the PCU. As the reactor starts to cool down the reactivity will become positive. The power rises again with the restoration of the nominal helium inventory. Thus, the power production returns to its equilibrium level of 268 MW_{th}. As soon as helium extraction from the PCU has stopped, the gas velocities and the pressure ratio in the circuit have reached their nominal values, and the same is true also for the reactor outlet temperature.

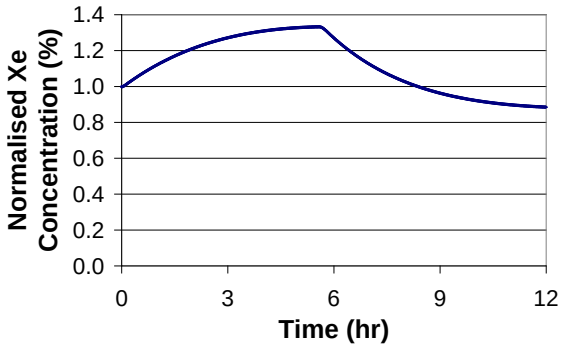

Fig. 5.23: Normalised xenon concentration during load following transient, three shaft configuration.

Fig. 5.23 shows the relative change in xenon density during the event. The initial concentration of 1% is the relative xenon concentration compared to its concentration in equilibrium. A decrease in reactor fission power results in a gradual build-up of the ^{135}Xe concentration. This is a result of the decay of ^{135}I and a decrease in xenon transmutation. A new equilibrium will result some time after the transition. ^{135}Xe has a very large absorption cross section for thermal neutrons, and with the increase, it would be impossible to return to the original fission power before the xenon concentration has decayed below a critical value. The excess reactivity in the core can override this xenon poisoning effect, and an up-word power transition will be possible at any requested time. The maximal xenon concentration is reached after 5.6 hours, and from this point on the xenon will decay to its end value.

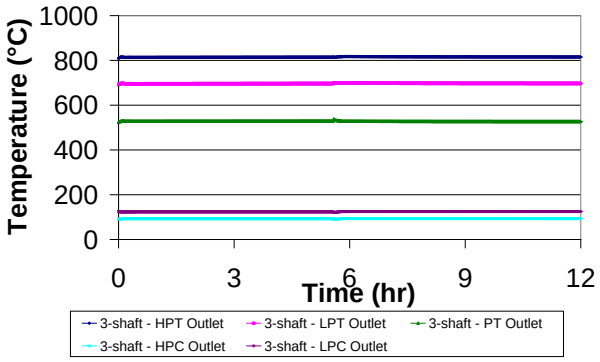

Fig. 5.24: Temperature evolution at turbines and compressors outlet during load following transient, three shaft configuration.

The volumes handled by the turbo-machines and the circuit temperatures remain almost constant, which is shown in Fig. 5.24. The machine efficiencies and therefore also the plant efficiency undergo practically no change with pure pressure level control. Hence, the advantage of this method of control is its economy. The efficiencies of both single and three shaft configurations are expected not to be degraded. However, the literature indicated, that multi shaft machines are in this case superior to single shaft ones [24].

From the transient demonstrated here it is evident that Flownex is also capable of calculating long-term transients with a time span in the order of magnitude of several hours.

5.4.3 Helium Leakage

Breaks in the pressure boundary have been classified into three break sizes [74]. Small breaks, often referred to as leaks, are holes of up to 65 mm in diameter. Medium breaks relate to an opening of an equivalent diameter, which is not greater than 230 mm. Large breaks are openings in the pressure boundary layer which are larger than 230 mm. A break of a medium or of

a large size can lead to a depressurised loss of flow, which is one of the accident scenarios investigated for the design of nuclear reactors. In the current accident, the pressure is lost due to a small crack in a pipe. The crack has a distinct diameter and a leakage area, which causes the mass flow circulating in the PCU to decrease. The size of the leakage area is assumed to be 0.003318 m^2, which corresponds to a crack with a diameter of 65 mm. Such a scheme could occur as a result of a pipe rupture at the outlet of the high pressure compressor, which refers to point 4 in Fig. 5.1 and Fig. 5.2. Helium will then flow out to the environment until the pressure is established at 100 kPa. The leakage is modelled as an orifice (restrictor). The restrictor is initially closed, and is opened at t=1 s. At t=6 s, a special signal indicates of the failure whereby rapid loss of helium of the system occurs. The counter-acting measure is a reduction of the system pressure by a decoupling of the generator from the grid.

The resulting mass, pressure, temperature and reactor thermal power transients are shown respectively in the Fig. 5.25-Fig. 5.28.

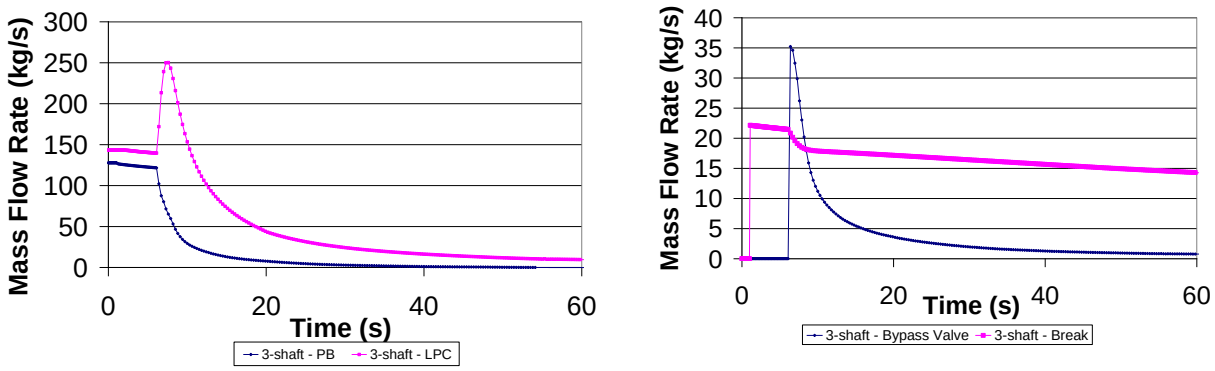

Fig. 5.25: Mass flow variation in reactor core and low pressure compressor, and mass flow variation in bypass valve and break during a pipe break transient, three shaft configuration.

Fig. 5.25 demonstrates the control strategy in the case of a pipe break. The break causes a continuous decrease in the circuit mass flow. The high mass flow rate through the bypass valve decreases the loss of helium from the system for an instant. As it was seen in previous transient cases, also here the compressors will tend to surge due to the strong changes in the operating conditions of the circuit. Therefore, local compressors bypass valves will open rapidly and completely. This is done in both single and three shaft configurations, in order to keep the compressors in a safe margin from the surge limit.

Fig. 5.25 further shows that the instantaneous pipe break leads to a rapid decrease in mass flow rate of the low pressure compressor, after a sharp increase due to the local bypass. As the reactor core and the turbines flow are being directly connected, the helium flow through the

reactor core decreases as well. After 50 s the helium circulation in the reactor core is zero. In the same time, the turbo-machines are brought to a complete stop due to the bypass valve, which is kept opened during the transient.

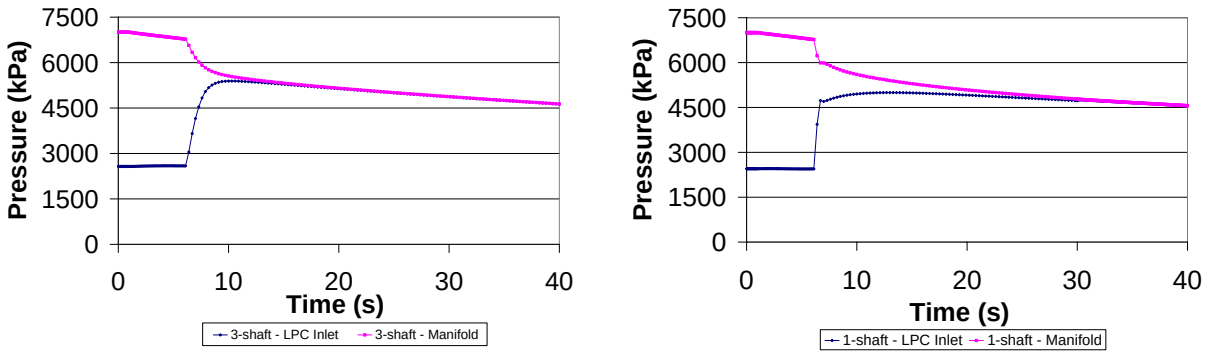

Fig. 5.26: System pressure at low pressure compressor inlet and at the manifold during a pipe break transient, three and single shaft configuration.

According to Fig. 5.26, a sharp decrease of 2000 kPa in the pressure of the low pressure compressor inlet is experienced in the first 10 s in the three shaft system. A similar level of pressure is experienced in the single shaft system at t=20 s. The opposite occurs at the manifold, which undergoes a strong increase in pressure. After a pressure equalisation has been reached, the pressure transient becomes notably flatter.

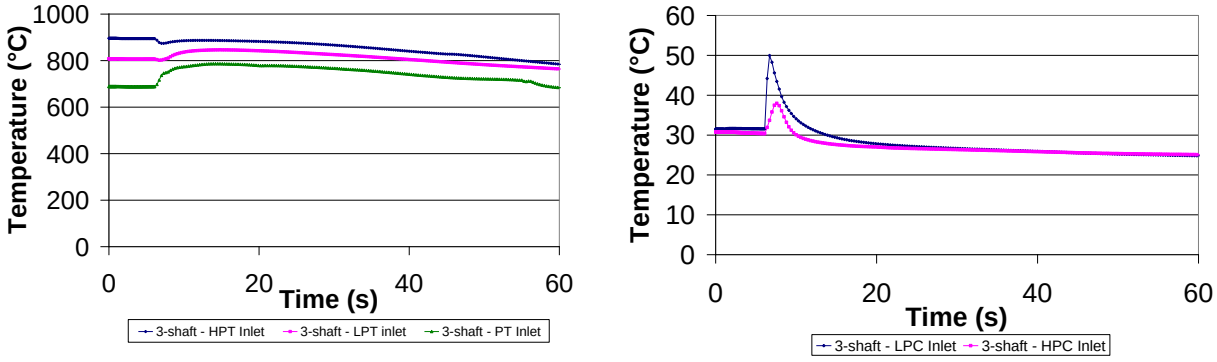

Fig. 5.27: Turbines' and the compressors' inlet temperature variations during a pipe break transient, three shaft configuration.

The temperature evolution at turbines and compressors inlet in the three shaft configuration is presented in Fig. 5.27. The turbines' inlet temperatures undergo a small increase followed by a stronger decrease. However, the relatively high thermal capacity of the three turbines has an effect which causes a balancing process of the temperatures to takes place more slowly than the corresponding pressure balancing process. The compressors show a similar behaviour as

the turbines, except for a peak and a temperature rise due to the quick and the full opening of the bypass valve.

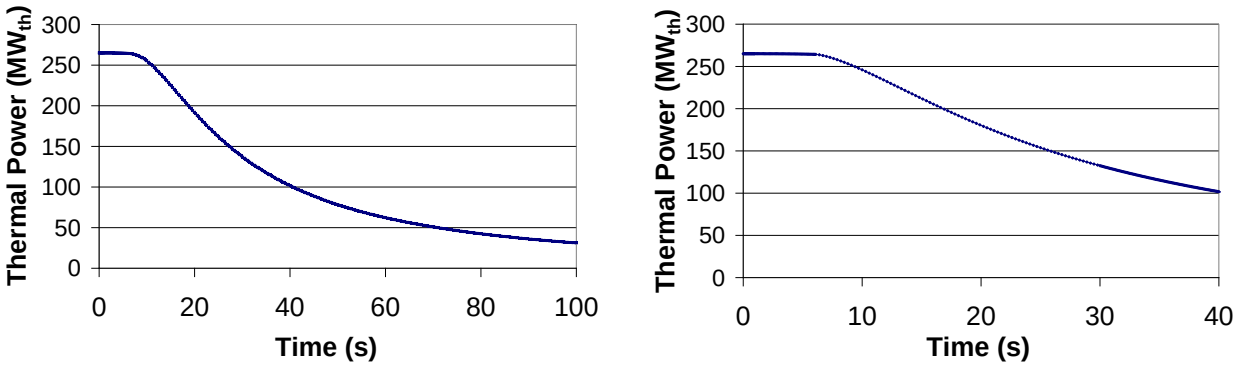

Fig. 5.28: Variation in reactor thermal power during a pipe break transient, three and single shaft configuration.

Fig. 5.28 shows the heat transferred to helium in the reactor core in both single and three shaft configurations. Heat removal from the core occurs continuously from the beginning of the transient. After the turbo-machines have stopped, heat extraction of the residual heat from the core occurs by means of natural convection. After 100 s, the reactor core thermal power is 39 MW_{th} in the three shaft system. On the other hand, the thermal output of the single shaft reactor decreases to 40% of the nominal value after 40 s. These are however not the end values.

6 Discussion and Conclusions

This thesis presents transient analyses of a Pebble Bed High Temperature reactor coupled to a PCU, which resembles to the project of the South African PBMR plant. In order to perform the analyses, a code system has been developed. This code couples the reactor core model code to the thermal hydraulic code of the PCU. This coupling has been developed in order to create a more realistic and a more detailed simulation of the entire system for the reactor safety analysis. This development renders the assumptions which should have otherwise been made concerning the time evolution of the boundary conditions for each of the separate systems: the reactor core on one hand and the PCU on the other hand.

The main calculation tool used for the transient analyses of the complete system is the thermal fluid network analysis code Flownex. Flownex focuses on models for the various components of the PCU, and encompasses a less detailed model for the reactor core. In order to validate the models for the individual components, Flownex models have been verified against the experimental results of the German facility EVO II.

6.1 Complete System Model

The design of the components of the complete Brayton cycle PCU was done with the aid of Flownex. The code encompasses the thermodynamic properties of a variety of fluids and gasses. Flownex encompasses detailed components models. It is therefore suitable for modelling power plants such as the direct closed Brayton cycle with a Pebble Bed Reactor as its heat source. Flownex is built in a modular way, and can be adapted for solving any kind of complex thermal-fluid networks or power plants. Flownex core model was developed with an emphasis on simulating a complete integrated system, which includes the reactor core and the PCU. This fact is of advantage, because it allows for the modelling of complex thermal-hydraulic networks, and especially of the complete plant within one code with fast calculation times. The PCU was connected to two different generic shaft configurations, namely: the single and the shaft. Component models needed for the simulation of the complete Brayton cycle have already been included in the subroutine of the code, and were deemed accurate enough for transient analyses of the complete plant. In order to simplify the simulation procedure, the design of the utilised reactor core model, as well as the principle design of the components in the primary circuit of the single and the three shaft configurations was kept as similar as pos-

sible. It has been shown that it is possible to depict a complete system model for both shaft configurations using Flownex.

6.2 Code Validation

A number of options exist for the verification and validation of a thermal-fluid system model. The most obvious option is a comparison with data from the actual plant, which is the method selected in this thesis. Most of the literature for the validation was gathered in the frame of the European project RAPHAEL. The importance of the validation is on one hand the modelling and construction of a complete power plant from scratch, using and interpreting the geometrical data and the information gathered from the literature. By doing so, a large variety of modelling challenges were confronted, such as the modelling of diffusing leakage flows, valves, and the thermal inertia of a tank wall. On the other hand, the validation provided the opportunity to validate Flownex calculations against experimental data derived from a large-scale Helium Brayton cycle installation. This modelling also assisted in the construction of the single shaft layout, as these circuits are very similar thermodynamically. The observed differences in the main system parameters, such as power, temperatures, pressures and mass flows are within a few percentages. Furthermore, Flownex models predict the same trends as the experimental results for a load following transient, except for the temperature evolution in tank 1. All differences found could be explained, and therefore the models can be considered acceptable for using in further analyses. Some of the models have been treated in a simplified way. In some cases, the simplifications do not introduce any additional uncertainties to the results, such as in the treatment of the valves connecting the storage tanks to the main circuit in the load following transient. On the other hand, the treatment of the leakage flows and the heat losses in the system should be improved in the future study. Another recommendation is to replace the pipe element, which substituted the heater element existing in the real installation, by a conductive heat transfer element. This element can be designed to model the heat transfer through solid materials, the solid-fluid convection interaction and the radiation heat transfer in the heater. In addition, the turbo-machines models in Flownex become less accurate having applied them for a different machine than the original design was assigned for. Hence, the transient analysis should be repeated in the future using the original turbo-machines' characteristics, or similar maps conducted from the turbo-machines geometry. The

retrieval of additional documents, and in particular documentation of supplementary transient cases, would allow for the extensions of the validation exercise.

6.3 Coupling Methodology and Reactor Models

WKIND is considered to be a detailed code system for the neutronics calculations of the reactor core. Therefore, it was used to replace Flownex reactor core model. As it is not viable to directly couple Flownex to other codes, an indirect coupling method was purposed. The coupling attempts to match characteristics values of WKIND core model with the Flownex PCU. These characteristics values are updated after every time step. The coupled programme combines the detailed neutronic and thermal hydraulic behaviour of the WKIND core model, which incorporates a 1D neutronics and thermal hydraulics part with the thermal hydraulics of the PCU, to assess detailed calculations of transients of the complete system.

Both core models are very useful to get proper boundary conditions for the core transients during accidents. However, Flownex core model was developed in order to assess a gain in the time needed for the calculations of the complete system model. On the other hand, WKIND core model enables the extension of the analyses and the solution of strong reactivity transients. In the first core related transient case, withdrawal of all control rods at a speed of 100 cm/s, the results obtained by WKIND core model are more important than the respective Flownex results, as WKIND correctly describes the temperature changes within the core. From the results attributed in this case it is evident that great differences exist between the capabilities and limitations of the two core models. Flownex core model simulates the fuel temperature using a homogeneous model, whereas WKIND calculation of the fuel particle temperature is done explicitly. By taking into account the position of the control rods, WKIND core model demonstrates a more realistic behaviour of the core. In the second transient, the control rods are withdrawn at a speed of 1 cm/s. In this case, both reactor core models have shown similar behaviour and the analysis results are similar for both cases.

From the transient analyses it is evident that the thermal inertia of the reactor is so large, that the influence of various disturbances on the dynamic behaviour of the core is hardly noticeable. During a load rejection transient, the core outlet temperature is almost constant. Thus, the strong negative temperature coefficient is shown to be favourable both from a safety point of view and for the reduction of temperature variations during off-design operation. This is beneficial for the operation at elevated reactor inlet temperatures as occurring in this case.

Both rector core models have shown good agreement in the transient analyses results, with respect to the single and the three shaft system layouts. The results also met the safety requirements of the plant, whereby the inherent safety aspect of the PBMR is shown. The study demonstrates that the design of PCU using the WKIND core model prevents the temperature from exceeding 1600°C even during strong reactivity transients. In this transient, reactivity was inserted, and that has to be compensated by a negative temperature feedback, i.e., by higher temperatures. Once the rods withdrawal has stopped, the negative feedback is stronger and therefore the power rapidly decreases. In order to obtain and to maintain the higher temperatures, more power is needed.

The complete system simulation coupled to a reactor model core results in obtaining realistic boundary conditions for the core inlet parameters. It has been shown that Fownex point kinetics approximation of the neutronic calculations works well for the operational region of interest, except for the case of strong reactivity disturbances. It has been proven that the neutronic calculations can be greatly reduced in their complexity using the Flownex point kinetics reactor core model. However, WKIND core model is advantageous, offering an accurate solution even in the latter case. Therefore, it would be beneficial to incorporate power profile changes during control rod movement in Flownex core model. In the current coupling, a pipe component assimilates the reactor core as a heat source with an artificial resistance in the form of friction to get the correct pressure drop. However, the indirect coupling method could be improved by replacing Flownex core model with a pipe with variable losses. This will result in a new calculated pipe loss factor, which better predicts the correct thermo hydraulic behaviour of the core. Furthermore, it is recommended to extend the coupling by using 2D and even 3D core neutronics. Such coupling will not pose a great challenge, as the interface between Flownex and the external core is almost identical in all cases.

6.4 Transient Analyses

The direct coupling of the PCU with a High Temperature Pebble Bed Reactor has a variety of dynamical aspects. The close interaction between the reactor core flow, the turbine power and the pressure ratio leads to strong pressure and temperature transients, which are decisive for most structural design requirements. It can be concluded that the single and the three shaft configurations do not differ greatly in their dynamic response. Providing similar core boundary conditions during transient simulations for both systems proves that only negligible dif-

ferences exist in the mass flow circulating through the core during a reactor shut down procedure. However, the transient behaviour of the two circuits differs substantially during a load rejection transient. Here, the opening of a bypass valve was used, and it was shown that this action was capable of successfully controlling both systems, allowing them to return to stable operating conditions. Opening the bypass valve resulted also in a large change in pressure ratio over the power turbine and the compressors in both systems, which strongly influenced the efficiencies of the turbo-machines. It is evident that during a loss of load transient, the main components in both systems undergo sharp changes in pressures and temperatures. Close interactions between the core mass flow, the turbine power and the system pressure ratio lead to this outcome. Higher turbo-machinery efficiencies achieved in the single shaft system indicate the advantage of this configuration in a load rejection transient. With a free running power turbine as in the three shaft configuration, the generator speed is more difficult to control. In the three shaft configuration, the tendency of the power turbine to over speed has been prevented by using a complicated sequence of control actions. In addition, this system requires a resistor bank with a minimum continuous rating of 10 MW_{el} in order to limit the power turbine over speed and to provide the plant house load during the event. The complexity involved in the design of the three shaft configuration with an additional large resistor will end up at higher costs and risks. On the other hand, the single shaft configuration, which is easier to control, requires a very long shaft and long tubes, which can contribute to an additional risk for breaks. The single shaft configuration has another built-in limitation of the compressors and the turbine shafts rotating at the generator speed. This has the effect of a disadvantageous part load performance of this system, and therefore it is recommended to further investigate the behaviour of the systems using stress and risk analysis. In the load following transient the helium inventory is reduced to 40% within about 6 hours, and shortly after the reduction the inventory is restored to 100%. This transient barely affects the working points of the turbo-machinery. According to the literature, the three shaft configuration provides an improved operational stability in this case. This is due to the fact that the compressors follow their operating line, instead of a constant speed line, thus increasing the flexibility, offering a quick response to load increase. Based on the simulation results it can be concluded that the dynamic behaviour of the plant is correctly predicted over a wide range of conditions and at time scales, varying from a few seconds to several hours. It has been demonstrated that the control system of the PCU plays an important role in determining the complete behaviour of the plant. The implicit formulation of Flownex code makes it possible not only to calculate

the system behaviour for a certain given design, but also to modify and reduce the geometry needed to obtain a requested system performance. This is the case, for example, during loss of load and helium leak simulations, where the turbo-machines operate away from their original design point. Here, Flownex will simulate up to the point where the flow through the turbo-units is too low. With the aid of suitable bypass valves added, it was possible to proceed the simulation, by adjusting the bypasses opening diameter according to the varying behaviour of the turbines and the compressors. In the case of a helium leak, a rapid pressure equalisation accompanied by a turbo-machines trip was shown. Also here, a decoupling of the generator from the grid was initiated. Furthermore, the calculated turbo-machines speed was decreased until reaching a complete stop in both the single and three shaft systems.

6.5 Final Conclusion

The indirect coupling method can provide improved boundary values and predict accurate system behaviour for the analyses of the complete plant safety when interfacing Flownex and WKIND. A quick response to a range of power demands, using a simple design of the control system, advocates the single shaft system. However, further investigation should be done to rectify this, especially during long-term part load performance of the system.

7 References

[1] Verkerk, E.C., 2000. Dynamics of the pebble bed nuclear reactor in the direct Brayton cycle. Ph.D. Thesis, Delft University of technology, The Netherlands.

[2] General Atomics, USA, Home Page: http://www.ga.com/gtmhr/gtmhr1.html.

[3] Ullman's Encyclopedia of Industrial Chemistry, 2007. Wiley - VCH GmbH.

[4] Moore, R.A., Kantor, M.E., Brey, H.L., and Olson, H.G. 1982. HTGR experience, programs, and future applications, Nuc. Eng. Des. 72, pp. 153-174.

[5] Current status and future development of modular high temperature gas cooled reactor technology (IAEA-TECDOC-1198), 2001, Vienna, Austria.

[6] Matzie, R. A., 2006. Overview of HTR technology, Proceedings of HTR 2006, 3rd International Topical Meeting on High Temperature Reactor Technology, October 1-4, 2006, Johannesburg, South Africa

[7] PBMR, South Africa, Home Page. [Web:] http://www.PBMR.com.

[8] Barnet, H., Singh J. and Hohn, H., 1990. "Nuclear process heat – AVR lessons for the future", Nuclear AVR – Experimental high-Temperature reactor, Association of the German Engineers (VDI) – The Society for Energy Technologies, VDI-Verlag GmbH, Düsseldorf, pp.352-366.

[9] Lohnert, G., 1990. Technical design features and essential safety-related properties of the HTR-Module, Nuc. Eng. Des. 121, pp. 259-275.

[10] Schenk, W., Pitzer, D. and Nabielek, H, 1986. Spaltproduktfreisetzungsverlauf von Kugelbrennelementen bei Störfalltemperaturen, Oktober 1986, Jül-2091.

[11] Weisbrodt, I.A., 1995. Summary report on technical experiences from high temperature helium turbo-machinery testing in Germany, Proceedings of Technical Committee meeting on Design and Development of gas-cooled reactor with closed cycle gas turbines, Beijing, China, 30 October – 2 November 1995, pp. 177-250.

[12] Greyvenstein, G.P. and Rousseau, P.G., 2003. Design of a physical model of the PBMR with the aid of Flownet, Nucl. Eng. Des., 173, pp.119-129.

[13] Bammer, K., and Deuster, G. 1974. Das Heliumturbinen-Kraftwerk Oberhausen: Auslegung und Aufbau, Energie und Technik, 26 (1), pp. 1-6.

[14] Zenker, P., 1976. Selected piping problems encountered in the helium turbine installation in Oberhausen. 3R international, 15. Jahrgang, Heft 4, April 1976, pp. 141 – 145.

[15] Zenker, P., 1974. Einige Aspekte zum Bau der 50-MW-Heliumturbinenanlage der Energieversorgung Oberhausen AG., Atomkernenergie (ATKE), 1974 Bd. 23, pp. 99-104.

[16] Fruthschi, H. U., 2005. Closed-cycle gas turbine experience and future potential, ASME Press, New York.

[17] Niekerk, W.M.K., Rousseau, P.G., and Greyvenstein, G.P. 2003. Operation and simulation of a three-shaft, closed-loop, Brayton cycle model of the PBMR power plant. International Conference on Advances in Nuclear Power Plants, 4-7 May, 2003, Cordoba, Spain.

[18] Zohng, D., Xu, Y., 1995. Progress of the HTR-10 project, Proceedings of a Technical Committee meeting on Design and Development of gas-cooled reactor with closed cycle gas turbines, Beijing, China, 30 October – 2 November 1995, pp. 25-30.

[19] Xu, Y. and Sun, Y., 1996. HTR-10 Severe accident management, Proceedings of an IAEA technical committee meeting on high temperature gas-cooled reactor technology development (IAEA-TECDOC-988), Johannesburg, South Africa, 13-15 November, 1995, pp. 93-100.

[20] Sun, Y., Gao, Z., 2003. Benchmark Problem of the HTR-10 Control Rod Withdrawal without Scram (ver. 2003-12), Institute of Nuclear Energy Technology, Tsinghua University, Beijing, China.

[21] Walter, A., Schulz, A., Lohnert, G., 2006. Comparison of Two Models for a Pebble Bed Modular Reactor Core Coupled to a Brayton Cycle, Nuc. Eng. Des. 236, pp. 603-614.

[22] Matzner, D., 2004. PBMR project status and the way ahead, 2nd International Topical Meeting on High Temperature Reactor Technology, 22-24 September 2004, Beijing, China.

[23] Koster, A., Matzner, H.D., Nichols, D.R., 2003. PBMR design for the future, Nuc. Eng. Des. 222, pp. 231-245.

[24] Decher, R., 1994. Energy conversion systems – flow, physics and engineering, Oxford University Press, New York.

[25] Dong, Y., Unger, H.M. and Fröhling, W., 2001. Comparison of plant efficiencies of various power conversion systems for high temperature reactor modules, Kerntechnik, 66 (2001), 1/2, pp. 8-14.

[26] Lederer, B.J., Wildberg, D.W., 1992. Reaktorhandbuch, Kerntechnische Grundlagen für Betriebspersonal in Kernkraftwerken, Carl Hanser Verlag, München-Wien.

[27] Matsuo, E., Tsutsumi, M., Ogata, K. and Nomura, S., 1995 .Conceptual design of helium gas turbine for MHTGR-GT. Proceedings of technical committee meeting on design and development of gas-cooled reactor with closed cycle gas turbines, Beijing, China, 30 October – 2 November 1995, pp. 95-109.

[28] Zahng, Z. and Jiang, Z., 1995. Design of indirect gas turbine cycle for a modular high temperature gas cooled reactor. Proceedings of technical committee meeting

on design and development of gas-cooled reactor with closed cycle gas turbines, Beijing, China, 30 October – 2 November 1995, pp.85-93.

[29] Greyvenstein, G.P., 2002. An implicit method for analysis of transient flows in pipe networks, Int. J. Numer. Meth. Eng., 53, pp.1127-1143.

[30] Ravenswaay, J.P., Greyvenstein, G.P., Willem M.K., Niekerk, W.M.K. and Labuschagne, J.T., 2004. Verification and validation of the HTGR systems CFD code Flownex, 2nd International Topical Meeting on High Temperature Reactor Technology, 22-24 September 2004, Beijing, China.

[31] Landman, W.Y., Van Heerden, E., Ravenswaay, J.P. and Greyvenstein, G.P., 2003. Flownet Nuclear Architecture, Implementation and Verification and Validation, ICAPP 2003 (International Congress on Advanced Nuclear Power Plants), 4-7 May, Cordoba, Spain.

[32] De Geus, Aer and Stempniewicz, 2006. Application of Spectra on PBMR V704 design, Proceedings HTR 2006: 3rd International Topical Meeting on High Temperature Reactor Technology, October 1-4, 2006, Johannesburg, South Africa.

[33] Star CD-Methodology, Manual Version 3.10, 2000, Computational Dynamic, London.

[34] Rousseau, P.G., Du Toit, C.G. and Landman, W.Y., 2004. Validation of a transient thermal-fluid systems CFD model for a packed bed high temperature gas-cooled nuclear reactor, 2nd International Topical Meeting on High Temperature Reactor Technology, 22-24 September 2004, Beijing, China.

[35] Coetzee, R.V., Der Merwe, V. and Rousseau, P.G., 2003. FLOWNEX Version 6 USER MANUAL, M-Tech Industrial, Potchefstroom, South Africa.

[36] Walter, A., Schulz and A., Lohnert, G., 2004. Comparison of Two Models for a Pebble Bed Modular Reactor Core Coupled to a Brayton Cycle, 2nd International Topical Meeting on High Temperature Reactor Technology, 22-24 September 2004, Beijing, China.

[37] Feltes, W., 1993. HTR - Program Description of ZIRKUS, Siemens Report Nr. KWU BT71/93/0009/.

[38] Bernnat, W. and Feltes, W., 2003. Models for reactor physics calculations for HTR pebble bed modular reactors, Nuc. Eng. Des. 220, pp. 331-347.

[39] Lamarsh, J.R. and Baratta, A.J., 2001. Introduction to nuclear engineering. New Jersey: Prentice Hall.

[40] Schulz, A., 2004. Entwicklung einer Komponente zur Kopplung von externen Simulationsmodulen an das thermofluidische Anlagen-Simulationsprogramm Flownex, IKE.

[41] Marais, D., 2007. Validation of the point kinetic neutronic model of the PBMR, Master of Engineering (Nuclear), Potchefstroom Campus of the North-West University, Potchefstroom, South Africa.

[42] Landman, W.A. and Greyvenstein, G.P. 2004. Dynamic systems CFD simulation code for the modelling of HTGR power plants, 2nd International Topical Meeting on High Temperature Reactor Technology, 22-24 September 2004, Beijing, China.

[43] Greyvenstein, G.P. and Rousseau, P.G., 2002. Basic principles of HTR thermal hydraulics, HTR/ECS, High Temperature Reactor School, November 4-8 2002, Cadarache, France.

[44] Wylie, E.B., Streeter V.L., 1993. Fluid Transients in Systems. Englewood Cliffs, NJ: Prentice-Hall.

[45] Anderson D. A., Tannehill, J. C. and Pletcher, R. H., 1984. Computational fluid mechanics and heat transfer, McGraw-Hill, New York.

[46] Shames, I. H., 1982. Mechanics of Fluids. McGraw-Hill, New York.

[47] Streeter, V.L. and Wylie, E.B., 1979. Fluid Mechanics. 7th ed., McGraw-Hill Book Company, Johannesburg.

[48] Holman, J.P., 1989. Heat transfer. McGraw-Hill, New York.

[49] Kays, W. M. and London, A.L., 1964. Compact Heat Exchangers. McGraw-Hill Series in Mechanical Engineering, Custom Edition.

[50] FLOWNEX Version 7.0 USER MANUAL - part 2, November 2006, M-Tech Industrial, Potchefstroom, South Africa.

[51] FLOWNEX Version 6.8 USER MANUAL - part 1and 2, August 2005, M-Tech Industrial, Potchefstroom, South Africa.

[52] Greyvenstein, G.P. and Rousseau, P.G., 2002. One-dimensional reactor model for the integrated simulation of the PBMR power plant, Proceedings of 1st International Conference on Heat Transfer, Fluid Mechanics and thermodynamics, 8-10 April, 2002, Kruger Park, South Africa.

[53] Du Toit, C.G., Greyvenstein, G.P., Rousseau, P.G., 2003. A comprehensive reactor model for the integrated network simulation of the PBMR power plant, International Congress on Advanced Nuclear Power Plants, 4-7 May 2003, Cordoba, Spain.

[54] Greyvenstein, G.P., 2006. The application of systems CFD to the design and optimisation of High-Temperature Gas-Cooled nuclear power plants, Proceedings of ASME POWER 2006 Conference Georgia World Congress, May 2-4, 2006, Georgia, Atlanta.

[55] Kugeler, K. and Schulten, R., 1989. Hochtemerpaturreaktortechnik. Springer-Verlag, Heidelberg.

[56] Stoecker, W. F., 1989, Design of thermal systems, McGraw-Hill, New York

[57] Kindt, T. and Kohtz, N., 1993. ZKIND – ein Simulationprogramm für Reaktivitätstransienten in Kugelhaufen-Hochtemperaturreaktoren. KWU BT71/93/0018, 1993.

[58] Bammert, K., Krey, G. und Krapp, R., 1974. Die 50-MW-Heliumturbine Oberhausen, 19th Annual International Gas Turbine Conference and Products Show, Schweizerische Bauzeitung, 92 Jahrgang, Heft 11, 14 März 1974, pp. 235-240.

[59] Bammert, K, Johanning, J., and Weidner, E. 1983. Instrumentierung und Verfahren zur Messung des dynamischen Verhaltens der Heliumturbinenanlage Oberhausen. Atomkernenergie-Kerntechnik, 43 (4), pp. 225-239.

[60] Bammert, K., 1975. A general review of closed cycle gas turbines using fossil, nuclear and solar energy, September 1975, Verlag Karl Thiemig, München.

[61] Frutschi, H. U., 2005. Closed-cycle gas turbines - operating experience and future potential", ASME, New York.

[62] Bentivoglio, F. and Geffraye, G., 2006. Validation of the CATHARE code against experimental data from Brayton cycle plants. Proceedings of HTR 2006, 3rd International Topical Meeting on High Temperature Reactor Technology, October 1-4, 2006, Johannesburg, South Africa.

[63] Bammert, K., 1988. Beitrag zur Dokumentation über die 50 MW-Heliumturbinenanlage. Bericht, Institut für Strömungsmaschinen, Universität Hannover.

[64] Pirson, J., Ehster, S., Komen, E. M. J., Niessen, H. F., Van Hove, W., 2006. Safety related matters dealt with in the RAPHAEL European FP6 project, Proceedings of HTR 2006, 3rd International Topical Meeting on High Temperature Reactor Technology, October 1-4, 2006, Johannesburg, South Africa.

[65] Zenker, P., 1988. 10 Jahre Betriebserfahrung mit der Heliumturbinenanlage Oberhausen, VGB Kraftwerktechnik 68, heft 7, Juli 1988.

[66] Widlund, O., Geffraye, G., Bentivoglio, F., Messié, A., Ruby, A., Saez, M., Tauveron, N. and Bassi, C., 2005. Overview of gas-cooled reactor applications with Cathare, 11th International Topical Meeting on Nuclear Reactor Thermal hydraulics (NURETH-11), October 2-6, 2005, Avignon, France.

[67] Trevor Dudley et al. The thermal hydraulic model for the PBMR plant training simulator, Proceedings HTR 2006: 3rd International Topical Meeting on High Temperature Reactor Technology, October 1-4, 2006, Johannesburg, South Africa.

[68] Reitsman, F. et al., 2006. The PBMR steady-state and coupled kinetics core thermal hydraulics benchmark test problems, Nucl. Eng. Des. 236, pp. 657-668.

[69] Rademer, T., Bernnat, W., and Lohnert, G., 2004. Coupling of neutronics and thermal hydraulics codes for the simulation of transients of pebble bed HTR reactors, 2nd International Topical Meeting on High Temperature Reactor Technology, September 22-24, 2004, Beijing, China.

[70] Ben Said, N., Lohnert, G., Buck, M., Bernnat, W., 2006. The impact of design on the decay heat removal capabilities of a modular pebble bed HTR, Nucl. Eng. Des. 236, pp. 648-656.

[71] Botha, B.W. and Rousseau, P.G., 2002. Simulation investigation of control options for full load rejection in the PBMR closed cycle gas turbine power plant**,** International Gas Turbine Institute Turbo Expo (IGTI 2002), 3-6 June 2002, Amsterdam, Holland.

[72] Van Rooyen, W.J., Krueger, D.L.W., Mathews, E.H. and Kleingeld, M., 2006. Simulation and optimisation of gas storage tanks filled with heat sink, Nuc. Eng. Des., 236 (2), pp. 156-163.

[73] Verkerk, E.C. and Kikstra, J.F., 2003. Comparison of two models for a high temperature reactor coupled to a gas turbine, Nuc. Eng. Des., 220, pp. 51-65.

[74] Schmitz, W., Koster, A., 2006. Air ingress simulations using CFD, Proceedings of HTR 2006, 3rd International Topical Meeting on High Temperature Reactor Technology, October 1-4, 2006, Johannesburg, South Africa.

Institut für Kernenergetik und
Energiesysteme

Universität Stuttgart

Pfaffenwaldring 31

D-70550 Stuttgart